RELATIVE RISK TO SEABIRDS FROM FUTURE OFFSHORE WIND ENERGY DEVELOPMENTS IN DANISH WATERS: SPATIAL DISTRIBUTION AND CUMULATIVE DEVELOPMENT SCENARIOS

Technical Report from DCE – Danish Centre for Environment and Energy No. 367 2025

AARHUS
UNIVERSITY
DCE – DANISH CENTRE FOR ENVIRONMENT AND ENERGY

RELATIVE RISK TO SEABIRDS FROM FUTURE OFFSHORE WIND ENERGY DEVELOPMENTS IN DANISH WATERS: SPATIAL DISTRIBUTION AND CUMULATIVE DEVELOPMENT SCENARIOS

Technical Report from DCE – Danish Centre for Environment and Energy No. 367 2026

Saana Isojunno[1]
Lindesay Scott-Hayward[1]
Claus Lunde Pedersen[2]
Heidi Maria Thomsen[2]
Morten Frederiksen[2]
Thomas Bregnballe[2]
Jacob Sterup[2]
Rasmus Due Nielsen[2]
Thorsten Skovbjerg Balsby[2]
Monique MacKenzie[1]
Ib Krag Petersen[2]

[1] CREEM, School of Mathematics and Statistics, University of St Andrews
[2] Aarhus Universit, Department of Ecoscience

AARHUS
UNIVERSITY
DCE – DANISH CENTRE FOR ENVIRONMENT AND ENERGY

Data sheet

Series title and no.:	Technical Report from DCE – Danish Centre for Environment and Energy No. 367
Category:	Scientific advisory report
Title:	Relative risk to seabirds from future offshore wind energy developments in Danish waters: spatial distribution and cumulative development scenarios

Author(s):	Saana Isojunno[1], Lindesay Scott-Hayward[1], Claus Lunde Pedersen[2], Heidi Maria Thomsen[2], Morten Frederiksen [2], Thomas Bregnballe [2], Jacob Sterup [2], Rasmus Due Nielsen [2], Thorsten Skovbjerg Balsby[2], Monique MacKenzie[1], Ib Krag Petersen[2]
Institution(s):	[1] CREEM, School of Mathematics and Statistics, University of St Andrews [2] Aarhus University, Department of Ecoscience

Publisher:	Aarhus University, DCE – Danish Centre for Environment and Energy ©
URL:	https://dce.au.dk
Year of publication:	January 2026
Editing completed:	January 2026
Referee(s):	Anthony David Fox
Quality assurance, DCE:	Camilla Uldal
External comments:	Comments can be found here
Financial support:	Energistyrelsen.
Please cite as:	Isojunno, S., Scott-Hayward, L., Pedersen, C.L., Thomsen, H.M., Frederiksen, M., Bregnballe, T., Sterup, J., Due Nielsen R., Skovbjerg Balsby T., MacKenzie, M. Petersen, I.K. 2025. Mapping relative risk to seabirds from offshore wind energy developments in Danish waters. Aarhus University, DCE – Danish Centre for Environment and Energy, 123 pp. Technical Report No. 367

Abstract:	Based on 352 days of aerial Distance Sampling line transect surveys of birds in Danish marine areas over the past 24 years, we developed a relative risk analysis for birds and offshore wind farm development. The assessment was based on abundance estimates for 17 marine bird species and their susceptibility towards offshore wind farm development. Using habitat, displacement and collision risk layers we classified the Danish marine areas in least and greatest risk of impacts to marine birds, as well as considered the potential relative risks under future cumulative development scenarios.

Keywords:	Seabird, offshore wind farm, spatial planning, sensitivity analysis, risk assessment, risk ranking, cumulative risk.
Front page photo:	Flying long-tailed ducks in snow. Photo by Rasmus Due Nielsen.
ISBN:	978-87-7648-021-9
ISSN (electronic):	2244-999X
Number of pages:	123

Contents

Summary

This report aimed to estimate the spatial distribution and cumulative risk to seabirds from a set of proposed future wind turbine locations to inform spatial planning in Danish national marine waters. The risk analysis approach described in this report followed closely that of a previous report (Isojunno et al., 2025) which developed seabird sensitivity maps for the region, providing spatially relative risk assessment based on historical survey data to the most at-risk species at each map location. In the present work, several important updates were made to the risk analysis methodology and input data to enable the estimation of cumulative risk under future development scenarios, alongside an update to the sensitivity maps. Additional survey data were also included to improve the spatial and temporal coverage of the data underpinning the sensitivity maps. These allowed the estimation of seasonal density distribution maps for key species found in Danish marine waters year-round. Combined with knowledge of the seasonal presence of each species in Danish marine waters, the present work also provides both seasonal and year-round sensitivity maps. Furthermore, survey data were time-weighted in the spatial analysis to represent the most recent distributions as the most relevant baseline for future scenario planning.

As in the previous work, the risk analysis considered three potential hazards to seabirds associated with offshore wind farm development: potential habitat degradation, displacement, and collision. The risk analysis quantified both 1) expected levels of species risk to each hazard, i.e., rates of habitat overlap, displacement, and collision, and 2) allowable levels of risk, based on desired target levels of protection and existing protections for each population and their habitat in Danish marine waters. Relative risks were expressed as the ratio between the expected (1) and allowable (2) levels of risk, benchmarking expected risks against target protections. The target protections, and thus the allowable levels of risk, for each species were set specific to each hazard: habitat protection level (HPL), target protection level from displacement (TPLd) and target protection level from mortality (TPLm). This benchmarking enabled the comparison of risks to different species and hazards relative to their allowable levels. An expert elicitation process was employed to inform the target protection and other non-spatial input parameters, as well as quantify associated parameter uncertainty.

Overall, the results of the sensitivity mapping were consistent with our previous findings, indicating robustness to key assumptions. Coastal and shallow areas maintained high risk ranking across all three hazards, displacement in particular. Offshore areas were again identified as having higher relative collision risk, especially for kittiwakes and other gull species. Additionally, seasonal maps suggested the highest risk of collision was during the summer months when longer daylength increased risk to present species which were most active during the day.

The cumulative risk analysis found substantial variation in relative risk between species and different hazards under development scenarios with increasing number of turbines installed. When discounting any area-based protection offered by SPAs, allowable levels of risk were exceeded for the displacement of diver and grebe species under a future development scenario with 1,045 additional turbines compared to present. When future wind farms

were assumed to not impact populations within designated SPAs, the expected cumulative risks were reduced relative to the allowable thresholds. These findings underscore the importance of comprehensive area-based and other management measures to counter potential risks to seabird populations from offshore wind development.

Resumé

I denne rapport estimeres den rumlige kumulative risiko for havfugle i relation til udbygningsplaner for havvindmølleparker i danske farvande. Risikovurderingsmetoden fulgte tæt tilgangen i en tidligere rapport (Isojunno et al., 2025), som udviklede følsomhedskort for regionen baseret på historiske optællingsdata og leverede en rumlig relativ risikovurdering for de mest sårbare arter på hvert kortlagt område. I nærværende rapport blev der foretaget flere væsentlige opdateringer af både metode og inputdata for at muliggøre estimering af kumulativ risiko under fremtidige udbygningsscenarier samt for at opdatere følsomhedskortene. Supplerende optællingsdata blev inddraget for at forbedre den rumlige og tidsmæssige dækning af datagrundlaget bag følsomhedskortene. Dette muliggjorde estimering af sæsonbestemte tætheder for nøglearter, der forekommer i danske havområder året rundt. Kombineret med viden om arternes sæsonmæssige tilstedeværelse giver nærværende arbejde både sæsonspecifikke og helårlige følsomhedskort. Derudover blev optællingsdata tidsvægtet i den rumlige analyse for at sikre, at de nyeste fordelingsmønstre vægtes højest som det mest relevante udgangspunkt for fremtidig planlægning. Som i det tidligere arbejde omfattede risikovurderingen tre potentielle påvirkninger af havfugle forbundet med etablering af havvindmølleparker: potentiel habitatforringelse, fortrængning og kollisionsrisiko. Risikovurderingen kvantificerede både 1) de forventede risikoniveauer for hver art i forhold til hver påvirkning – dvs. graden af habitatoverlap, fortrængning og kollisionsrate – og 2) de tilladte risikoniveauer, baseret på ønskede beskyttelsesniveauer og eksisterende beskyttelse af hver bestand og dens levesteder i danske havområder. De relative risici blev udtrykt som forholdet mellem de forventede (1) og de tilladte (2) risikoniveauer, hvilket gjorde det muligt at sammenholde de forventede risici med de målrettede beskyttelsesniveauer. De målrettede beskyttelsesniveauer – og dermed de tilladte risici – blev fastsat specifikt for hver påvirkning: habitatbeskyttelsesniveau (HPL), målbeskyttelsesniveau for fortrængning (TPLd) og målbeskyttelsesniveau for dødelighed (TPLm). Denne benchmarking muliggjorde sammenligning af risici på tværs af arter og påvirkninger i forhold til deres respektive tolerancer. Et ekspertpanel blev anvendt til at informere de målrettede beskyttelsesniveauer og andre ikke-rumlige inputparametre samt til at kvantificere usikkerhed i disse parametre. Overordnet var resultaterne fra følsomhedskortlægningen i overensstemmelse med tidligere fund, hvilket indikerer robusthed over for centrale antagelser. Kystnære og lavvandede områder fastholdt høje risikorangeringer for alle tre påvirkninger, især fortrængning. Offshore-områder blev igen identificeret som havende højere relativ kollisionsrisiko, særligt for rider og andre mågearter. De sæsonspecifikke kort viste desuden, at kollisionsrisikoen var højest om sommeren, hvor længere dagslys øger risikoen for arter, der er til stede og mest aktive i dagtimerne. Den kumulative risikovurdering viste betydelig variation i relativ risiko mellem arter og påvirkninger under udbygningsscenarier med stigende antal installerede mølleparker. Når der ikke blev taget højde for den arealbaserede beskyttelse i fuglebeskyttelsesområder (SPAs), blev de tilladte risikoniveauer overskredet for fortrængning af lommer og lappedykkere under et fremtidigt udbygningsscenarie med 1.045 yderligere møller sammenlignet med i dag. Når det antages, at fremtidige havvindmølleparker ikke påvirker bestande inden for udpegede SPAs, blev de forventede kumulative risici reduceret i forhold til de tilladte grænser. Disse resultater understreger betydningen af omfattende arealbaserede og andre forvaltningsmæssige tiltag for at imødegå potentielle risici for havfuglebestande i forbindelse med udbygning af havvind.

1 Introduction

Vulnerability assessments and sensitivity maps have been developed for a wide range of marine species, including seabirds and marine mammals, to inform spatial planning of offshore activities (Garthe & Hüppop, 2004; Furness et al., 2013; Bradbury et al., 2014; Certain et al., 2015; Kelsey et al., 2018; Best & Halpin, 2019; Verling et al., 2021; Fauchald et al., 2024). Both vulnerability assessments and sensitivity maps are prioritization tools that aim to rank levels of concern for different species (vulnerability assessments, e.g., Willmott et al., 2013; Green et al., 2025) and locations (sensitivity maps, e.g., Bradbury et al., 2014; Certain et al., 2015; Fauchald et al., 2024), and sometimes under specific development scenarios (e.g., Southall et al., 2023). Vulnerability assessments are typically carried out by a systematic scoring of factors thought to increase species susceptibility to impacts, such as adult survival, habitat specialism and flight altitude. Sensitivity maps combine these species-specific vulnerabilities with spatial distribution information to indicate areas that are liable to impacts due to the presence of vulnerable species. While there is some consistency and consensus on which seabird species are generally the most vulnerable to displacement and collision (e.g., Garthe & Hüppop, 2004; Willmott et al., 2013; Certain et al., 2015; Kelsey et al., 2018; Fauchald et al., 2024), methods to quantify vulnerability and to map sensitivity vary widely, with little guidance on best-practice approaches, assumptions, or treatment of uncertainty in the context of marine wildlife risk assessments (though see e.g., Cox, 2008; Linkov et al., 2009; Duijm, 2015 for discussion in other risk assessment contexts).

The "spatial risk-ranking" algorithm developed by Isojunno et al., 2025 provided several advances to previously published vulnerability assessments and sensitivity mapping approaches. The proposed algorithm aims to replicate the causal pathways of impact as closely as possible, albeit in a simple cross-sectional approach based on aerial survey data. This assumes populations are well-mixed and without significant individual variation, rather than individual-based models (IBM) that track individual movements and differences in exposure over time. However, the inputs to and outputs from the algorithm are fully quantitative, continuous-valued parameters that can be validated against empirical data and other quantitative assessment approaches, such as IBMs or population viability analyses (PVA). Parameter uncertainty is propagated through the entire algorithm, ensuring uncertainty both in the spatial distribution of species as well as non-spatial input parameters are incorporated within the confidence intervals of the risk analysis outcomes. Importantly, the outcomes of the risk analysis are defined with respect to explicit assessment targets, ensuring interpretability and comparability of results.

Risk-based approaches to environmental assessment are popular because they are consistent with risk management frameworks and administrative processes that require risk managers to consider both the likelihood and the potential consequence of unwanted outcomes (Gibbs & Browman, 2015; Raimondo et al., 2018; Stelzenmüller et al., 2020; Verling et al., 2021). Based upon this literature, we define species risk as the likelihood and consequence of unwanted outcomes to populations. Following the relative risk analysis approach of Isojunno et al., 2025, we quantify risk relative to assessment targets. While we do not aim to quantify absolute risk to populations, our aim is to inform about the relative magnitude differences in risk between different

species, hazards, and wind farm development scenarios. This goes a step further than risk ranking, which can only consider the rank order of different risks from the lowest to the highest risk scenario, and not the magnitude changes in risk from the lowest to the highest risk scenario. It is important to understand how much risks increase as species are exposed to a growing number of developments (hereafter, termed 'cumulative risk'). This knowledge enables informed decisions in situations where exposure is predicted to increase over time, such as when wind farm expansion is planned to cover increasingly large areas. While spatial risk ranking can inform about the areas where those cumulative risks can be minimized, risk ranking cannot inform about how slow or fast risks accumulate over time as more wind turbines are being installed. This is why in the present work, where we aim to evaluate cumulative risk, we have focused improving upon the methodology to estimate relative magnitude differences in risk, beyond the risk-ranking analysis presented in Isojunno et al., 2025.

Relative magnitude differences in risk are expected to be more sensitive to input parameters and model assumptions than risk ranking. More precise information is required to estimate differences between values, than rank order values, with statistical confidence. For example, more information is required to state that one species is five times at greater risk of collision than another species (estimating the order of magnitude of difference), than state that one species is at greater risk than another species (only the relative difference, not its magnitude, is estimated). To address this greater need for precision, we employed an expert elicitation process to estimate input parameter values, which in our previous report relied on published vulnerability scores (Isojunno et al., 2025). A literature review was carried out to provide the experts with an evidence dossier from which to draw conclusions, following a pre-defined protocol for making impartial, expert judgements as part of a two-stage Delphi process (MacMillan & Marshall, 2005; Hemming et al., 2018). Because we expected the relative magnitudes of risk to be sensitive to uncertainty in input parameters, we also used the between-expert variation in values to quantify parameter uncertainty. This uncertainty was then propagated through the algorithm and incorporated in the confidence intervals for each relative risk value. This way, we could evaluate differences in relative magnitude of risk with a degree of confidence. Furthermore, we tested the robustness of our results to key assumptions, such as the inclusion of existing area-based protections.

The developed analysis approach succeeded in the estimation of cumulative risk for different species and hazards. We found clear support for variation in the relative magnitude of cumulative risks to different species and hazards. For some species and scenarios, such as the risk of displacement on diver species, there was also substantial uncertainty around the magnitude increase in risk under future scenarios. The main cumulative risk results are presented in **Figure 3.10** - **Figure 3.12** and **Table 3.4**, with associated confidence intervals. The updated sensitivity maps are provided in **Figure 3.2** and **Figure 3.7**. For ongoing spatial planning purposes, the updated maps should be used instead of the previously published maps (Isojunno et al., 2025). The Discussion provides further guidance on the interpretation of the cumulative risk scenarios, potential caveats and considerations to reduce uncertainty in future risk assessments.

2 Methods

2.1 Relative risk analysis

2.1.1 Overview

This analysis aimed to estimate the spatial distribution and cumulative risk to seabirds from proposed future wind farm developments in Danish marine waters. For the rationale and development of the risk-based analysis approach for spatial risk ranking, we refer the reader to Isojunno et al., 2025. These are only briefly outlined here, with emphasis on highlighting changes to the methodology to estimate cumulative risk. An updated glossary of terms is provided in Appendix 1.

As in the previous work, the risk analysis considered three potential hazards to seabirds associated with offshore wind farm development: potential habitat degradation, displacement, and collision with turbine blades. The risk analysis quantified both 1) expected levels of species risk to each hazard, i.e., rates of habitat overlap, displacement, and collision, and 2) allowable levels of species risk, based on any existing and desired, target levels of protection for each population and their habitat in Danish marine waters. Relative risks were quantified as the ratio between the expected (1) and allowable (2) levels of risk. The risk ratio benchmarked the expected risks to each species in the numerator against allowable risks in the denominator, bringing relative species risks to the same scale with respect to targets. An expert elicitation process was employed to inform the assessment targets and other non-spatial input parameters, as well as quantify associated parameter uncertainty. The spatial input data consisted of species density distribution maps, which were primarily used to inform the expected level of risks at each grid location (**Figure 2.1**).

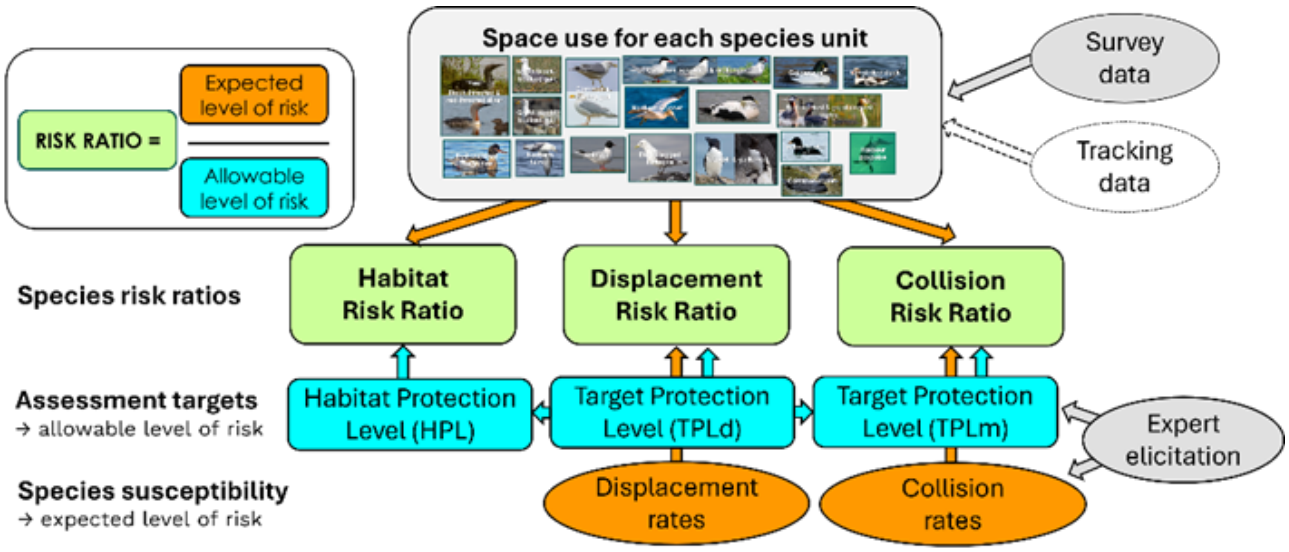

Figure 2.1. Conceptual overview of the approach to the risk analysis. Relative risks (light green) were quantified to inform both the spatial risk ranking of areas (sensitivity maps) and cumulative risk. Relative risks were expressed as the ratio between expected and allowable levels of risk. Inputs to the numerator and denominator are shown in orange and cyan, respectively. The allowable level of risk was informed by species- and hazard-specific target protection levels (cyan). Data sources are shown in grey: aerial survey data were used to inform the implemented algorithm (dark blue arrows). Tracking data were analysed to inform species space utilization (Isojunno et al., 2025) but was not incorporated in the present risk analysis.

2.1.2 Assessment targets

Relative risk was defined with respect to target protection levels for species units and their habitats, following our previous report (Isojunno et al., 2025)(see Appendix 1 for updated Glossary). These assessment targets were specified for each species or species group that were analysed together in the risk-ranking algorithm (hereafter, species unit). The individual species included within each species unit are listed in **Table 2.1** and explained in further detail in **Section 2.2.1**.

To account for the different levels of the potential consequences of displacement versus mortality on populations, we specified two target protection levels for each species unit: Target Protection Level from Displacement (TPLd), and Target Protection Level from Mortality (TPLm). Both were defined as the desired level of protection for each species unit and expressed as the proportion of the current population abundance for each species unit in the Danish EEZ marine region, as in the previous analysis. The separation of TPLd and TPLm introduced an additional parameter compared with the previous analysis, which used a single TPL value to describe the desired level of complete protection for each species unit in Danish national waters, given current population status, trends, and resilience to existing threats.

We also considered the proportion of each species' range that should be protected from any additional habitat alteration, the Habitat Protection Level (HPL). As in the previous analysis, the aim of the HPL was to reflect the dependence of each species on spatially limited resources and was used to ringfence core areas from further wind energy development. Unlike the previous analysis, however, the HPL was also informed by TPLd. This update was made to account for species, such as the goldeneye, that are habitat specialist but are not necessarily affected by this specialism due to good habitat availability and favourable population status. Similarly, TPLd was used to adjust TPLm. The calculation of each protection level based on the expert-elicited parameters is described in the sections on expert elicitation and input parameters, below.

As in our previous work, we considered existing area-based protections in the risk analysis. To achieve this, the allowable level of birds at risk of displacement was adjusted to reflect estimated species abundance outside any Special Protection Areas (SPAs) designated for each species. To present a full range of potential outcomes, we compare the main version of the risk analysis (no area-based protection) to an SPA-version that assumed 100% of target protection for displacement and mortality could be achieved within protected areas for designated species.

2.1.3 Quantifying relative risks

Relative risk of each hazard (habitat alteration, displacement, collision) for each modelled species unit i and development scenario x was expressed as a risk ratio. The risk ratios were calculated between the expected outcomes (numerator) and "allowable" outcomes based on the assessment targets for each species unit (denominator). The expected outcomes were calculated for three metrics, one for each hazard: the degree of overlap between core habitat and the hypothetical wind farm, the expected number of birds at risk of displacement, and the expected number of birds at risk of collision. Risk ratio values of > 1 could therefore be interpreted as the expected outcome exceeding allowable levels by this factor value. Conversely, risk ratios < 1 would indicate

that the allowable thresholds have not been exceeded. Species-unit-specific values for target protection levels were used to calculate the denominator for each hazard, enabling comparisons of relative risk between the modelled species units with different assessment targets (hereafter referred to as "relative species risk").

Relative risk was calculated with respect to a hypothetical development area x and associated exposure to each hazard. For risk-mapping, risk ratios were calculated for each grid location under a future scenario where a wind farm footprint would cover each 1x1 km grid cell area. For cumulative risk, the development areas consisted of specific development scenarios including existing and future placement of wind turbines over time (**Section 2.1.4**). Other than this difference in development scenarios, the risk ratio calculations for risk-mapping and cumulative risk were equivalent. Thus, in the equations below, the index x represents a development scenario, either at a single grid location (risk-mapping) or a polygon representing a development scenario in a particular area (cumulative risk). For habitat and collision risk, the area of exposure was defined as the footprint of a hypothetical wind farm. For displacement, the area of exposure included both the footprint and a buffer zone representing the spatial extent of displacement for each species unit.

The relative species risks of exceeding the HPL threshold (h_i^*) for each species unit i, grid cell y and development scenario x were calculated as the risk mapping risk ratio ($R_{h[i,y]}$) and cumulative risk ratio ($R_{h[i,x]}$):

$$R_{h[i,y]} = \frac{q_{i,y}}{(1 - h_i^*)}$$

and

$$R_{h[i,x]} = \frac{\sum_y^E q_{i,y}}{\sum_y^A q_{i,y}}$$

where $q_{i,y}$ is the habitat overlap metric, representing the degree of habitat overlap with species unit i in each grid cell location y. More specifically, $q_{i,y}$ was quantified as the fraction of the species range with a lower density than the estimated density in each 1x1 km grid cell $n_{i,y}$. To calculate the cumulative risk ratio over development areas containing multiple grid cells ($R_{h[i,x]}$), the grid cell values $q_{i,y}$ were summed over the development scenario area (E) to represent expected level of risk in the numerator and then divided by the sum of the grid cell values outside the core area defined by the HPL (A) to represent the allowable level of risk. Species range was defined as the area predicted to contain 0.95 (i.e., 95%) of the species unit's abundance in Danish marine waters. Thus, $q_{i,y}$ represents the species' core habitat overlap with the development area relative to its range. In risk-mapping scenarios considering existing area-based protections, $R_{h[i,y]}$ was set to its maximum value within any designated SPAs and a surrounding buffer zone, defined by the expected spatial extent of displacement for the species unit (β_i). In other words, each species unit was ringfenced a core area based on its distribution and HPL, and any additional areas under SPA designations.

The relative species risk of collision and displacement were expressed as the ratio between the expected number of birds at risk from each hazard under the development scenario x, and the allowable number of birds at risk, calculated based on the species unit abundance and target protection levels. The risk ratios for collision and displacement were calculated respectively as

$$R_{c[i,x]} = \frac{\lambda_i \cdot n_{i,x}}{N_i \cdot (1 - m_i)}$$

and

$$R_{d[i,x]} = \frac{\sum_m^M n_{i,m} \cdot \alpha_i}{N_i \cdot (1 - p_i)}$$

where p_i and m_i are the target protection levels from displacement and mortality, respectively, and N_i is the estimated abundance in the study area for each species unit i. The numerator in each equation aimed to reflect the expected number of birds potentially at risk. For collision risk, this was calculated as the product of proxy collision rate (λ_i) and the estimated number of birds within the development area x ($n_{i,x}$). In other words, the number of birds at risk of collision was specified to increase linearly with bird density at any given location. The number of birds at risk of displacement was calculated similarly as the product between the species unit displacement rate (α_i) and estimated number of exposed birds, but accounting for the spatial extent of displacement (β_i). For the cumulative risk scenario, the number of exposed birds was estimated by summing the estimated counts within the development area and buffer zone whose extent from the edge of the wind farm was determined by the spatial extent of displacement parameter for the species unit (β_i). Similarly for the risk-mapping, the number of exposed birds was summed over M grid cells in the neighbourhood of each grid cell x, with the radius of the neighbourhood determined by the extent parameter β_i.

The displacement and collision risk ratio calculations above assume that the placement of wind farms is the primary planning tool by which species risks can be reduced. However, some of the target protection levels could also be achieved by other area-based protections, beyond the selection of low-risk areas for wind farm development. To assess the potential benefits of such additional measures, we considered scenarios where existing SPA designations contribute to meeting the target protection level for designated species. Importantly, these scenarios assume that the placement of future wind farms is restricted to areas outside SPAs.

To adjust the risk ratio for each species unit, we firstly estimated the species unit abundance that could potentially benefit from area-based protections, N_i^a. The value N_i^a was estimated by summing predicted counts for grid cells that were within SPAs designated for the species but excluding grid cells close to existing or proposed wind turbines. "Close" was defined as 2 km for collision, and within the spatial extent parameter β_i for displacement. To provide an extreme contrast to the original scenario without any area-based protections, we considered a scenario where 100% of the resulting number of birds were protected, but we also explored scenarios with partial effectiveness (with 50% of N_i^a protected). Incorporating a proportional effectiveness parameter ε_i, the number of birds benefiting from area-based protections in the population can be written as $N_i^p = \varepsilon_i \cdot N_i^a$. The remaining part of the population $N_i^u = N_i - N_i^p$ was considered as not benefiting from the SPAs designated for the species unit. Thus, the abundance of each species unit was partitioned to "protected" and "unprotected" parts, based on the spatial coverage and assumed effectiveness of any SPAs designated for species within the unit.

Should a target protection level be fully achieved by the area-based species protections, the remainder of the population was considered to not require further protection. In other words, when $\frac{N_i^p}{N_i} \geq TPL_i$, the target protection level for the unprotected portion of the population (TPL_i^u) was set to zero. When the area-based protections did not fully achieve the target

($\frac{N_i^p}{N_i} < TPL_i$), the TPL_i^u was calculated based on the number of birds remaining from the target after subtracting those protected by SPAs:

$$TPL_i^u = max(TPL_i \cdot N_i - N_i^p, 0)/N_i^u$$

For the unprotected part of the population, a risk ratio could then be calculated as the expected level of impact (e.g., for collision, $\lambda_i \cdot n_{i,x}$) divided by the allowable level $N_i^u \cdot (1 - m_i^*)$ where m_i^* is the TPL_i^u for collision. To represent the risk ratio for the whole population, the resulting risk ratio was weighted by the unprotected proportion of the population:

$$R_{c[o,x]}^* = \frac{N_i^u}{N_i} \cdot \frac{\lambda_i \cdot n_{i,x}}{N_i^u \cdot (1 - m_i^*)} + \frac{N_i^p}{N_i} * 0$$

Thus, the overall risk ratio was calculated as a weighted average of the protected and unprotected population risk ratios, where the risk ratio of the protected population is zero. Simplifying this equation above, we obtain an equation similar to the original risk ratio, but with the target protection level TPL replaced by the adjusted target level for the unprotected population TPL_i^u:

$$R_{c[o,x]}^* = \frac{\lambda_i \cdot n_{i,x}}{N_i \cdot (1 - m_i^*)}$$

This relative risk metric can be interpreted as an adjusted risk ratio that assumes a level of protection within SPAs for designated species, and that these areas are not available to wind farm development. Thus, it is an adjusted risk ratio between the expected rate of impact and the allowable rate for the population that is influenced by the placement of wind farms outside SPAs (**Figure 2.2**).

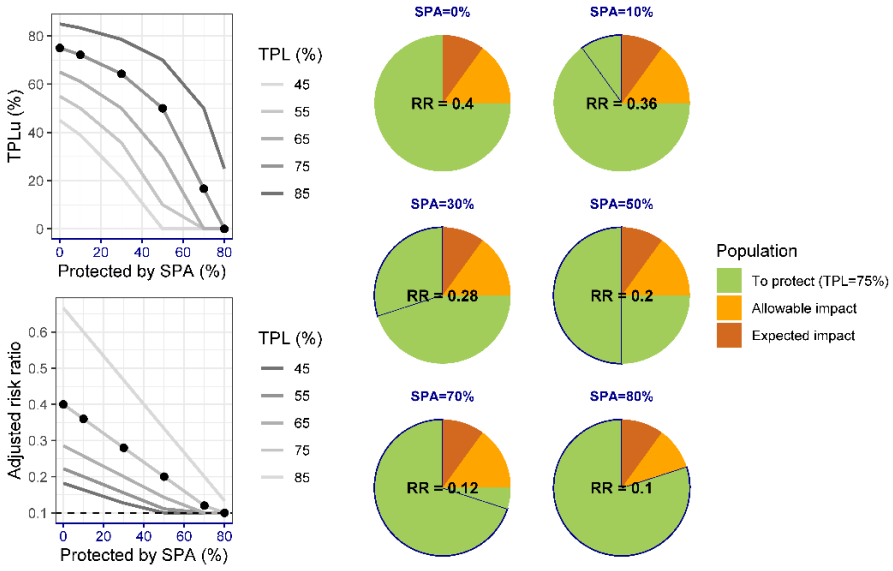

Figure 2.2. An illustration of the risk ratio adjustment made to account for SPA protection of designated species. In this example, the expected level of impact is set to 10% of the population. The pie chart on the right shows the partitioning of a population with 75% TPL into the proportion that is the target of protection (green), assumed to be protected by SPA designations (within blue outline), allowable for impact (orange and brown) and expected impact (brown). The leftmost panels show how the target protection outside SPAs (TPL_i^u) and the adjusted risk ratio (R^*) decline as greater percentage of the species unit abundance is assumed to be protected by SPAs, for hypothetical species examples with different TPLs (45-85%).

2.1.4 Wind farm development scenarios

Two types of hypothetical future development scenarios were considered: one for the risk-mapping, and another for the cumulative risk analysis.

The risk-mapping algorithm aimed to inform the choice between alternative locations for future wind farm development. We therefore conceptualized each grid cell location to represent an alternative location for a future wind farm. To quantify this, spatially relative risks were calculated for each grid location assuming the grid cell area in the location was covered by the footprint of a 1x1 km wind farm.

The cumulative risk analysis aimed to quantify relative increase in risk between baseline and a specific future development scenario. The development scenario consisted of 1,045 proposed turbine locations by the year 2030. The proposed turbine locations were not associated with specific lease areas, installation order, or alternatives. Therefore, the primary objective of the cumulative risk analysis was to quantify the potential differences in risk between baseline (representing status quo, given existing turbines) and the set of proposed turbine installations in 2030.

To provide additional information, we considered intermediate development scenarios between the baseline and 100% of the proposed future turbines. To achieve this, we "stretched" the installation of turbines over one year in 2030 to cover a longer time period, using an installation rate comparable to that experienced for existing turbines (~50 turbines a year). With a constant installation rate, the start, middle, and end points of this stretched timeline represented the current baseline, 50% and 100% development scenarios, irrespective of the amount of stretching caused by the assumed installation rate. However, the risk associated with any installation will depend on its placement in high vs low-risk areas. To provide a reasonable best-case scenario for installation, we assumed that turbines in the lowest risk areas (identified as part of the risk-mapping) would be installed first. This way, the relative risk associated with the midpoint of the timeline represented the expected risk of installing 50% of the lowest-risk turbines. Similarly, the difference in risk between the 50% and 100% scenarios represented the expected additional risk should 50% of the highest-risk turbines be installed.

2.1.5 Expert elicitation

The aim of the expert elicitation process was to derive a set of evidence-based input parameters and associated parameter uncertainty to the risk analysis, considering expert interpretation is required to derive the values from published literature. Each expert was asked to make evidence-based and impartial judgements on both their best estimate and 95% plausible value for each input parameter, for each species unit. Experts were asked to assume the role of an impartial observer, and consider the most likely values for each parameter, given its definition and empirical evidence to support it.

A brief literature review was carried out to collate relevant publications to evidence the parameter values. The experts were provided with this evidence dossier and invited to contribute additional sources to the dossier. The purpose of the evidence dossier was to ensure consistency in the empirical evidence upon which different experts based their judgments.

The expert elicitation was set up as a two-stage Delphi process. In the first stage, experts were asked to make individual judgements, independent of other experts. After these initial assessments, the experts convened to discuss their individual assessments and explore differences as well as identify any parameter values for which there was a greater consensus. Following the meeting, experts were offered the opportunity to update their initial assessment.

"Expert" in the elicitation context referred to a scientist with an ability to critically evaluate the empirical evidence for each parameter value. The experts included six experts associated with the project (ADF, CLP, HMT, IKP, MFR, TJSB; see Datasheet) and were selected to represent a range of relevant subject matter expertise in seabird ecology and monitoring, collision risk modelling, and/or displacement studies. The experts were asked to provide input on as many input parameters as possible, irrespective of their subject matter expertise. However, experts were not required to provide input to every parameter, if they felt unable to do so.

For most parameters, we already had an initial set of values based on our previous report (Isojunno et al., 2025). Most of the experts in the group were not blind to these values due to their involvement in co-authoring and reviewing the report. This starting point was formalized by providing an initial set of parameters in the assessment sheets that the experts were asked to provide their estimates. These included the parameter values from the previous report, as well as values collated from the literature for additional parameters that were added to the risk analysis. The experts were then free to either update the parameter values or not, as they saw appropriate. The assessment sheet, instructions, and evidence dossier are provided as Electronic supplementary material.

2.1.6 Input parameters

For each modelled species unit, we set values for TPLd (p_i^*), TPLm (m_i^*), HPL (h_i^*), proxy collision rate (λ_i), proxy displacement rate (α_i), and the expected spatial extent of displacement (β_i). Expert elicited parameter values were used to inform the displacement rates (α_i, β_i) directly, while the values for the three protection levels (TPLd, TPLm, HPL) and collision rate (λ_i) were calculated based on additional parameters that were part of the expert elicitation (population status, importance of Danish marine waters to the species, habitat specialism, and collision risk parameters)(**Figure 2.3**).

The TPLd was derived from two expert-elicited parameters, population status and importance of Danish marine waters to the population status. To make judgements about population status for the species, experts were asked to consider OSPAR and HELCOM assessments, alongside EU Red List status, depending on which listing they considered most relevant to the population found in Danish marine waters. The population status was scored on a 5-point ordinal scale, matching the IUCN red list categories (1 – least concern, 2 – near-threatened, 3 – vulnerable, 4 – endangered, 5 – critical). To make judgements about the importance of Danish marine waters to each species unit, experts considered the role of Danish marine waters in maintaining or achieving favourable conservation status for the population as whole. This was scored on a 3-point ordinal scale (low, medium, high). "High" importance was defined as overall population status depending on its continued use of Danish marine waters. "Medium" importance of Danish marine waters was defined as sufficient importance to impact overall population status, while "Low" was

defined as little influence on overall population status. The TPLd value was then assigned based upon both scores using a conversion matrix (**Figure 2.4**). The range (60-95%) and distribution of values in the conversion matrix was informed by expert-elicited values from the first stage of the Delphi process, before the experts convened and it was decided that a systematic conversion of the TPLd values based on both scores would be preferable. TPLd values within each population status category were increased based on Danish importance, except for the critical population status which received the highest value of 95% irrespective of Danish importance. While many experts were not comfortable in providing judgements on these percentages directly, all experts were comfortable scoring population status and importance of Danish importance to the overall population.

To inform target protection level from mortality (TPLm), an allowable level of mortality was calculated based on the potential biological removal (PBR) (Wade, 1998), expressed as a proportion of population abundance:

$$TPLm\ (\%) = (1 - PBR) * 100$$

Wade (1998) proposed PBR to estimate allowable limits to human-caused mortality of cetacean and pinniped populations. The formulation here follows adjustments made to estimate PBR for seabird populations (O'Brien et al., 2017):

$$PBR = 0.5 * (r - 1) * (1 - p_i^*)$$

where r is the maximum annual population growth rate, estimated from annual adult survival probability and age at first reproduction (Niel & Lebreton, 2005, parameter λ in eq. 15 therein) and p_i^* is the recovery factor. Species-unit-specific values for adult survival and age at first reproduction were derived from a literature review carried out on seabird populations in the UK (Horswill & Robinson, 2015). The demographic parameters were provided to the expert panel as part of the expert elicitation procedure (Electronic supplementary materials). The recovery factor p_i^* was equated to TPLd. The recovery factor is a value between 0 and 1 and is commonly used to set more precautionary harvest rates for threatened populations and when there is more uncertainty around demographic parameter estimates. In the present analysis, we only considered population status (TPLd) in the recovery factor, as uncertainty in population abundance estimates was accounted for in the workflow by resampling from the density surfaces (**Section 2.1.7**, Risk analysis workflow). Because both TPLd and PBR were expressed as proportion of population abundance, the minimum abundance parameter was not included in the calculation of PBR.

To inform HPL, experts were asked to consider the percentage of each species range in Danish waters that should be under area-based protection from offshore wind development, given the habitat specialism of each species. Habitat specialism was defined as the degree to which each species requires at-sea habitats that are specific to particular areas or sites in Danish marine waters. Similar to the TPLd, the expert assessment of HPL was changed from direct elicitation of percentage values to a systematic allocation of percentage values based on expert-elicited habitat specialism score, which was then scaled by the TPLd values. Habitat specialism was scored on a 5-point ordinal scale: 1 – very flexible, habitat generalist, 2 – mostly flexible, 3 – intermediate, 4 – mostly specialist, 5 – inflexible, habitat specialist. While experts were generally

comfortable providing the HPL percentage values directly, the score-based approach helped align different interpretations of the HPL from the initial assessment. The initial assessment of HPL values was used to inform the allocation of HPL values to each habitat specialism category and associated adjustment by TPLd. Based on the range of HPL values from the initial assessments, and feedback from the consensus meeting, the proportional HPL values were rescaled from the specialism score and then adjusted by TPLd using (specialism score + 1)/10 x TPLd/100.

To inform species-specific collision rates, the following parameters were collated from the literature and presented to the experts for assessment: proportion of time spent flying during the day ($f_{i,d}$), proportion of time spent flying during the night ($f_{i,n}$), proportion of flights at rotor height (r_i), flight speed (v_i), microavoidance rate during the day ($\delta_{i,d}$), and microavoidance rate during the night ($\delta_{i,n}$). Proxy collision rate during the day was calculated based on each expert-elicited value as

$$\lambda_{i,d} = (1 - \alpha_i) * f_{i,d} * r_i * (1 - \delta_{i,d})/v_i$$

The calculation was repeated for night time ($\lambda_{i,n}$), and the day and night rates were then combined using

$$\lambda_i = \lambda_{i,d} + p_{i,n}\lambda_{i,d}$$

Where p_n is the average proportion of night hours over a full year, calculated based on the presence/absence of each species unit in Danish marine waters (**Table 2.1**) and the interval between sunset and sunrise using the package "suncalc" in R (v0.5.1)(Thieurmel, 2017).

The proxy collision rate was used instead of formal collision risk modelling (CRM) to reduce computational time. To explore whether the collision proxy could reproduce CRM outputs in terms of absolute and/or relative magnitude between species, collision risk modelling was carried out using the "stochLAB" R package (Caneco et al., 2022). The CRM was run for each of the 17 species units with the equivalent species-specific input parameters ($f_{i,n}$, r_i, v_i, $\delta_{i,d}$) while holding input parameters related to wind farm installation and activity constant. Displacement rate (α_i) and proportion of time flying during the day ($f_{i,d}$) were used to adjust the input density of birds to the CRM, expressed as number of daytime in-flight birds/km^2 per month, for 12 months of the year. Morphometric data (wing span, body length) for each species unit were obtained by averaging species-specific values from stochLAB defaults, when available, and otherwise supplemented by equivalent UK values made freely available by RSPB (e.g., https://www.rspb.org.uk/birds-and-wildlife/red-breasted-merganser). The wind farm scenario, held constant across species, was specified to include 49 turbines spaced at 800 m apart on a square footprint, *i.e.* with length and breadth of 4.8 km. Rotor radius was set to be 80 m and air gap 36 m. Wind availability, speed, blade pitch, and downtime parameters were set at example values provided by stochLAB. The CRM was run using the Band model assumption (i.e., flight height distribution assumed to be uniform within rotor-swept zone vs outside, determined by the r_i parameter; Band et al., 2007; Johnston et al., 2014) and without species-specific parameter uncertainty. The CRM outputs were then converted to rates per turbine and per bird. Finally, the CRM rates were compared with the bootstrapped proxy collision rate estimates for each species (median and 95% percentiles).

Figure 2.3. Input data and parameters to the algorithm.

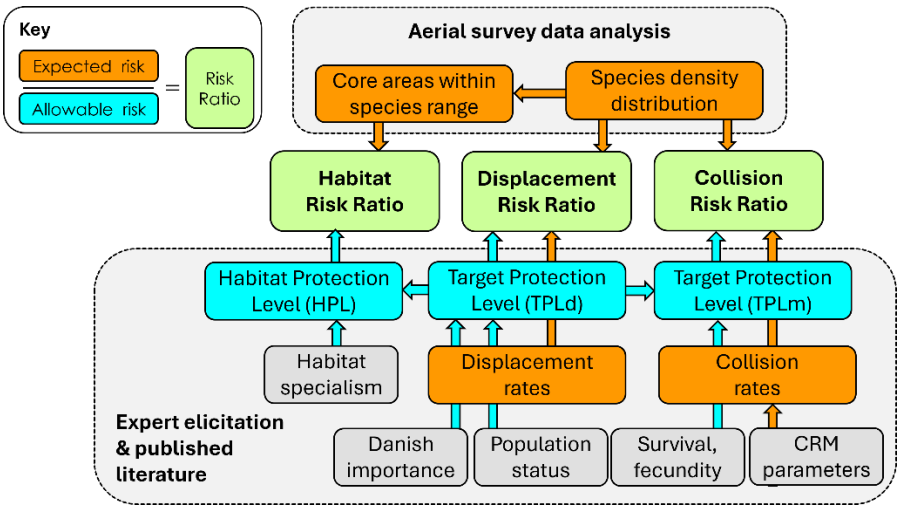

Figure 2.4. Scoring matrices used to derive TPLd and HPL based on expert-elicited parameters.

TPLd (% of population)	Danish Importance		
Conservation status	Low	Med	High
1 - Least Concern (LC)	60%	65%	70%
2 - Near Threatened (NT)	65%	70%	75%
3 - Vulnerable (VU)	70%	75%	80%
4 - Endanegered (EN)	80%	85%	90%
5 - Critically endangered (CR)	95%	95%	95%

HPL (% of species DK range)	Example TPLd (%)		
Habitat specialism	65%	75%	95%
1 - very flexible, habitat generalist	13%	15%	19%
2 - mostly flexible	20%	23%	29%
3 - intermediate	26%	30%	38%
4 - mostly specialist	33%	38%	48%
5 - inflexible, habitat specialist	39%	45%	57%

Table 2.1. Species included in the analysis. EURING = EURING species code, Species unit = an abbreviated label indicating the species or species groups that were analysed together as an ecologically similar species unit in the spatial risk-ranking algorithm, EU list = European species status following BirdLife International, 2021 red-listing; LC = least concern, NT = near threatened, VU = vulnerable, EN = endangered. N_{obs} = sample size of species observations.

EURING	Name (Danish)	Name (English)	Scientific name	Family	Species unit label	EU list	N_{obs}
59	Lom sp.	Diver sp.	*Gavia sp.*	Gaviidae	Diver		7272
20	Rødstrubet lom	Red-throated diver	*Gavia stellata*	Gaviidae	Diver	LC	4886
30	Sortstrubet lom	Black-throated diver	*Gavia arctica*	Gaviidae	Diver	LC	113
100	Gråstrubet lappedykker	Red-necked grebe	*Podiceps grisegena*	Podicipedidae	Grebe	VU	1071
90	Toppet lappedykker	Great crested grebe	*Podiceps cristatus*	Podicipedidae	Grebe	LC	990
129	Lappedykker sp.	Grebe sp.	*Podicipedidae sp.*	Podicipedidae	Grebe		355
220	Mallemuk	Northern fulmar	*Fulmarus glacialis*	Procellariidae	Fulmar	VU	3172
710	Sule	Northern gannet	*Morus bassanus*	Sulidae	Gannet	LC	7333
2180	Hvinand	Goldeneye	*Bucephala clangula*	Anatidae	Goldeneye	LC	2815
2120	Havlit	Long-tailed duck	*Clangula hyemalis*	Anatidae	Longtailed	LC	11482
2060	Ederfugl	Common eider	*Somateria mollissima*	Anatidae	Eider	EN	69626
2130	Sortand	Common scoter	*Melanitta nigra*	Anatidae	Scoter	LC	88559
2150	Fløjlsand	Velvet scoter	*Melanitta fusca*	Anatidae	Velvetscoter	VU	7971
2210	Toppet skallesluger	Red-breasted merganser	*Mergus serrator*	Anatidae	Merganser	NT	6593
5900	Stormmåge	Common gull	*Larus canus*	Laridae	Gull	LC	3630
5920	Sølvmåge	Herring gull	*Larus argentatus agg.*	Laridae	Gull	LC	49477
5910	Sildemåge	Lesser black-backed gull	*Larus fuscus*	Laridae	LBBG	LC	1035
6000	Svartbag	Great black-backed gull	*Larus marinus*	Laridae	GBBG	LC	7952
5780	Dværgmåge	Little gull	*Hydrocoloeus minutus*	Laridae	Littlegull	LC	2377
6020	Ride	Black-legged kittiwake	*Rissa tridactyla*	Laridae	Kittiwake	VU	6462
6150	Fjordterne	Common tern	*Sterna hirundo*	Laridae	Tern	LC	8
6160	Havterne	Arctic tern	*Sterna paradisaea*	Laridae	Tern	LC	625
6159	Hav/fjordterne	Arctic/Common tern		Laridae	Tern		2111
6110	Splitterne	Sandwich tern	*Thalasseus sandvicensis*	Laridae	Tern	LC	1149
6259	Terne sp.	Tern sp.	*Sterninae sp.*	Laridae	Tern		475
6360	Alk	Razorbill	*Alca torda*	Alcidae	Alcid	LC	780
6345	Alk/lomvie	Razorbill/Guillemot		Alcidae	Alcid		18681
6340	Lomvie	Common guillemot	*Uria aalge*	Alcidae	Alcid	LC	3736
6380	Tejst	Black guillemot	*Cepphus grylle*	Alcidae	Alcid	LC	83

2.1.7 Risk analysis workflow

The complete risk analysis workflow comprised of the following steps: 1) spatial risk ranking to produce sensitivity maps, 2) creating an annual time course for future installations by ranking proposed future wind turbine locations by their combined risk to seabirds, from the lowest to the highest risk turbines, and 3) estimation of cumulative risk over the time-line of installations, including both the commission of existing wind farms as well as the hypothetical installation order of proposed future wind farms. Uncertainty was estimated using a bootstrap procedure, whereby the above three steps were repeated multiple times, each time drawing a different set of input parameters and data, to generate a distribution of outcomes to represent uncertainty in analysis outcomes.

The generation of sensitivity maps followed the spatial risk-ranking algorithm of Isojunno et al., 2025 with updated inputs. Relative risk maps were generated in four main steps (**Figure 2.5**). First, risk ratios were calculated in each grid cell of the study area based on the predicted density distributions for each of the 17 modelled species units. This created 17 risk ratio maps for each of the three hazards (habitat alteration, displacement, and collision). Next, a combined map of risk ratios was generated for each hazard by taking the maximum value for each grid cell across the species units. This second step created three risk ratio maps, each representing maximum species risk at each grid location relative to the assessment targets. In a third step, the maximum risk ratio values were ranked in space. This was achieved by taking the quantiles of the risk ratio values across the prediction grid. The resulting values between 0 and 1 represent the ranking of each grid cell by their risk ratio value. For example, a quantile value of 0.95 at a grid location would indicate that 95% of the study area had lower risk ratio values than the value at the grid location. Finally, in a fourth step, the spatially relative risk maps for each of the three hazards were combined based on their maximum value. Thus, the final combined map presents maximum values across the three hazard maps.

Risk maps were created for each season (winter, spring, summer, autumn) as well as year-round. Seasonal maps were based on the available density distribution estimates of species present in that season (**Section 2.2.1**). Three different methods to generate year-round risk-maps were evaluated. The first two methods summarized risk ratios for each species unit as either maximum values (Method 1) or simple average values (Method 2) across the four seasons. The third method calculated year-round risk based on year-round density distribution maps for each species. For species that were modelled density distribution separately for winter-spring and summer-autumn (**Section 2.2.1**), the two density distributions were averaged with season duration in days as weights. Compared to Method 3, Methods 1 & 2 did not account for the duration of each season. Method 3 can be interpreted as accounting for the cumulative use of at-sea areas when species are present in Danish marine waters, while Methods 1 and 2 represent maximum and average risk across the present seasons, respectively. All three methods aimed to represent year-round risk when the species are present in Danish marine waters, and thus risks were not reduced by strongly seasonal species' absence in certain times of the year (**Table 2.2**). The year-round risk maps presented in the report are based on Method 3, but we provide results based on Methods 1 and 2 in **Appendix 3** for comparison.

Input parameter uncertainty was propagated through the entire risk-analysis via bootstrapping. Bootstrapping was applied both to the cumulative risk and spatial risk-ranking calculations. Both sets of calculations were repeated 500 times, each time using a different bootstrap prediction for species unit densities and set of expert-elicited input parameters. Expert-elicited input parameters were re-sampled independent of the expert, so that for each iteration (a re-run of the analysis), the input parameters could come from multiple different experts. Uncertainty in the risk-analysis outcomes was then represented by summarizing the distribution of the resulting 500 cumulative risk scenarios and risk maps. To represent uncertainty, we used both the ratio of standard deviation to mean (i.e., coefficient of variation) and 95% percentiles to represent the 95% confidence interval.

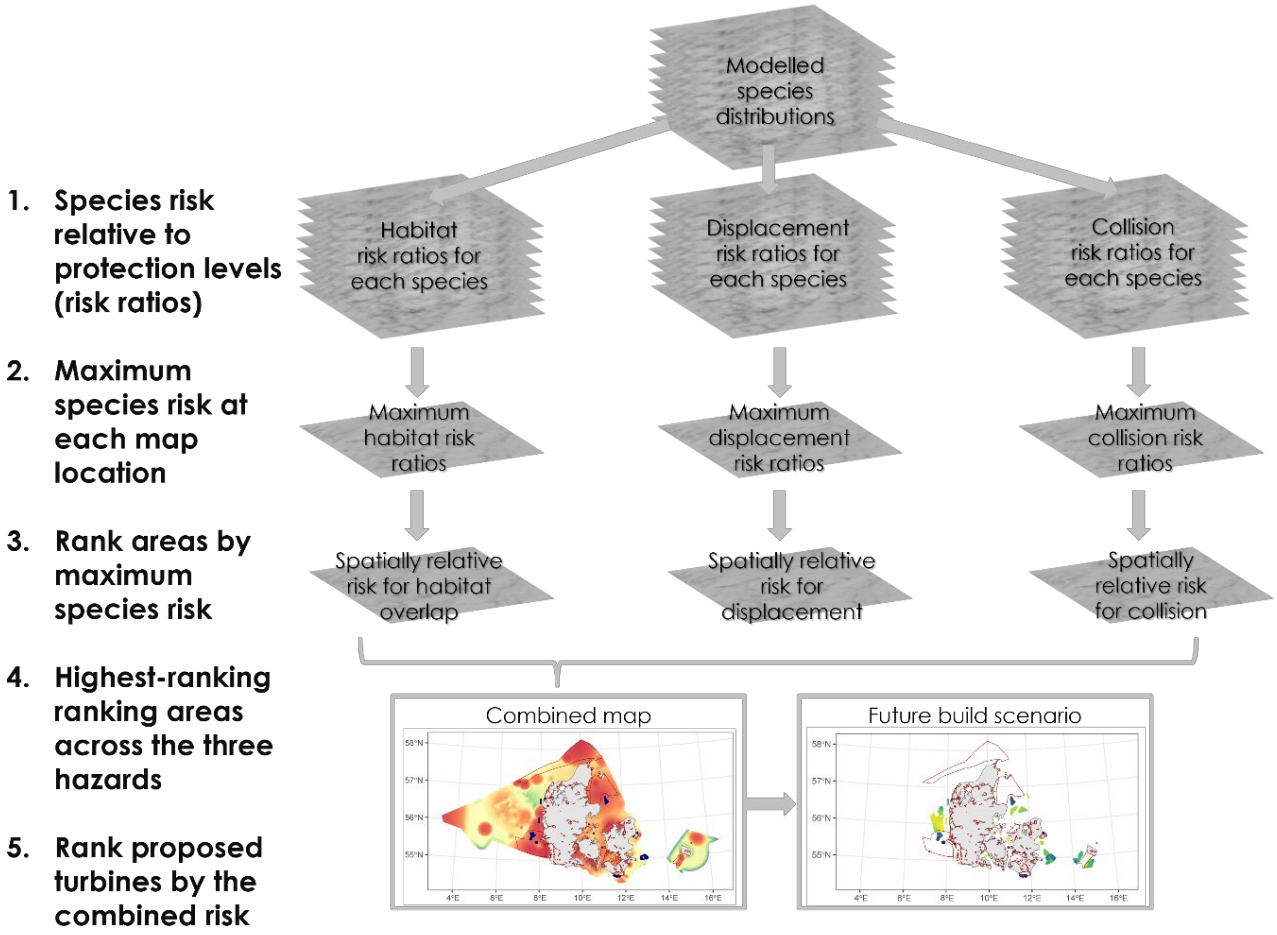

Figure 2.5. Overview of the spatial risk-ranking algorithm and key input parameters. The algorithm was applied to 17 species units, some of which combined ecologically similar species identifiable from aerial surveys (see **Table 2.1**).

2.2 Aerial survey data analysis

2.2.1 Modelled species and seasons

Spatial density distribution maps were estimated separately for 17 seabird species units, representing either individual species or species groups (**Table 2.1**). Ecologically similar bird species that are challenging to identify to species level from aircraft were grouped together. The groups included red- and black-throated divers (hereafter, divers), red-necked and great crested grebe (hereafter, grebes), common- and herring gull (hereafter, "grey gulls"), common-, arctic-, and sandwich terns (hereafter, terns), and razorbills and common guillemots (hereafter, alcids). For brevity, the 17 species and species groups (**Table 2.1**) are referred to as the modelled species units. Abbreviated species unit labels in figure legends are provided in **Table 2.1** (e.g., the two grey gull species are abbreviated to species unit "Gull"), but for additional clarity, more descriptive names are provided in tables and text where space allows.

For species units present in Danish waters year-round (grebes, fulmar, gannet, goldeneye, eider, common scoter, velvet scoter, merganser, grey gulls, great black-backed gull, kittiwake, alcids), two density surfaces were estimated, one combining data from winter and spring surveys and the other combining data from summer and autumn surveys. Hereafter, these two maps are termed "winter-spring" and "summer-autumn", respectively. Strongly seasonal species were estimated a single density surface but only

including data from seasons that the species units was considered present in Denmark (**Table 2.2**). This avoided introducing uncertainty to the static density distribution maps that was solely due to seasonal variation in presence-absence. For example, divers are almost totally absent during summer, and therefore only surveys from autumn, winter, and spring were included in the spatial analysis for this species unit.

Table 2.2. Definition of seasons and exclusion of species survey data within some of these. For strongly migratory species or species groups, survey data were excluded from seasons that the modelled species unit were a-priori determined as absent in Danish marine waters.

Season	Start date	Absent species units
Spring	1 March	
Summer	15 June	Divers, long-tailed duck, little gull
Autumn	15 September	Long-tailed duck, terns
Winter	15 November	LBBG, terns

2.2.2 Survey data sample size and coverage

Visual aerial surveys were used to collect data on seabirds using line transect Distance Sampling methods (Buckland et al., 2001). The dataset consisted of 352 aerial surveys from 299 different days between 1999-2025. The surveys covered 222,814 km of transect line, with each segment approximately 500 m long and up to 1000 m wide. Of the total 357,354 species detections, 324,409 were of the species selected for modelling in this project, and 310,819 of which were retained in analysis after a data validation exercise to account for any left-right bias indicating undue influence by sighting conditions, such as sun glare (Isojunno et al., 2025, Appendix 2 therein).

The surveys provided an extensive spatial coverage over Danish marine waters, though with lower effort in the offshore regions of the North Sea (**Figure 2.6**). Survey effort was concentrated in the winter and spring periods (**Figure 2.7**); the start date for each seasonal period (spring, summer, autumn and winter) is given in **Table 2.2**. The largest number of observations came from common scoter, common eider and the two grey gull species (N > 15,000) while the fewest observations were of lesser black-backed gull, little gull, and the grebe species unit (N < 3000) (**Table 2.1**, **Figure 2.8**).

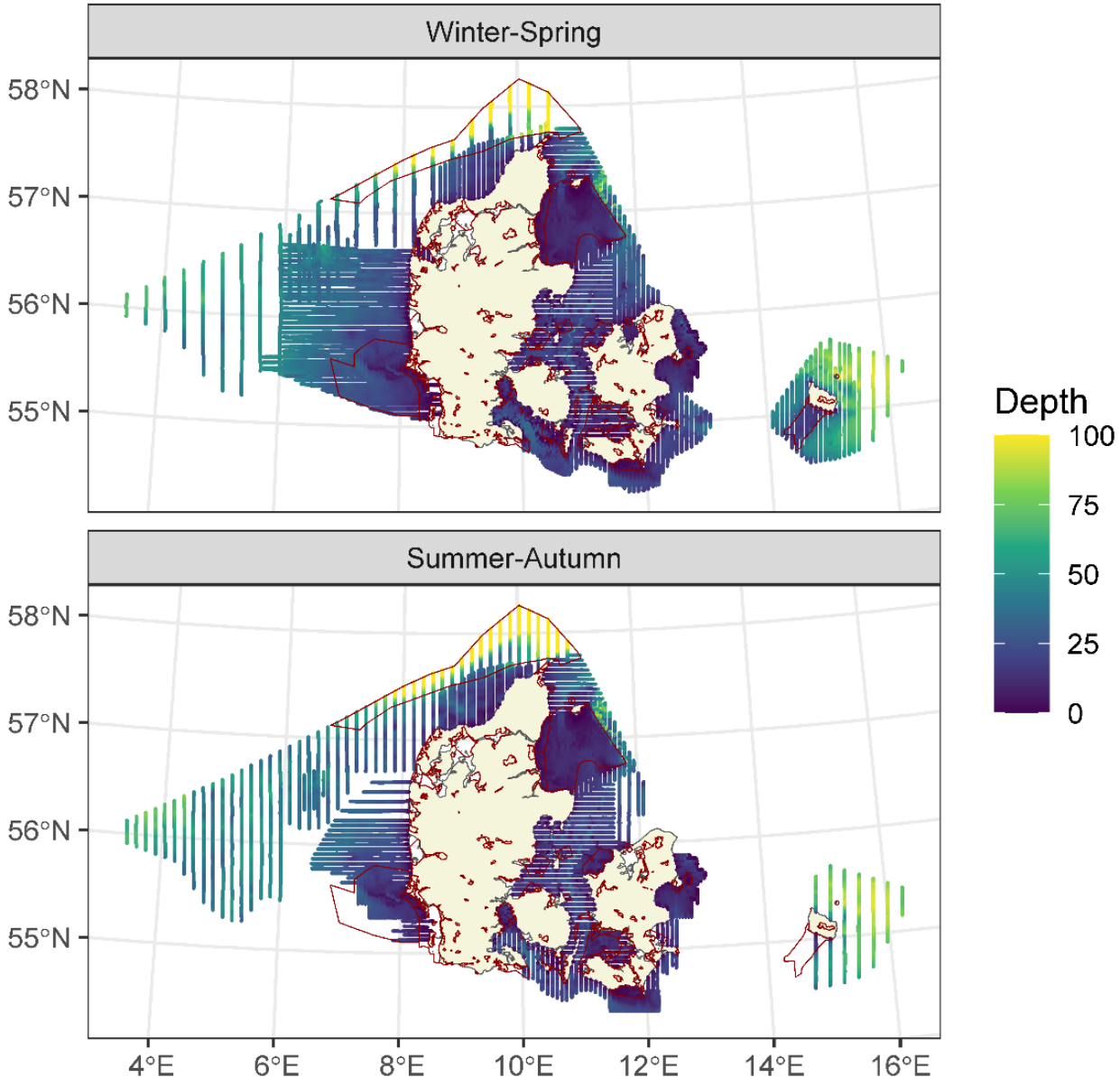

Figure 2.6. Spatial coverage of surveys by season. Each segment is coloured by the associated water depth. Seasons are defined in **Table 2.2**. Red polygons delineate SPAs, irrespective of species designation.

Figure 2.7. Temporal coverage of surveys by season and year. Seasons are defined in **Table 2.2**.

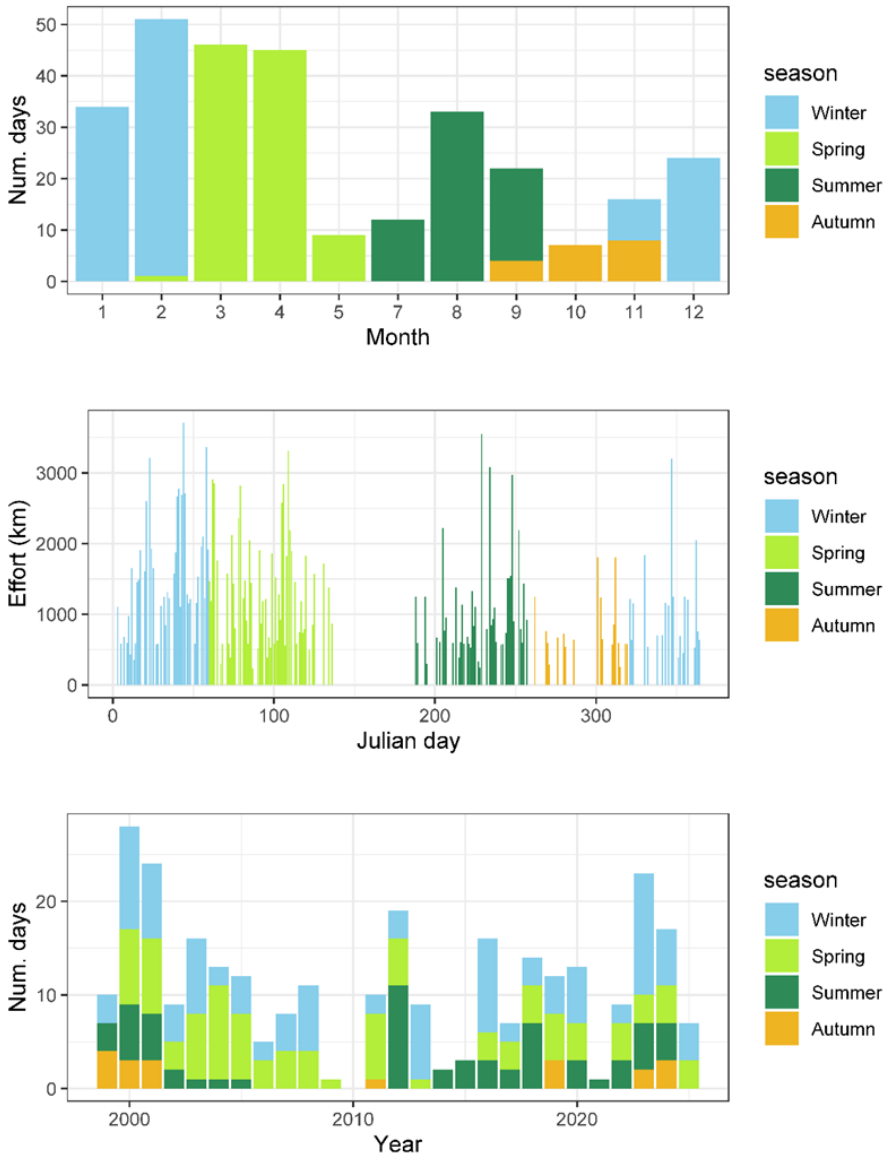

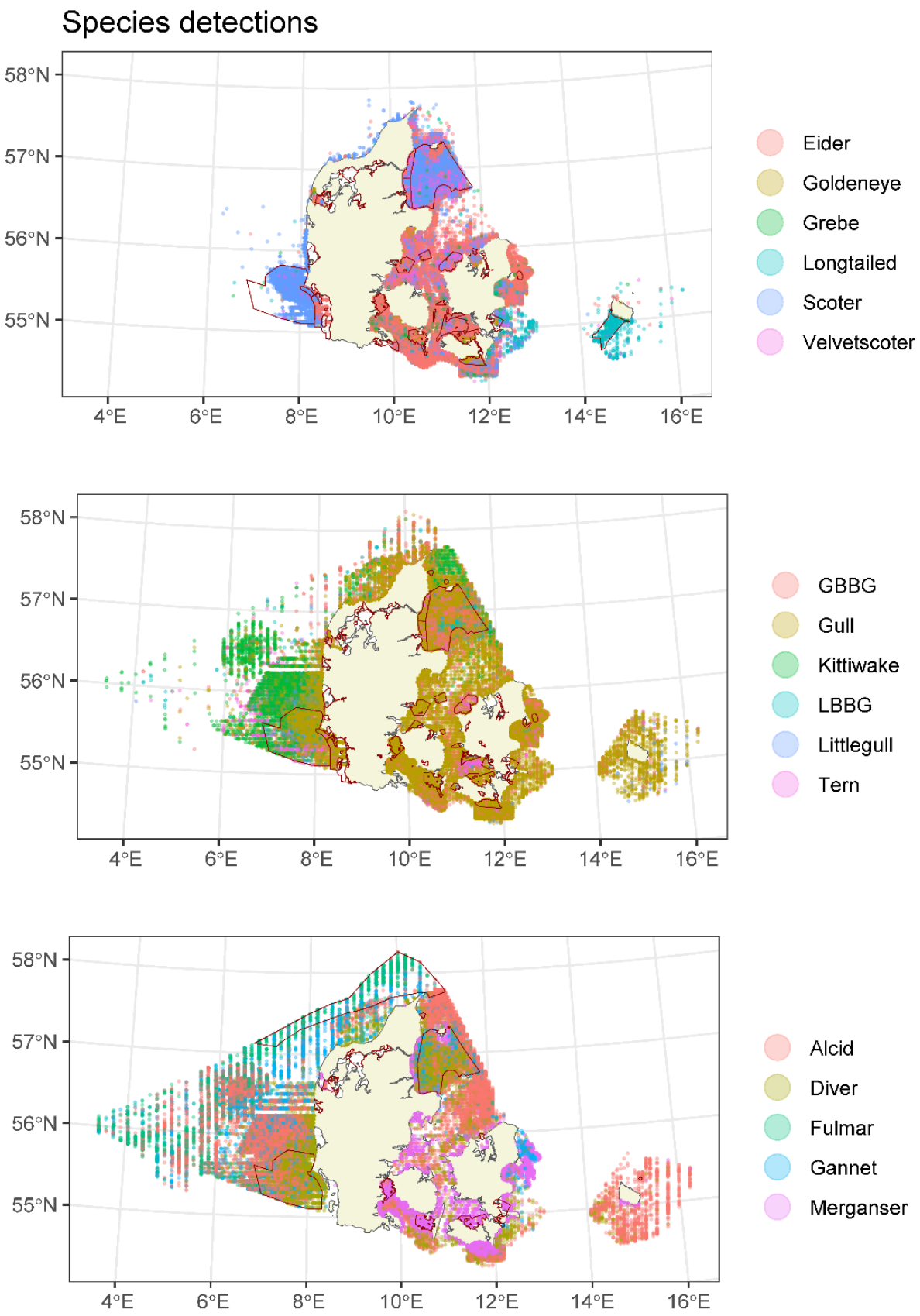

Figure 2.8. Spatial distribution of species detections, pooling surveys across all seasons and years. Species labels in the legend refer to modelled species units listed in **Table 2.1**. Most recent data are shown on top; though presented in transparent colour, species units with fewer detections may be hidden behind species with greater numbers of detections. A mix of colours indicates more balanced number of recent detections from different species units. Red polygons delineate SPAs designated for one or more species within each species unit in each panel.

2.2.3 Survey data modelling methods

The survey data modelling followed previously published methods (Scott-Hayward et al., 2023a), and are only briefly summarized here. For further details on the nationwide survey data analysis, we refer the reader to our previous report (Isojunno et al., 2025). A Distance Sampling analysis was carried out to estimate the number of birds in each survey segment given the distribution of observations relative to distance from the observers. The resulting count per unit area estimates, corrected for detectability, were then carried forward to a spatial analysis with the aim to estimate bird density for all Danish marine waters at 1 x 1km resolution. Candidate explanatory variables in the spatial analysis included water depth, distance to coast, and a two-dimensional term using geographic coordinates to account for surface patterns, which could result from unmodelled environmental variability. The count data were collected along survey lines in sequence, and so consecutive observations were likely to be correlated in space and time. With a spatial term included and limiting residual spatial correlation, any temporal autocorrelation in model residuals was accounted for by using robust standard errors as part of the modelling framework. Uncertainty was estimated using a parametric bootstrap (n=500), which propagated uncertainty through both the Distance Sampling and spatial analyses. All models were fitted using the MRSea R package (Scott-Hayward et al., 2023b; R Core Team, 2024) and were subject to various diagnostic checks (e.g. assessment of the assumed mean-variance relationship, a key assumption check).

The following updates were made to the analysis methods detailed in our previous report (Isojunno et al., 2025). Additional survey data were included to improve the spatial and temporal coverage of the data underpinning the sensitivity maps, and to allow the estimation of separate distributions for the winter-spring and summer-autumn periods for species units found in Denmark year-round (i.e., species units other than those listed in **Table 2.2**). Furthermore, survey data were time-weighted in the spatial analysis to represent the most recent distributions as the most relevant baseline for future scenario planning. The frequency weights were calculated as the inverse of the whole number of years between the survey date and a future date (1/year difference). The future date was set at 15th June 2026, thus ensuring that the calculation of year followed the beginning of the summer period, rather than the calendar year. The weights were then rescaled so that they would sum to the total sample size. The weights were selected to represent the uncertainty associated with potential distributional and abundance changes occurring on an annual basis, at an unknown rate. This assumed that as each year passed, the distribution and abundance could have made a step change from the previous year. Similar to a random walk, the distribution and abundance across years could be stationary, but the variance between the current and past year would increase in proportion to the number of years elapsed between them. Thus, the most recent year was allocated the highest frequency weight. The second-last year was allocated half of this maximum weight, the third-last year the third, and so on.

To evaluate potential shifts in distributions, two diagnostic maps were produced for each species unit: one representing the most recent distribution, and another representing a historical distribution (Appendix 2). The maps were based on the outputs of the distance analysis and therefore accounted for detectability, but without smoothing density estimates in space. To generate the maps, the distance-corrected density values for each species unit and survey segment were calculated time-weighted averages in 10 km hexagons. To

represent the most recent distribution, the weighted average was calculated based on the time weights described above (emphasizing the most recent data the most). To represent a historical distribution, the weights were reversed in time (emphasizing the oldest data the most). The reverse time weighting followed the same calculation as the forward weights, but measuring time difference to a set past date (15th June 1998).

Minor modifications were also made to the spatial analysis to improve spatial model fit to the data. First, to select suitable sets of radii, spatial heterogeneity was evaluated at the level of each survey campaign and then summarized at the scale of the national waters. This avoided issues with estimating suitable radii sizes at the national scale where the study area is discontinuous due to the presence of land in the middle of the prediction grid. Secondly, a larger number and more spatially spread-out candidate knot locations were provided to the algorithm to allow better coverage and more nuance in the resulting density surfaces.

3 Results

3.1 Aerial survey data analysis

Observer and group size were the most frequently selected covariates to explain detection probability (**Table 3.1**) for each species or species group that were modelled together as a species unit (**Table 2.1**). The northern gannet and common scoter were estimated with the highest probabilities of detection ($p > 0.3$) while grebes were estimated the lowest probabilities ($p < 0.2$). Unsurprisingly, given the large number of detections, after adjusting for detectability, the common eider and common scoter were estimated to be the most abundant species units in the area covered by the surveys (**Table 3.1**).

Spatial analysis results for each species unit are summarized in **Table 3.2**. Spatial estimates of counts, associated uncertainty, and model diagnostics are provided for each species unit in **Appendix 2**.

Table 3.1. Summary of distance analysis results. Key = shape of detection function (hr = hazard rate, hn= half-normal), P(d) = average detection probability, SE = standard error, GOF $\chi 2$= Chi-square goodness-of-fit test statistic, N_{det} = sample size of species unit detections included in the analysis. Species unit = short label indicating species or species groups that were analysed together as a unit (**Table 2.1**).

Species unit	Key	Covariates	Number of parameters	P(d)	SE x 100	GOF χ^2	N_{det}
Alcid	hr	~ Observer + Group size	10	0.208	0.13	0.79	23261
Diver	hr	~ Observer + Behaviour + Group size	14	0.207	0.20	0.39	12248
Eider	hr	~ Behaviour + Group size	4	0.252	0.11	6.47	68990
Fulmar	hr	~ Observer + Group size	12	0.268	0.57	0.69	3134
Gannet	hr	~ Observer + Group size	10	0.340	0.52	90.66	7333
GBBG	hr	~ Observer + Group size	17	0.238	0.31	0.76	7913
Goldeneye	hr	~ Observer + Group size	16	0.290	0.66	0.56	2806
Grebe	hn	~ Observer + Group size	6	0.199	0.35	1.53	2415
Gull	hr	~ Observer + Group size	22	0.258	0.14	3.30	52861
Kittiwake	hr	~ Observer + Group size	18	0.248	0.35	1.74	6418
LBBG	hr	~ Observer + Group size	10	0.227	0.98	0.02	1032
Littlegull	hr		2	0.215	0.42	0.00	2377
Longtailed	hr	~ Observer + Group size + Behaviour	12	0.224	0.20	0.67	11467
Merganser	hr	~ Observer + Group size + Behaviour	10	0.276	0.41	4.34	6574
Scoter	hr	~ Observer + Group size	24	0.305	0.12	57.46	87089
Tern	hr	~ Observer	4	0.225	0.38	0.00	4353
Velvetscoter	hn	~ Observer + Group size	14	0.246	0.23	55.33	7957

Table 3.2. Summary of spatial modelling results. Candidate models included 1-dimensional terms (water depth or distance to coast) both with and without 2-dimensionsal surface estimate (1D2D and 2D Only models, respectively). CV score = cross-validation score, Species unit = label indicating species or species groups that were analysed together as a unit (**Table 2.1**).

Species unit	Seasons	Best model	1D terms	Dispersion parameter	CV score	Abundance	Lower 2.5%	Upper 97.5%
Alcid	winter, spring	Best 1D2D	Dist. to coast	34.0	22.4	116252	101728	141612
Alcid	summer, autumn	Best 1D2D	Dist. to coast	63.0	58.5	198475	157895	276357
Diver	winter, spring, autumn	Best 1D2D		27.0	3.6	22388	20498	25625
Eider	winter, spring	Best 1D2D		337.5	2673.2	688238	639921	741801
Eider	summer, autumn	Best 1D2D		362.7	833.8	136635	116855	159169
Fulmar	winter, spring	Best 1D2D	Dist. to coast	148.8	2.3	36172	26137	55520
Fulmar	summer, autumn	2D Only		29.5	118.7	72394	62574	93221
Gannet	winter, spring	Best 1D2D		22.9	1.3	17817	14304	25721
Gannet	summer, autumn	2D Only		13.9	1.1	7684	6662	8944
GBBG	winter, spring	Best 1D2D	Dist. to coast	62.0	4.8	18128	11163	45542
GBBG	summer, autumn	Best 1D2D	Dist. to coast	27.1	2.4	13205	10998	16957
Goldeneye	winter, spring	Best 1D2D		368.4	16.9	33737	28539	40826
Goldeneye	summer, autumn	Best 1D2D		2204.9	2.1	590	394	1009
Grebe	winter, spring	Best 1D2D		101.3	0.8	4908	4370	5687
Grebe	summer, autumn	Best 1D2D		7.7	0.1	996	823	1261
Gull	winter, spring	Best 1D2D	Water depth	117.3	194.4	108445	94713	160815564
Gull	summer, autumn	Best 1D2D		145.6	134.1	100229	89806	123777
Kittiwake	winter, spring	Best 1D2D	Water depth	34.1	3.4	13900	11867	16612
Kittiwake	summer, autumn	Best 1D2D		66.9	6.0	8161	6167	12337
LBBG	spring, summer, autumn	Best 1D2D		33.2	0.9	4131	3449	5711
Littlegull	winter, spring, autumn	Best 1D2D	Dist. to coast	148.8	1.9	1778	1530	2341
Longtailed	winter, spring	Best 1D2D		29.4	41.5	32773	28678	40003
Merganser	winter, spring	Best 1D2D		39.8	6.8	20042	18147	22864
Merganser	summer, autumn	Initial Model		511.1	1.3	2196	1375	3465
Scoter	winter, spring	Best 1D2D		523.3	7782.7	419003	375095	462942
Scoter	summer, autumn	Best 1D2D	Dist. to coast	223.1	1864.6	167431	150662	212626
Tern	spring, summer	Best 1D2D	Dist. to coast	38.0	9.0	7897	6995	9662
Velvetscoter	winter, spring	Best 1D2D		54.6	15.6	52439	46836	60755
Velvetscoter	summer, autumn	2D Only		218.7	20.0	17151	12437	26744

3.2 Expert-elicited input parameters

Application of the bootstrap procedure to the expert-elicited parameters resulted in a distribution of estimates for each input parameter (**Figure 3.1**). Some of these distributions showed bimodal distributions, such as the displacement rate for the divers. This indicated that the experts did not converge towards a single mean consensus value for this parameter, but rather there was divergence in expert judgements. For bimodal (or multimodal) distributions, summary statistics aiming to represent a single best estimate or central tendency for the distribution (such as mean or median) can be misleading. We have therefore elected not to present a table of best estimates for the input parameters. To account for the varying shape of the input parameter distributions, all the risk analysis outcomes presented in the report are based on bootstrap sampling from the input parameter distributions.

For collision rate, the bootstrapped distributions indicated wide confidence intervals for the most at-risk species (grey gulls, GBBG, LBBG, kittiwake, little gull) (**Figure 3.1**). That said, the distributions did not overlap with the species least at risk, such as divers and grebes. As well as high displacement rates, these species had relatively low proportion of time at the rotor-swept zone (≤0.3). Without flight speed, there was good concordance between the proxy collision rate and collision rates obtained from the collision risk modelling, both in terms of relative and absolute magnitude (**Appendix 3**, **Figure A3.2**). The inclusion of flight speed made relatively little difference to the proxy collision rate (**Appendix 3**, **Figure A3.1**), and therefore the proxy collision rate carried forward to the risk analysis was implemented without this parameter.

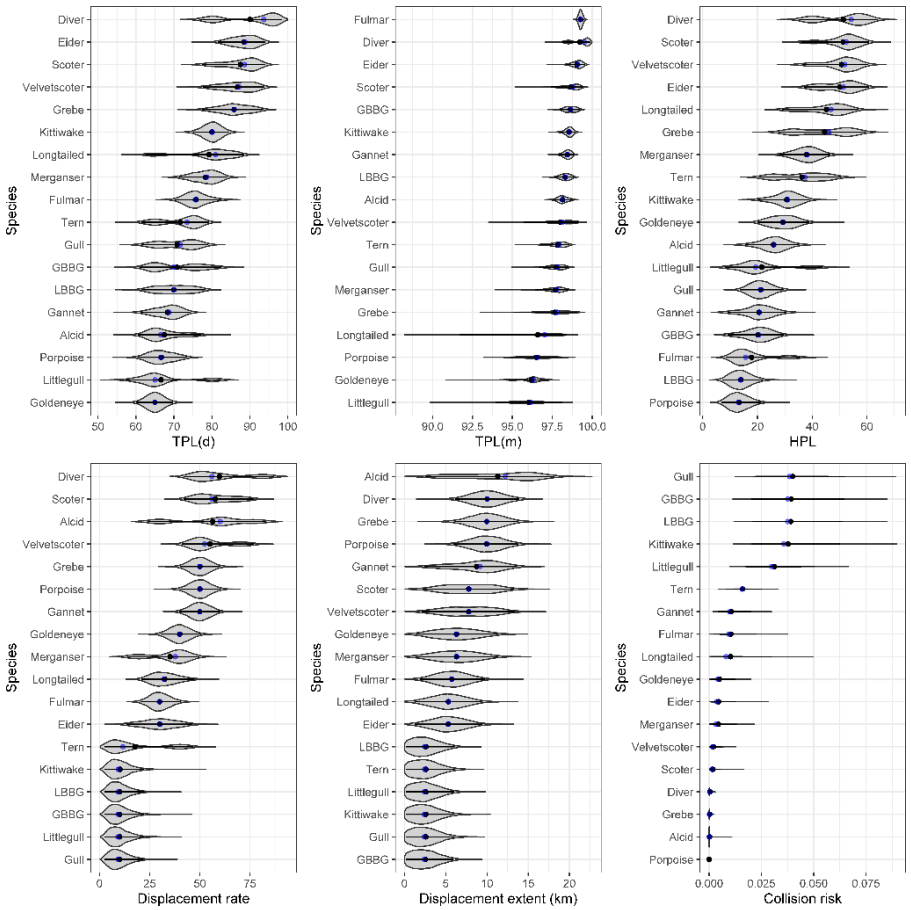

Figure 3.1. Distribution of input parameter values obtained through bootstrapping of the expert-elicited parameters. The violins represent the density distribution of each bootstrapped parameter distribution. The width of the violins are standardized across species (y-axis) and only show relative density distribution as a function of the parameter value (x-axis). Blue dots show medians, and horizontal black lines 95% confidence interval. Note that the y-axis ordering is based on the median values for each parameter and thus will be different for each panel. Modelled species within each species unit and associated labels are listed in **Table 2.1**. For example, "Gull" refers to the two "grey gull" species, herring and common gull.

3.3 Relative risk-mapping

Habitat overlap: The spatially relative species risk for habitat alteration, quantified as overlap, was the highest for species units with geographically narrow distribution ranges in inshore areas (**Figure 3.2**, **Table 3.3**). The highest-ranking areas for habitat risk matched areas with SPAs designated for the modelled species (**Figure 3.2**, **Figure 3.3**) indicating that the SPA designations successfully captured the high-use areas for these species. In areas identified as highest risk, species units that were most at risk from habitat overlap included divers, common scoters, eiders and velvet scoters (**Figure 3.4**). Comparing the lowest-risk areas to the highest-risk, the relative risk of habitat overlap was reduced substantially for all species, ranging from >95% reduction for 10 species units, to 72% and 60% reduction in the average risk ratio for the common scoter and alcid species (**Figure 3.5**, **Table 3.3**). The spatial distribution of habitat risk was relatively stable across seasons (**Figure 3.6**).

Displacement risk: The highest relative risk areas for displacement were found inshore (**Figure 3.2**), similar to habitat risk. Species units most at risk from displacement included divers, grebes, common scoters, and velvet scoters (**Figure 3.4**). Divers maintained their position as the highest-ranking species unit for displacement in the lowest-ranking areas, though the average risk ratio value was 47% lower than in the highest-ranking areas (**Figure 3.5**, **Table 3.3**). There was variation in the risk ratio reduction across species, suggesting that selecting the lowest-ranking areas from the combined map would be more effective in reducing the risk of displacement of some species (e.g., long-tailed duck, 88%) than others (e.g., alcids, 36%). Displacement risk ratios obtained the highest values during the summer and autumn. The spatial distribution of displacement risk was more concentrated during summer and autumn than during the winter and spring periods (**Figure 3.6**).

Collision risk: The collision risk map identified several potential hotspots of relative risk further offshore, especially in the northernmost part of the study area (**Figure 3.2**). The species that obtained the highest average risk ratios from collision included the GBBG, LBBG, kittiwake, and grey gulls (**Figure 3.4**), which were the top four species units at risk of collision both in the highest- and lowest-ranking areas. However, the average collision risk ratios for these species was 39-72% lower in the lowest-ranking areas compared to the highest-ranking areas in the combined map (**Figure 3.5**, **Table 3.3**). Collision risk ratios for the most at-risk species obtained the highest values during the summer, though the spatial distribution of collision risk was relatively stable across seasons (**Figure 3.6**).

Combined map: The final output of the spatial risk-ranking algorithm (**Figure 3.7**, top panel) combined the highest-ranking areas across the three hazards (i.e., the three panels in **Figure 3.2**). Combining the three spatially relative risk maps by their maximum value, the combined map identified only two areas that ranked in the lowest 33% across all three hazards, namely the offshore waters southeast of Thyboron in the North Sea and waters around Bornholm in the Baltic Sea (**Figure 3.5**). Furthermore, the identification of these areas contain uncertainty. Only a small number of grid cells were consistently identified in the lowest 33% quantile across all three hazards. For example, only 14 km^2 total area was identified in the bottom tertile 95% of the time (n=500 bootstraps). Lowering the threshold for correct identification to 90% (conversely, increasing the chance of misidentification to 10%), the lowest-risk area would increase to 80 km^2. On the other hand, much larger areas could be consistently identified as ranking in the top and bottom 50% across the three hazards with 95% confidence (**Figure 3.8**).

Figure 3.2. The relative risk for habitat overlap, displacement, and collision, expressed as the maximum risk ratio across species units. The maximum relative species risks were obtained as the maximum risk ratios for each grid cell in Step 2 of the algorithm (**Figure 2.5**) across all modelled species units (individual species or species groups modelled together **Table 2.1**). Existing wind turbines are shown in blue. Red polygons delineate SPAs, irrespective of species designation.

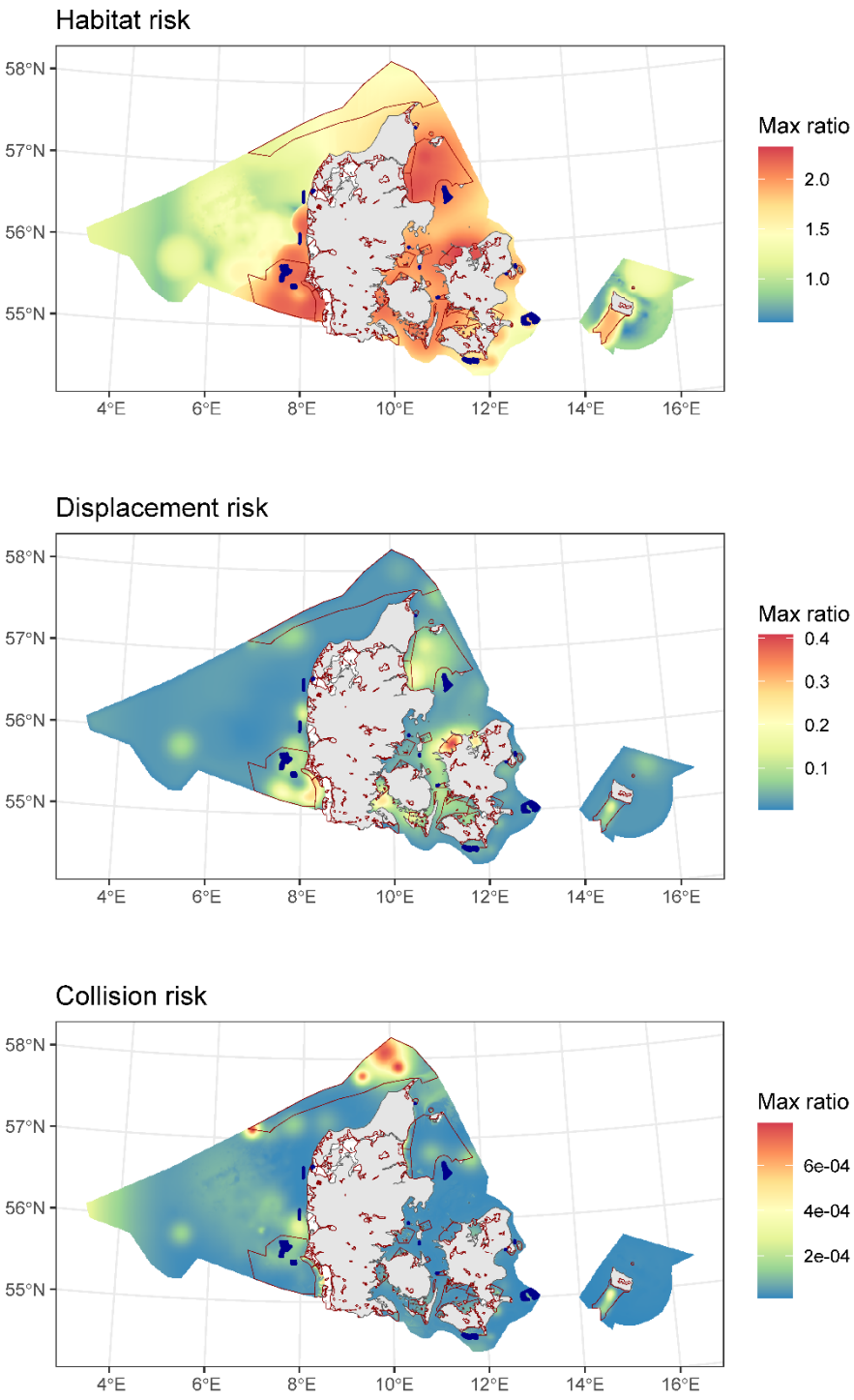

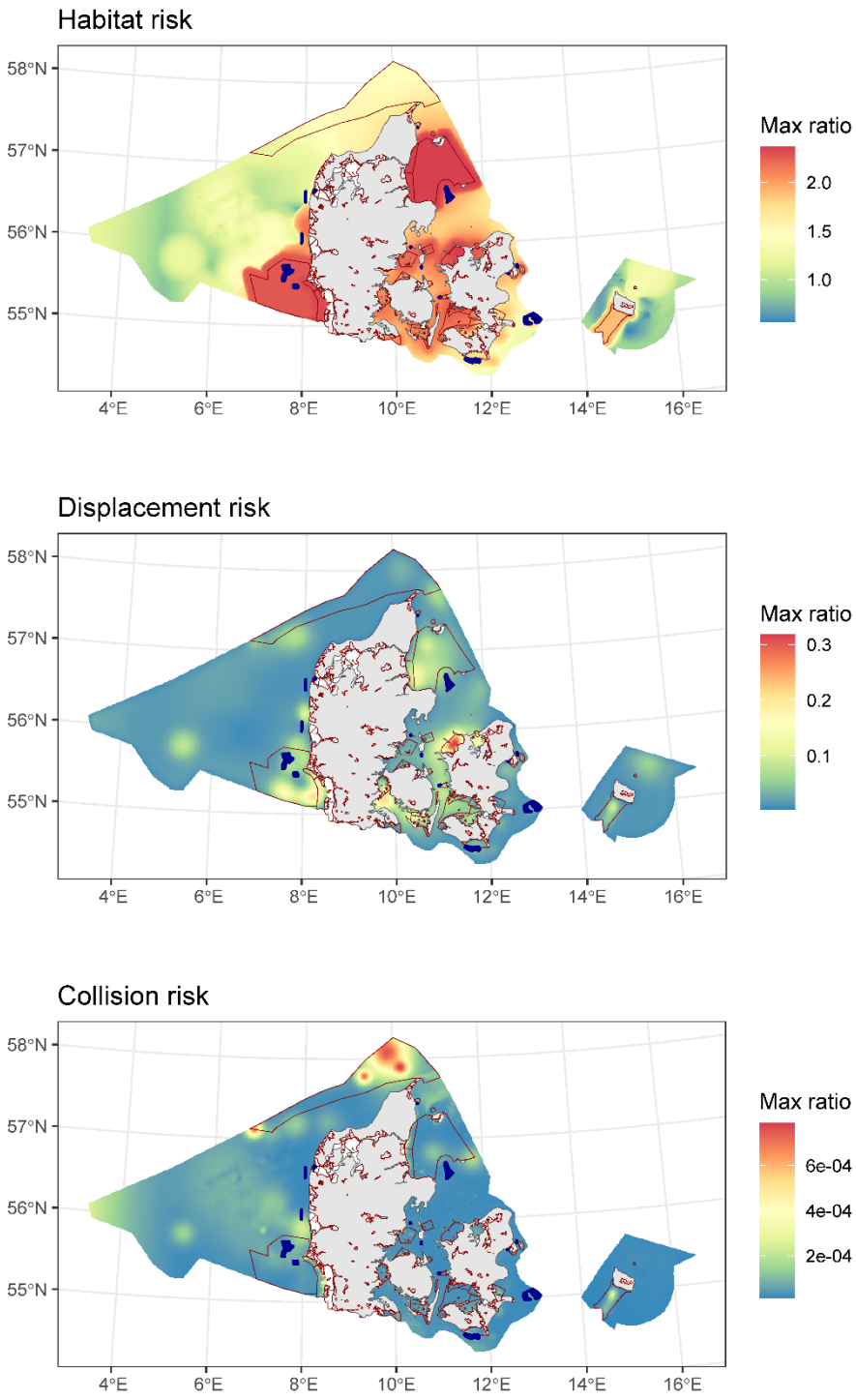

Figure 3.3. The relative risk for habitat overlap, displacement, and collision, expressed as the maximum risk ratio across species, when including SPA designations in the algorithm. In this version of the risk map, the species-unit-specific habitat risk ratio was set to the maximum of the species unit when within SPA designated to that species. Furthermore, abundance within SPAs was assumed to count towards the target protection levels for displacement (TPLd) and mortality (TPLm) for each species unit with designations (Section 2.1.3). Existing wind turbines are shown in blue. Red polygons delineate SPAs, irrespective of species designation.

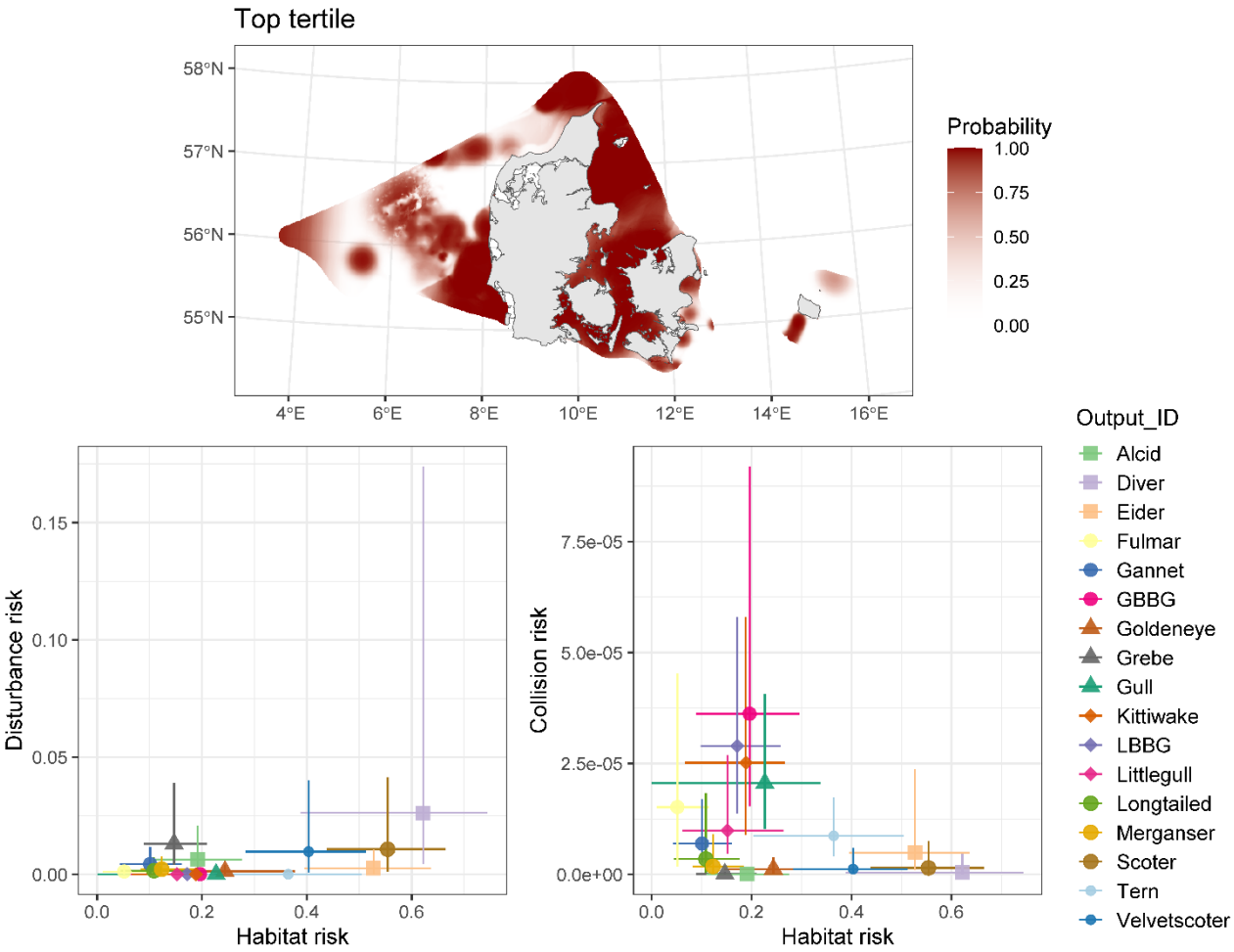

Figure 3.4. Areas identified as the highest spatial relative risk to species for each of the three hazards combined (top panel) and associated risk ratio values for each species unit (bottom panel). The probability that a location was ranked in the top tertile for at least one of the three hazards was estimated as a proportion from 500 bootstrap iterations. Average risk ratios are shown for areas in the combined map (**Figure 3.7**, top panel) that exceeded the third tertile (67% quantile), with symbols showing best estimates and lines 95% confidence intervals from the bootstrap (**Table 3.3**). Species labels in the legend represent modelled species units (individual species or species groups modelled together) listed in **Table 2.1**. Edges of the study areas are not shown, defined as grid cells with more than third of neighbouring grid cells <25 km falling outside the study area. This was done to remove bias in displacement risk estimates in edge areas where the number of birds outside the study area is not known.

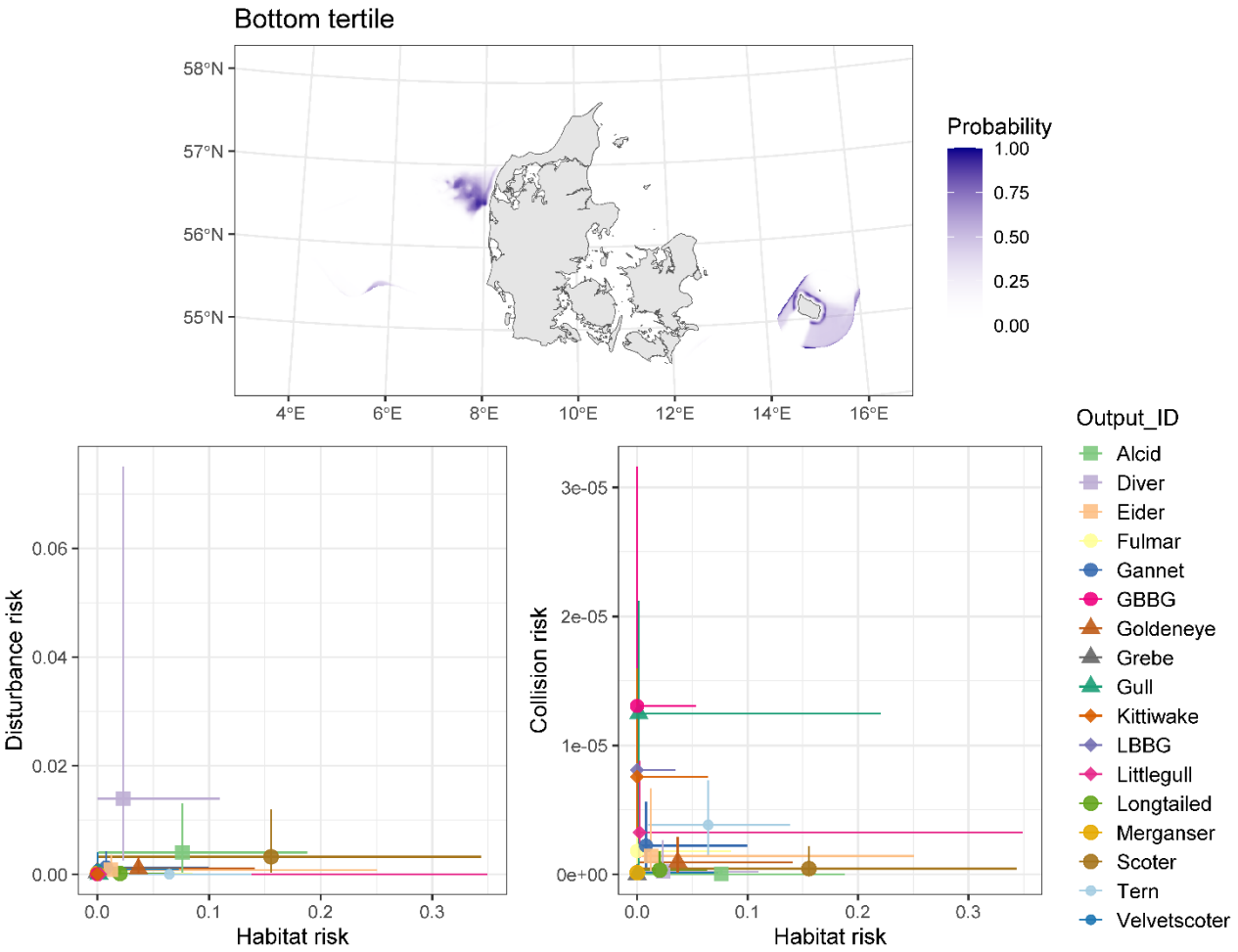

Figure 3.5. Areas identified as the lowest spatial relative risk to species for each of the three hazards combined (top panel) and associated risk ratio values for each species unit (bottom panel). The probability that a location was ranked in the bottom tertile for all the three hazards was estimated as a proportion from 500 bootstrap iterations. Average risk ratios are shown for areas in the combined map (**Figure 3.7**, top panel) that were below the third tertile (33.33% quantile), with symbols showing best estimates and lines 95% confidence intervals from the bootstrap (**Table 3.3**). Species labels in the legend represent modelled species units (individual species or species groups modelled together) listed in **Table 2.1**. Edges of the study areas are not shown, defined as grid cells with more than third of neighbouring grid cells <25 km falling outside the study area. This was done to remove bias in displacement risk estimates in edge areas where the number of birds outside the study area is not known.

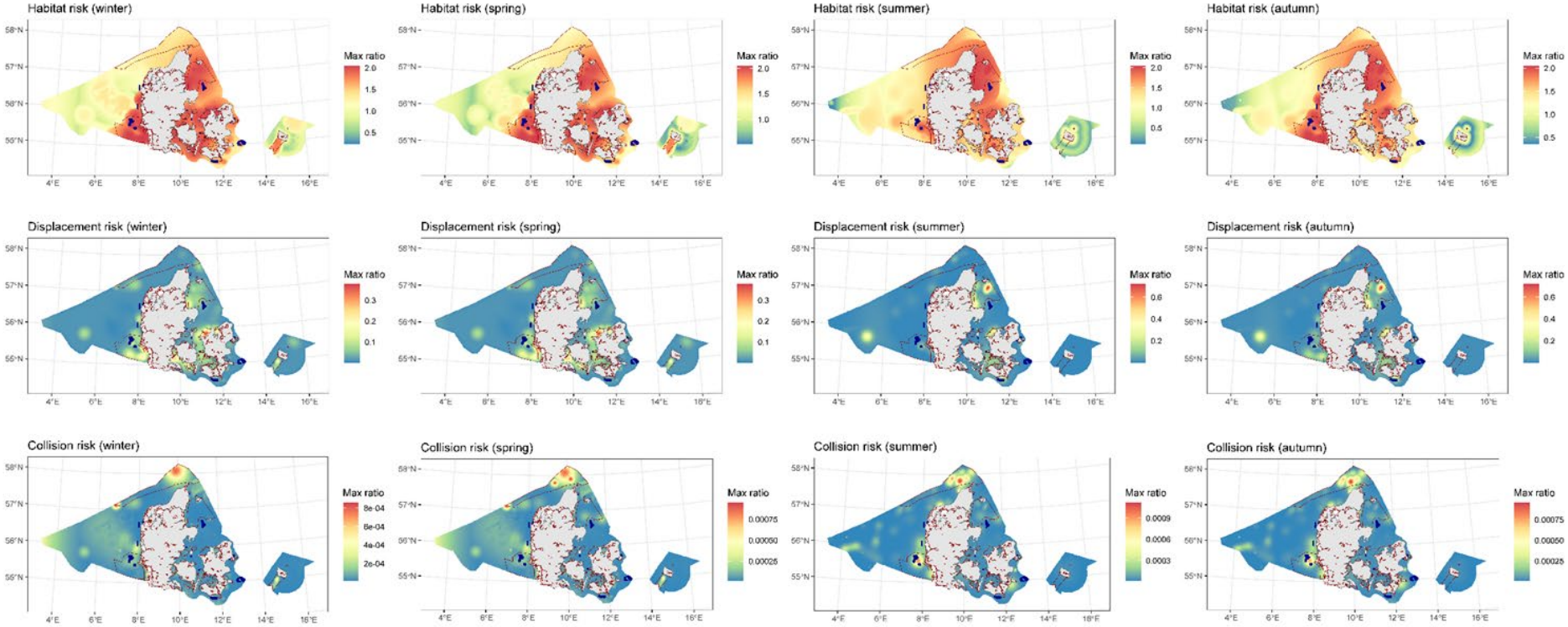

Figure 3.6. A comparison of risk ratios between different seasons. Risk ratios for each hazard are provided in each row, while the four columns represent the different seasons. Each seasonal map excludes species that are absent in Danish marine waters in that season (Table 2.2). For species present in Danish marine waters year-round, the seasonal risk ratio maps also reflect any changes in the estimated density distribution between winter-spring and summer-autumn.

Figure 3.7. The main output of the spatial risk-ranking algorithm with associated uncertainty (top and middle panels) and average number of species units that exceeded HPL thresholds (bottom panel). Top: the combined spatially relative risk map, showing the highest-ranking areas across the three hazard maps (habitat overlap, displacement, collision). The combined map represents the final output of the spatial-risk-ranking algorithm (**Figure 2.5**). Middle panel: coefficient of variation (CV) across 500 re-draws of the combined map based on bootstrapped count estimates. Bottom panel: the average number of species units that exceeded the HPL threshold over 500 bootstraps. Existing wind turbines are shown in blue. Red polygons delineate SPAs, irrespective of species designation.

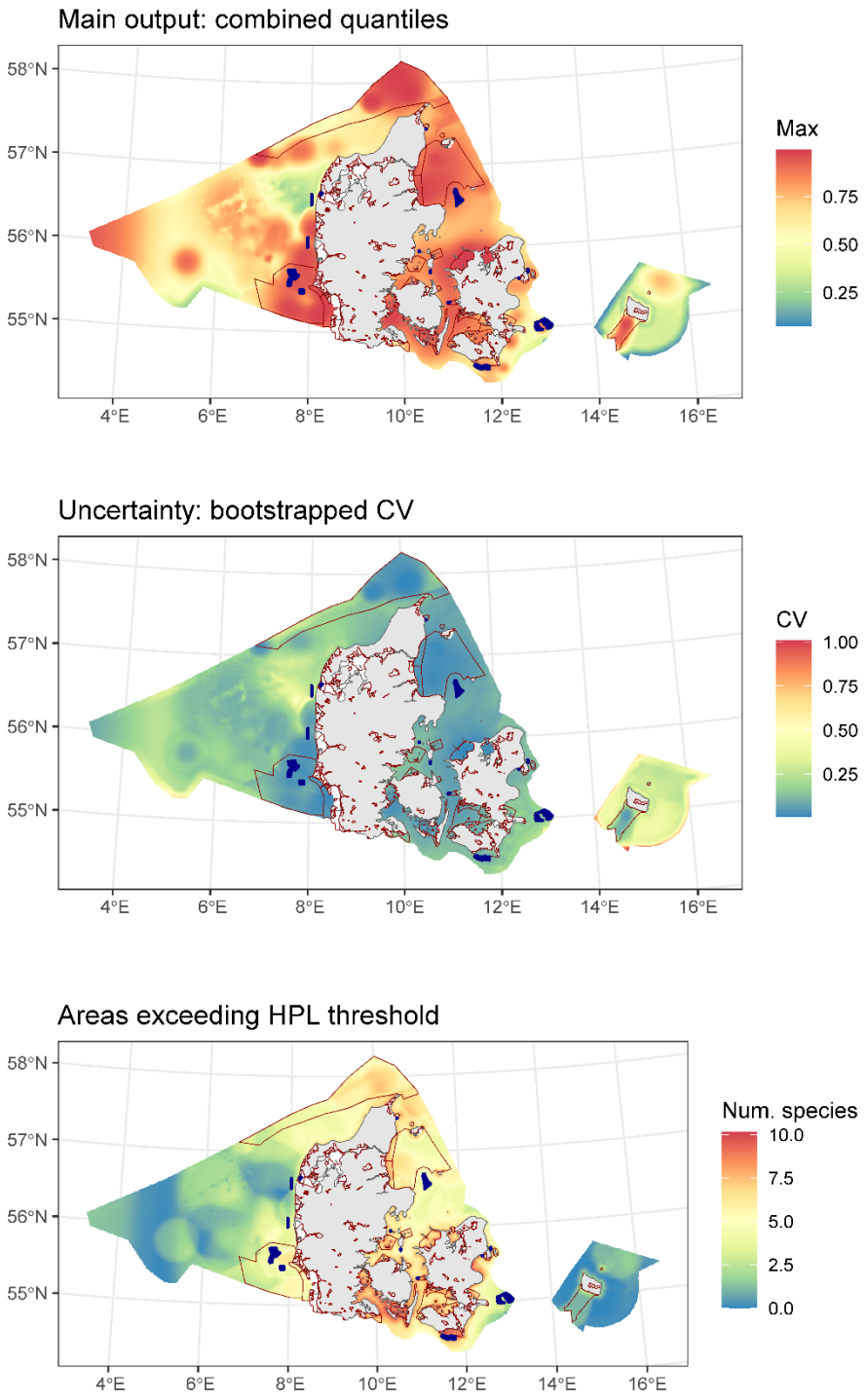

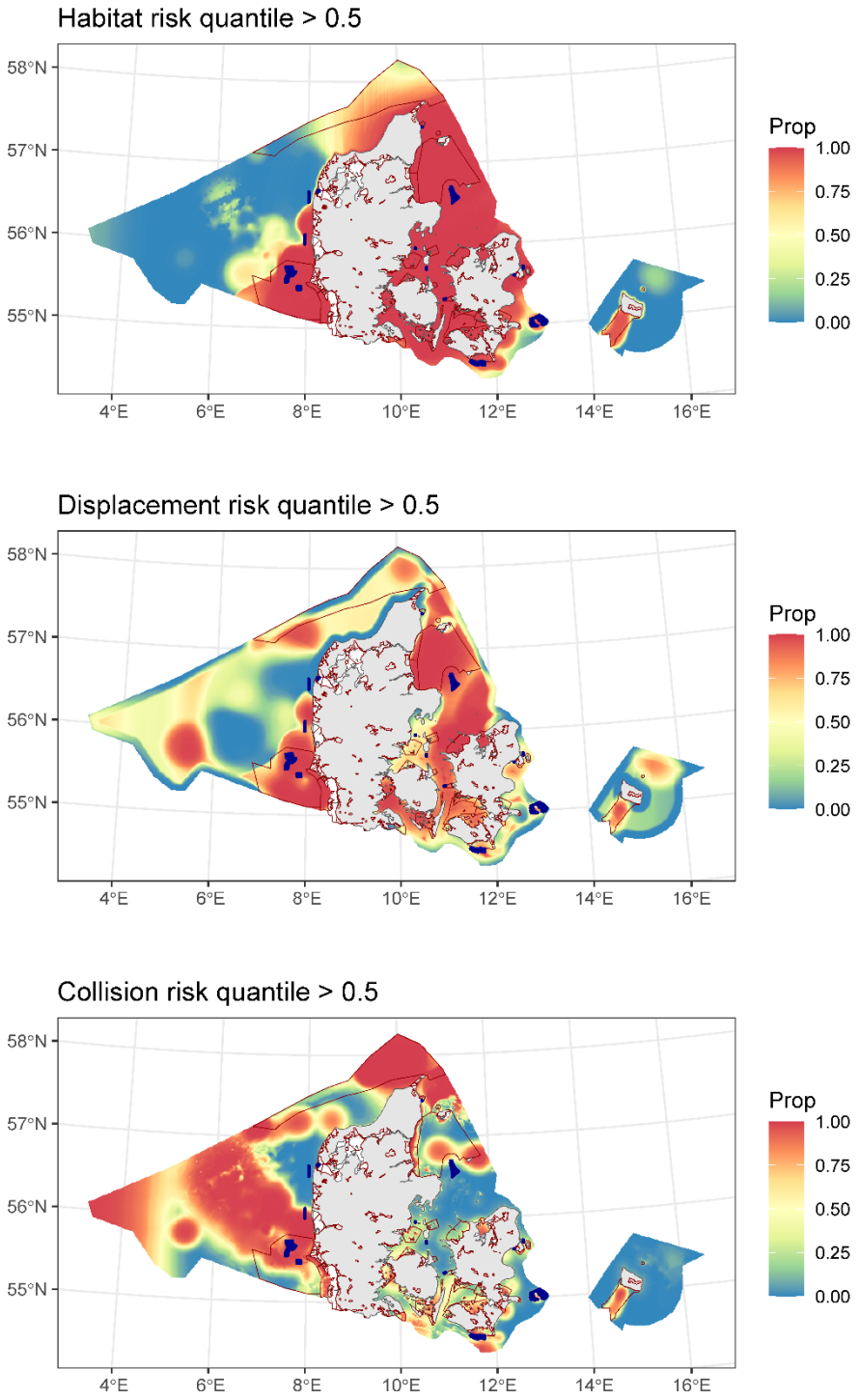

Figure 3.8. Proportion of bootstrapped risk maps that exceeded 50% quantiles for each hazard. The red areas can be interpreted as high confidence in the ranking of marine areas as higher risk than other areas in terms of habitat overlap, displacement and collision, respectively. Existing wind turbines are shown in blue. Red polygons delineate SPAs, irrespective of species designation.

Table 3.3. Summary of risk-mapping results. For each species unit the range is shown, defined as the area with 95% of abundance, and the area covered by SPAs designated for one or more species in the unit (% of prediction grid). Average risk ratios for each species and hazard are shown for areas in the combined map that exceeded the third tertile (67% quantile), with best estimates and 95% confidence intervals derived from the medians and 95% percentiles of 500 bootstrap iterations. Risk ratios were multiplied by 100 (habitat and displacement risk) or 10,000 (collision risk) to increase readability of small values. Species unit = species or species groups that were analysed together as a unit (**Table 2.1**).

Species unit	Species range (% of study area)	Species range (km^2)	SPA area (% of study area)	Average risk ratios (RR) in the top-ranking area			Reduction in average RR in the lowest-ranking area (%)		
				Habitat (RR x100)	Displacement (RR x100)	Collision (RR x 10,000)	Habitat	Displace-ment	Collision
Divers	33.1	34013	10	62.2 (74.5, 38.8)	2.62 (17.4, 0.44)	0 (0.05, 0)	96.2	46.8	43.9
Common Scoter	17.9	18336	11	55.4 (66.5, 43.8)	1.08 (4.14, 0.11)	0.01 (0.07, 0)	71.9	70	69.5
Eider	18.8	19249	9	52.7 (63.7, 39.5)	0.26 (1.07, 0.02)	0.05 (0.24, 0.01)	97.7	69.2	70.7
Velvet scoter	13.8	14146	6	40.4 (51.3, 28.3)	0.97 (4.02, 0.07)	0.01 (0.06, 0)	99.9	90.3	89.6
Terns	24.1	24691	9	36.5 (50.5, 20.4)	0.01 (0.1, 0)	0.09 (0.17, 0.04)	82.3	55.7	55.9
Goldeneye	31.8	32697	2	24.4 (37.8, 14.6)	0.13 (0.41, 0.01)	0.01 (0.04, 0)	84.9	19.8	18.8
Grey gulls	24.5	25176	0	22.7 (33.8, 0)	0.01 (0.05, 0)	0.21 (0.41, 0.1)	99.3	45.4	39.4
GBBG	18	18494	0	19.7 (29.7, 8.9)	0.01 (0.07, 0)	0.36 (0.92, 0.15)	100	65.9	63.9
Alcids	18.5	18997	0	19.2 (27.6, 10.9)	0.63 (2.07, 0.04)	0 (0, 0)	60.3	36.4	25.9
Kittiwake	21.1	21702	0	18.9 (26.8, 6.7)	0.01 (0.07, 0)	0.25 (0.58, 0.09)	100	70.6	69.9
LBBG	21	21590	0	17.2 (25.9, 9.9)	0.01 (0.06, 0)	0.29 (0.58, 0.14)	100	72.6	72.1
Little gull	11.6	11957	6	15.2 (26.5, 6.2)	0.01 (0.05, 0)	0.1 (0.27, 0.05)	98.5	67.2	67.2
Grebes	5.9	6055	1	14.7 (21, 8.9)	1.31 (3.9, 0.4)	0 (0.01, 0)	100	97.5	97.7
Merganser	9	9204	1	12.3 (18.5, 8.3)	0.22 (0.76, 0.01)	0.02 (0.09, 0)	100	91.6	92.5
Long-tailed duck	3.4	3533	1	10.9 (17.7, 4.5)	0.16 (0.73, 0.01)	0.03 (0.18, 0)	81.2	88.2	90.5
Gannet	16.6	17068	0	10.1 (16.2, 4.4)	0.43 (1.18, 0.02)	0.07 (0.17, 0.03)	92.1	70.8	67.9
Fulmar	7.3	7477	8	5.2 (11.5, 1)	0.12 (0.41, 0.01)	0.15 (0.45, 0.02)	100	88.3	88

3.4 Cumulative risks

Development scenarios: To create cumulative development scenarios, proposed future turbine locations (N=1,045) were ranked according to their combined risk quantile (**Figure 3.7**, top panel). Each turbine was then allocated a future installation year according to this rank, with approximately 50 turbines installed annually. This created an installation schedule that prioritized developments in the lowest-risk areas to seabirds (**Figure 3.9**). Existing turbines were incorporated in the development scenario based on their actual commission year.

Cumulative risk: Given the existing and hypothetical future installation schedule, cumulative risk was evaluated as magnitude increases in relative risk ratios as more turbines are installed over time. Thus, steeper curves can be interpreted as more rapid accumulation of risk. These cumulative risk curves are presented for each species unit and hazard separately (**Figure 3.10**, **Figure 3.11**, **Figure 3.12**). We make comparisons of cumulative risk and associated uncertainty between three main development scenarios (**Table 3.4**): current developments, including turbines from wind farms commissioned between the years 2000 and 2021; 50% development scenario, including the current turbines and 50% of the proposed future installations; and 100% development scenario, including the current and proposed future installations.

Given a particular development scenario, it is possible to compare the magnitude differences in relative risk both within species and across hazards, bearing in mind that these comparisons are contingent on the target protection levels. This is why each cumulative risk curve is paneled by the target protection level relevant to each hazard (habitat risk, HPL; displacement risk, TPLd; collision risk, TPLm). The relative risk values are generally expected to be greater in the panels representing higher protection levels, because they reduce the allowable levels of risk in the denominator of the risk ratio. However, when the development scenario overlaps with the core area of the species unit (habitat risk), or species density hotspots (displacement, collision risk), then the expected level of risk in the numerator will increase the risk ratio. For example, the long-tailed duck was not amongst the species with the highest target protection levels, yet the cumulative risk curves indicate higher relative habitat and displacement risk from the future development scenarios than most other species (**Figure 3.10**, **Figure 3.11**). Similarly, the cumulative risk curve for the little gull increased rapidly between the 50% and 100% development scenarios, despite relatively low TPLm for this species unit. This indicates that the future development areas coincide with the core areas and density hotspots for these species (**Figure 3.12**). Furthermore, species with high rates of displacement and collision will increase the influence of the numerator on the relative risk ratio. As an example, while the kittiwake had a lower TPLm than divers, the much higher collision rate (**Figure 3.1**) will increase the expected levels of risk for kittiwake and thus higher risk ratio for collision (**Figure 3.12**).

The influence of the target protection levels was also highlighted when comparing different versions of the cumulative risk analyses that made different assumptions about the effectiveness of SPAs to protect designated species. When SPA-based protections were allowed to contribute to the target protection level of designated species, displacement risks were reduced substantially relative to targets for divers, grebes, common and velvet scoters, and the longtailed duck (**Figure 3.13**). SPA designation also reduced the collision risk ratio for the little gull (**Figure 3.13**). With respect to species unit abundance,

SPA designations were estimated to protect common scoters the most, followed by velvet scoters, the longtailed duck, and little gull (Figure 3.14). This version of the risk analysis assumed 100% protection within SPA designated areas, but outside existing or planned development areas.

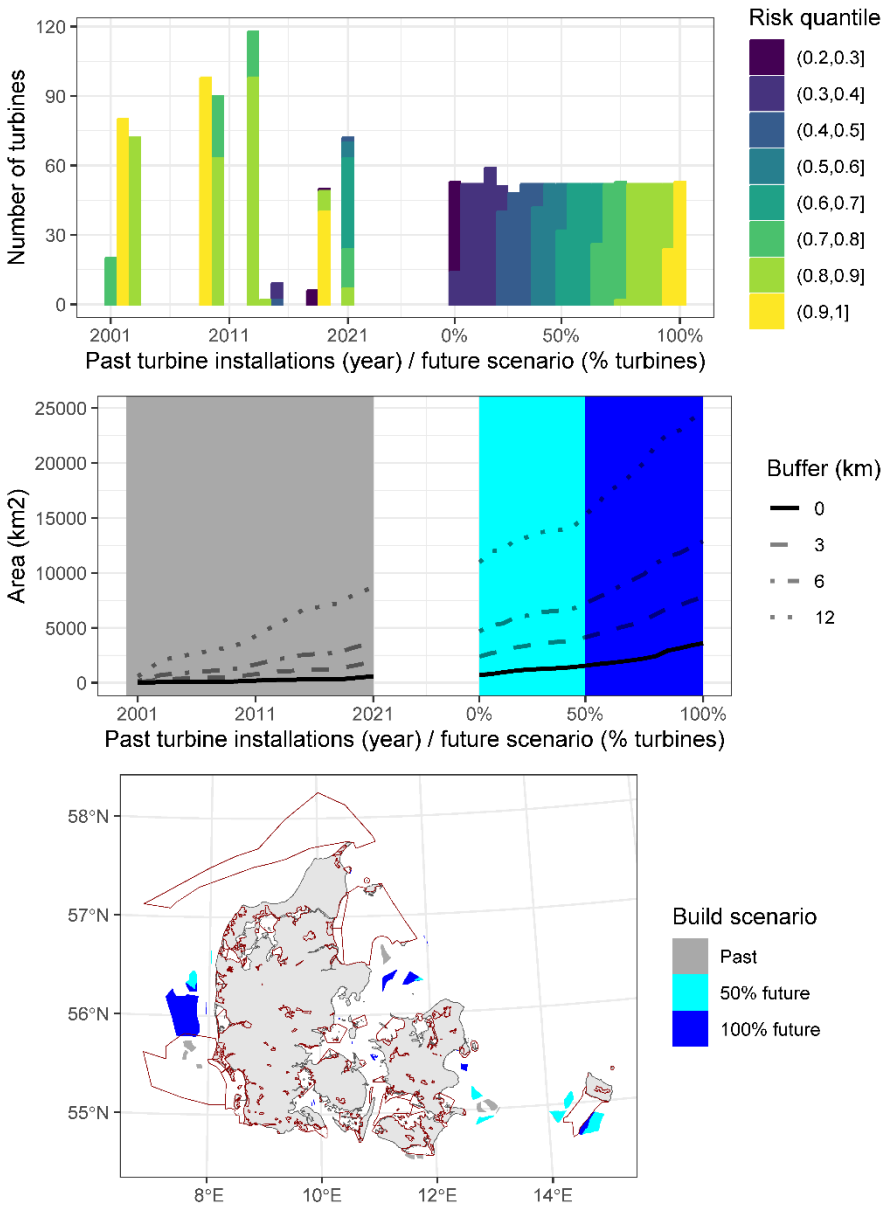

Figure 3.9. An illustration of the development scenario used to estimate cumulative risk. The top panel shows the annual number of turbines installed over time, colour-coded by the spatial risk ranking from the combined map (**Figure 3.7**). Turbines up to year 2021 were included according to their actual commission year, while proposed future locations for wind turbines were assigned an installation priority according to the spatial risk ranking. The middle panel shows the cumulative increase in the footprint of the development area, with and without different buffer zones around the footprint. Lighter and darker blue colours in the middle and lower panels show future scenarios where 50% vs 100% of the proposed turbines are installed, respectively.

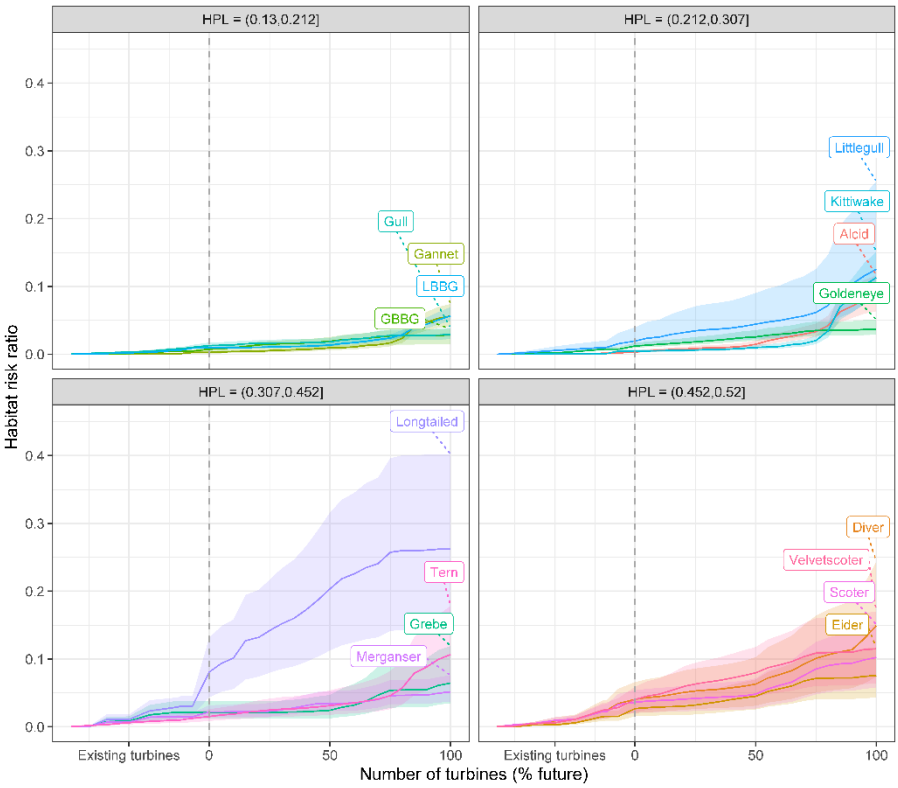

Figure 3.10. Habitat risk ratios for each species unit, cumulated over time with an increasing number of existing (2000-2021, n=617) and proposed future turbines (0-100% of total n=1,045). Different species units are colour-coded and shown in different panels from low to high habitat protection level (HPL). Lines show best estimates and shaded area 95% confidence intervals, derived from the median and 95% percentiles of 500 bootstrap iterations.

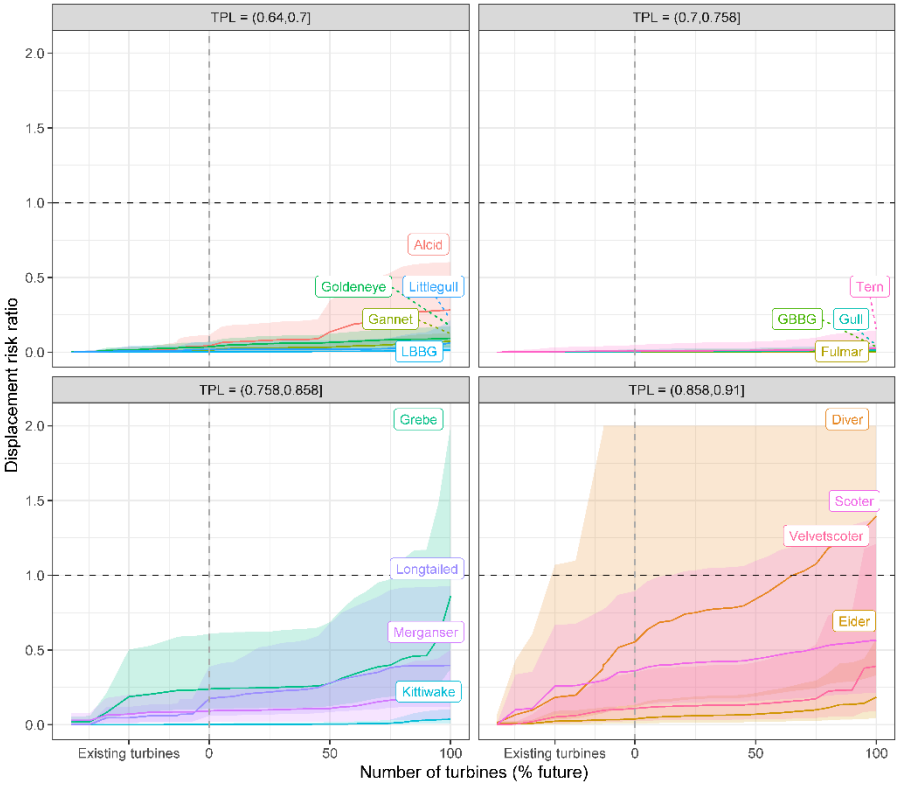

Figure 3.11. Displacement risk ratios for each species unit, cumulated over time with an increasing number of existing (2000-2021, n=617) and proposed future turbines (0-100% of total n=1,045). Different species units are colour-coded and shown in different panels from low to high target protection level for displacement (TPLd). Lines show best estimates and shaded area 95% confidence intervals, derived from the median and 95% percentiles of 500 bootstrap iterations.

Figure 3.12. Collision risk ratios for each species unit, cumulated over time with an increasing number of existing (2000-2021, n=617) and proposed future turbines (0-100% of total n=1,045). Different species units are colour-coded and shown in different panels from low to high target protection level for displacement (TPLm). Lines show best estimates and shaded area 95% confidence intervals, derived from the median and 95% percentiles of 500 bootstrap iterations.

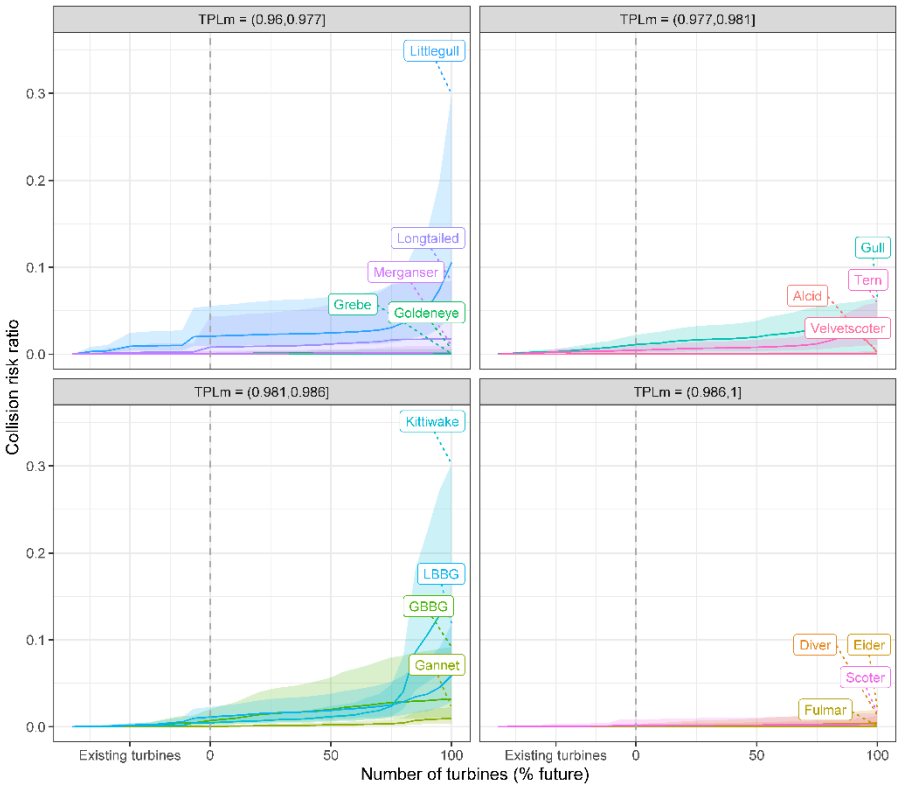

Figure 3.13. A comparison of cumulative risk ratios for displacement and collision under the 100% development scenarios (**Figure 3.9**) when area-based protections were included (blue) vs not (pink) in the risk analysis. When area-based protections were included in the analysis, they were used to adjust the allowable level of risk outside the SPAs. This assumed that SPAs would protect the designated species from any displacement and mortality, as long as they are not in the vicinity of existing or proposed wind turbines; and that the planning area for future wind farms is restricted to outside current SPAs (Section 2.1.3). The shaded areas in this violin plot represent the density distribution of outcomes from 500 bootstrap iterations and are scaled vertically to unity for each species unit. Solid circles show medians of the bootstrap distributions, which can be interpreted as our best estimate for relative risk for each species and scenario.

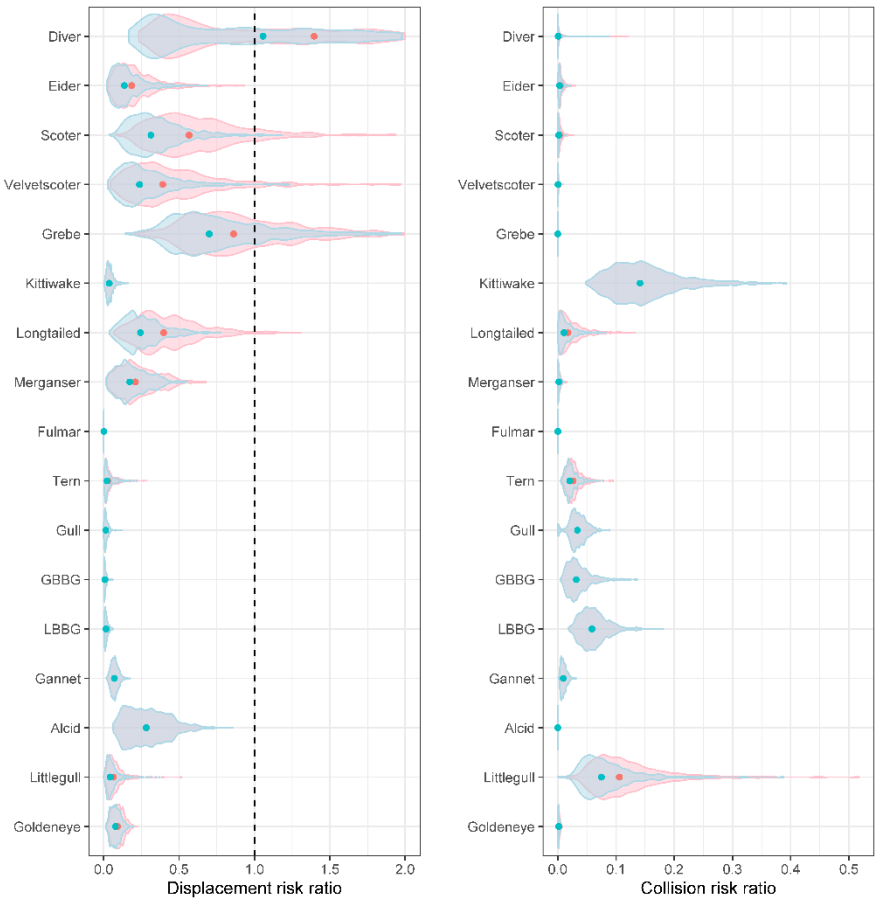

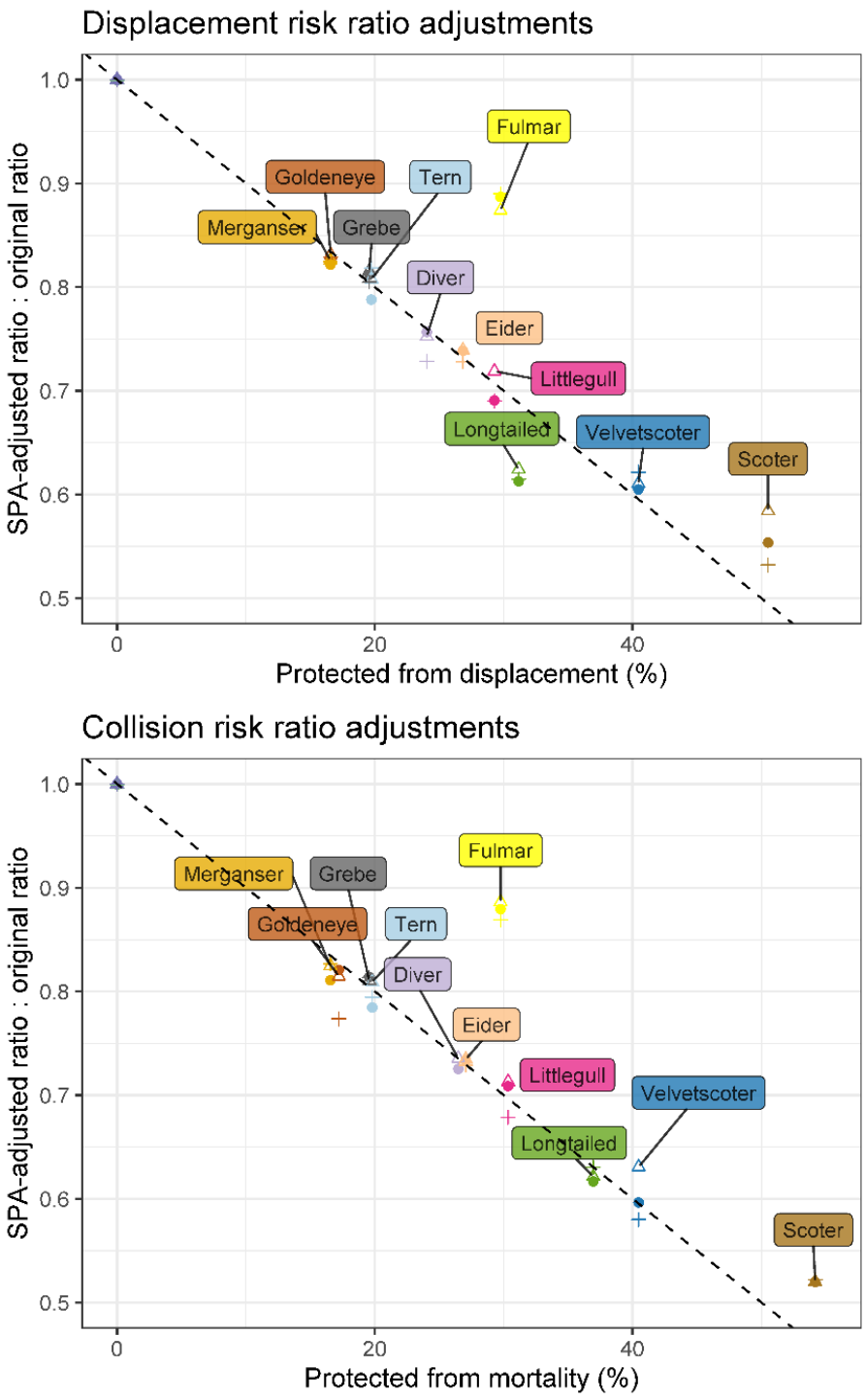

Figure 3.14. Comparison of risk ratio adjustments made to account for area-based protections for each species unit. X-axis shows the percentage of species unit abundance that was assumed to be protected in the SPA version of the risk analysis. This assumed SPAs would be 100% effective in protecting designated species when not close to existing or proposed turbines (Section 2.1.3). Y-axis shows the adjusted risk ratio under the SPA version of the risk analysis, divided by the original (no-SPA) risk ratio. The risk ratio was not adjusted for species without SPA designations (e.g., gulls), and therefore their x-axis value is zero and y-axis value is one. Common scoter had the highest % SPA-protection, which is the result of both the size of the area designated for this species, and the estimated abundance within the specific designated areas compared to outside. The dashed line shows the 1-to-1 line for reference. Deviations from this line are expected because the x-axis (% abundance protected) contains uncertainty from the spatial models (not shown in the figure). The different symbol shapes show median (circle) and 95% confidence intervals (triangle, cross) for the y-axis risk ratios.

Table 3.4. Cumulative risk ratios for each development scenario. For each scenario (Current, 50% and 100% future installations, **Figure 3.9**), median and 95% percentiles are shown for each risk ratio (HR = habitat risk, DR = displacement risk, CR = collision risk) from 500 bootstrap iterations.

Species unit	Current			50% development scenario			100% development scenario		
	HR	DR	CR	HR	DR	CR	HR	DR	CR
Divers	0.04 (0.02, 0.07)	0.55 (0.12, 2.95)	0 (0, 0)	0.06 (0.03, 0.1)	0.84 (0.19, 4.24)	0 (0, 0.01)	0.15 (0.07, 0.24)	1.4 (0.33, 6.69)	0 (0, 0.01)
Grebes	0.02 (0.01, 0.04)	0.24 (0.11, 0.61)	0 (0, 0)	0.02 (0.01, 0.05)	0.28 (0.12, 0.69)	0 (0, 0)	0.06 (0.03, 0.12)	0.86 (0.37, 2.15)	0 (0, 0)
Common scoter	0.04 (0.02, 0.05)	0.36 (0.13, 0.89)	0 (0, 0.01)	0.05 (0.03, 0.07)	0.44 (0.16, 1.1)	0 (0, 0.01)	0.1 (0.06, 0.15)	0.57 (0.22, 1.38)	0 (0, 0.02)
Long-tailed duck	0.08 (0.04, 0.13)	0.17 (0.06, 0.39)	0.01 (0, 0.04)	0.2 (0.11, 0.32)	0.28 (0.09, 0.68)	0.01 (0, 0.06)	0.26 (0.14, 0.4)	0.4 (0.12, 0.92)	0.02 (0, 0.08)
Velvetscoter	0.04 (0.02, 0.06)	0.11 (0.03, 0.35)	0 (0, 0)	0.08 (0.04, 0.12)	0.14 (0.04, 0.42)	0 (0, 0)	0.12 (0.06, 0.17)	0.39 (0.09, 1.21)	0 (0, 0)
Littlegull	0.02 (0.01, 0.04)	0.02 (0, 0.07)	0.02 (0.01, 0.06)	0.04 (0.02, 0.09)	0.02 (0, 0.08)	0.02 (0.01, 0.07)	0.13 (0.08, 0.26)	0.06 (0.01, 0.22)	0.11 (0.04, 0.3)
Alcids	0 (0, 0)	0.04 (0.01, 0.12)	0 (0, 0)	0.01 (0.01, 0.02)	0.14 (0.03, 0.35)	0 (0, 0)	0.09 (0.06, 0.12)	0.28 (0.09, 0.6)	0 (0, 0)
Eider	0.03 (0.02, 0.04)	0.04 (0.01, 0.13)	0 (0, 0)	0.05 (0.03, 0.07)	0.07 (0.02, 0.21)	0 (0, 0.01)	0.08 (0.04, 0.12)	0.19 (0.05, 0.57)	0 (0, 0.02)
Merganser	0.02 (0.01, 0.03)	0.09 (0.02, 0.23)	0 (0, 0)	0.03 (0.02, 0.05)	0.11 (0.02, 0.26)	0 (0, 0.01)	0.05 (0.04, 0.08)	0.21 (0.04, 0.5)	0 (0, 0.01)
Kittiwake	0 (0, 0.01)	0 (0, 0.01)	0 (0, 0.01)	0.01 (0.01, 0.01)	0.01 (0, 0.02)	0.01 (0.01, 0.02)	0.11 (0.08, 0.15)	0.04 (0.01, 0.1)	0.14 (0.07, 0.3)
Terns	0.02 (0.01, 0.03)	0.01 (0, 0.05)	0 (0, 0.01)	0.03 (0.02, 0.05)	0.01 (0, 0.07)	0.01 (0, 0.02)	0.11 (0.06, 0.18)	0.03 (0, 0.15)	0.03 (0.01, 0.06)
LBBG	0.01 (0.01, 0.01)	0 (0, 0.01)	0.01 (0, 0.02)	0.01 (0.01, 0.02)	0.01 (0, 0.02)	0.02 (0.01, 0.04)	0.06 (0.05, 0.07)	0.01 (0, 0.05)	0.06 (0.03, 0.12)
Goldeneye	0.01 (0.01, 0.02)	0.04 (0.01, 0.07)	0 (0, 0)	0.03 (0.02, 0.04)	0.07 (0.02, 0.12)	0 (0, 0)	0.04 (0.03, 0.05)	0.09 (0.03, 0.18)	0 (0, 0.01)
Gannet	0 (0, 0)	0.01 (0, 0.03)	0 (0, 0)	0.01 (0.01, 0.01)	0.03 (0.01, 0.07)	0 (0, 0.01)	0.06 (0.04, 0.07)	0.07 (0.03, 0.13)	0.01 (0, 0.02)
GBBG	0.01 (0, 0.01)	0 (0, 0.01)	0.01 (0, 0.02)	0.02 (0.01, 0.03)	0 (0, 0.02)	0.02 (0.01, 0.06)	0.03 (0.02, 0.04)	0.01 (0, 0.04)	0.03 (0.01, 0.09)
Grey gulls	0.01 (0.01, 0.02)	0.01 (0, 0.02)	0.01 (0, 0.02)	0.02 (0.01, 0.02)	0.01 (0, 0.03)	0.02 (0, 0.04)	0.03 (0.02, 0.04)	0.01 (0, 0.05)	0.03 (0, 0.06)
Fulmar	0 (0, 0)	0 (0, 0)	0 (0, 0)	0 (0, 0)	0 (0, 0)	0 (0, 0)	0 (0, 0)	0 (0, 0)	0 (0, 0)

4 Discussion

We have developed and presented an approach to evaluate cumulative risk to seabirds from future offshore wind energy developments throughout Danish marine waters, updating the relative risk analysis and sensitivity maps by Isojunno et al., 2025. Risks for each hazard (habitat alteration, displacement, collision) were quantified relative to explicit assessment targets and according to their respective pathways of impact (**Figure 2.1**, **Figure 2.5**). Species- and hazard-specific cumulative risk estimates showed differences in how fast or slow risk levels can accumulate, relative to assessment targets, as more offshore wind turbines are installed. Seasonal variation in species presence and density was incorporated as part of the spatial analysis, enabling the production of both year-round and seasonal sensitivity maps. The analytical approach used quantitative input parameters that can be informed by results from empirical displacement studies, collision risk modelling, and population modelling. The risk analysis was able to quantify potential magnitude differences in risk, as well as provide spatial and species rankings. Another advantage of the fully quantitative algorithm is that uncertainty can be propagated through the entire process. While we outline several important caveats to the use of relative risk approaches, the developed analysis approach provides a tool for spatial prioritization and evaluating magnitude differences in risk between cumulative risk scenarios, as well as associated uncertainties.

4.1 Relative risk analysis: interpretation and caveats

When interpreting the main outputs of the relative risk analysis, the risk ratios, it is important to bear in mind that they depend on the denominator – the allowable level of risk, which is calculated based on the target protection levels. The expert elicitation revealed that there is considerable uncertainty about what the numerical values for these protection levels should be. Uncertainty around these and other parameter values were estimated as part of the expert elicitation process and are represented in the confidence intervals of the presented risk ratios. However, it is possible that the expert elicitation process did not capture the full range of uncertainty in all parameters. In other words, the parameter values and associated uncertainty is likely to differ with different experts on the panel. As a precautionary approach, we recommend using the upper limit of the 95% confidence intervals to guide decision-making.

The use of explicit assessment targets has the advantage of providing clear benchmarks against which expected risks are compared. That said, without validation against population modelling, there is uncertainty about whether the protection levels scale appropriately with population consequences. For example, many population modelling studies have shown that potential biological removal (PBR) is not always a precautionary management measure for seabird populations under density dependence (e.g., O'Brien et al., 2017). Whether PBR is a sufficient benchmark to express relative risk to populations is less well understood. In any case, relative risk approaches such as the risk ratios presented here cannot be used to evidence negligible impact on seabird populations. This would require modelling population consequences more explicitly, e.g., in a population projection or viability analysis (Miller et al., 2019; Searle et al., 2019; Horswill et al., 2022; Merrall et al., 2024). Population modelling could also consider the contribution of subpopulations or stocks to population viability, e.g., in a metapopulation analysis framework. This could help validate

commonly used metrics of regional or national importance in vulnerability assessments. Similarly, here, experts were asked to score the importance of Danish marine waters to the conservation status of each species unit, which was then used to adjust the target protection levels (**Section 2.1.5, Figure 2.3**).

The expected levels of risk were informed by published literature reviews, which reflects current knowledge on impacts of offshore wind farms constructed to-date (e.g., Dierschke et al., 2016; Masden & Cook, 2016; Cook et al., 2018, 2025; Lamb et al., 2024; literature included in expert elicitation process are provided in Electronic supplementary materials). We did not attempt to predict how collision rates, displacement rates or the spatial extent of displacement could change as future offshore wind technology evolves towards larger turbines which are spaced further apart. It is possible that such changes, or other time-dependent processes such as habituation, will influence the susceptibility of different species to hazards differently, and consequently both the spatial distribution and cumulative species risks.

The updated sensitivity maps can be used to identify potential development areas that minimize the risk of habitat alteration, displacement and collision to the modelled seabirds within the study area of Danish marine waters. The maps should not be used to extrapolate risks for non-modelled species, life history contexts, or hazard types not currently implemented in the algorithm, such as effects during the breeding season, barrier effects during daily commuting between colonies and at-sea foraging areas, or collision risk during migration.

An important difference to previous sensitivity mapping approaches is that the maps presented here combine multiple species by maximum values, rather than sums or weighted averages, at any given location. This means that a high relative risk for one species cannot be compensated for by multiple low-risk species at the same location. This ensures a precautionary approach where the maps can be used to minimize risk for all species given their assessment targets, rather than the majority of species of concern.

Spatially relative risk means that values in each grid location are ranked with respect to all other grid locations in the study area. Because the combined map represents maximum spatial rankings across the three hazards, the combined map treats each hazard with equal weight. In reality, for a given species, the same number of birds impacted by habitat alteration, displacement, or collision are likely to have three different levels of population impact; some of which the hazard-specific target protection levels aim to capture. We therefore caution against relying on the combined map alone for decision-making. It is also important to note that the current approach to quantifying relative habitat risk considers all habitat alteration as unwanted, which does not account for potential positive effects, e.g., through reef effects or habitat enhancement. However, it would be possible to include such effects in the algorithm when more knowledge becomes available about possible positive effects of offshore wind farm structures for some species.

We present results for species units, some of which combined more than one ecologically similar species (**Table 2.1**). This approach was considered a pragmatic first approach to the multi-species assessment, as not all species are fully identifiable from aerial surveys. Because abundance estimates were made for each species unit, and maximum values were used to combine relative risks across multiple species, this choice did not influence the weighting of individual species on the multi-species hazard maps for potential habitat alteration,

displacement and collision. In other words, the combined relative risk maps based on species units would be the same as maps based on individual species, as long as the input parameters for each species within each species unit were specified to be the same. However, it is worth noting that the maps presenting number of species exceeding HPL thresholds (**Figure 3.7**, bottom panel) summarize the number of species units, rather than individual species.

The relative risk analysis was based on abundance and distribution data from cross-sectional surveys, rather than individual-based monitoring, and as such, assume that relative risks are proportional to species density. In other words, the approach does not account for any heterogeneity in space use or susceptibility to hazards within each population. Actual risks to populations emerge from the risks accumulated to their constituent individuals, which can vary within and between individuals over time and space. Cross-sectional metrics of impact can be expected to proxy actual impacts in well-mixed populations with space use resembling the ideal free distribution. However, the approach may under- or over-estimate risks when the population is not well-mixed, such as due to individual site fidelity, or differential exploitation of resources between age- and sex-classes.

We considered the most recent distribution data as the most relevant "pre-exposure baseline" for future development scenarios. To represent the most likely recent distributions, we used time-weighting in the spatial analysis that pooled aerial survey data across multiple years (1999-2024). The time-weighting was akin to attributing recent data with greater sample sizes than older data. As well as more representative of distributional patterns found in more recent data, the resulting estimated distribution will have greater uncertainty in areas that were not surveyed recently. This approach was taken to allow for changes in species abundance or density during the 25-year survey period, without having to model the changes explicitly – this would have been challenging, with many unknowns and outside the scope of this project, given variations in the spatial and temporal coverage of the survey data, and potentially complex interactions with the development of existing wind farms.

Seasonal variation in species presence in Danish marine waters was accounted for in two ways. First, seasonal sensitivity maps provide spatial risk ranking for the species present in that season (**Table 2.2**). These maps included season-specific distribution maps (winter-spring or summer-autumn) for species present in Denmark year-round. Thus, variation in the spatial distribution of risks between different seasons (winter, spring, summer, autumn) can be caused both by the presence/absence of strongly seasonal species, and any changes in distribution between winter/spring and summer-autumn, for those species that are present year-round. To generate year-round sensitivity maps, the seasonal distribution maps for the year-round residents were averaged, accounting for the duration of each season as weights. This assumes that risk is proportional to the average density of the species year-round.

The density distribution maps were estimated without correcting for availability bias (Dunn et al., 2024). This means that the presented estimated abundances can somewhat under-estimate the underlying, true abundance of birds present in Danish waters, particularly for diving species such as razorbills/common guillemots and divers.

4.2 Implications for spatial planning

Within the constraints of the assumptions outlined above, the risk analysis shows that spatial planning has substantial scope to reduce the potential risk of habitat alteration, displacement and collision to seabird species. Prioritizing the lowest-risk areas from the combined map (**Figure 3.5**) is expected to reduce risk for all assessed species units (**Section 2.2.1**). That said, the extent to which risks are reduced, i.e., the effectiveness of such prioritization, depends on species and hazard types (**Table 3.3**). The cumulative risk analysis further highlighted that prioritizing developments in lower-risk areas is expected minimize and even maintain current levels of risk for most of the assessed species. For example, the relative risk of displacement for grebes and collision risk for little gull were almost unchanged when the lower-risk turbines were installed first (up to 50% of the proposed set of turbines). When the turbines in the higher-risk areas were also developed (50-100% of the proposed turbines), the risks accumulated more rapidly. A notable exception to this pattern is the diver species unit, which showed a steady increase in displacement risk as more turbines are installed. For this species unit, the 100% development scenario is likely to breach the target protection level of displacement.

The analysis provides two key metrics for risk-aware spatial planning: how close the expected levels of risk are to target protection levels (the value of risk ratios), and its probability distribution (the likelihood of risk ratios), given uncertainty in the underlying species distributions, assessment targets and other input parameters. The probability distribution is useful for decision-making, because it can be used to minimize "regret", i.e., the likelihood of missing assessment targets. Only a very small proportion of the Danish marine area could be identified as low risk with high confidence for all species and hazard types, providing limited options for very risk-averse decision-making (**Figure 3.5**). Uncertainty maps (**Figure 3.7**, **Figure 3.8**) provide a transparent means to discuss risk tolerance and the likelihood of selecting a planning area that is not as low-risk to seabirds as intended. Similarly for the cumulative risk scenarios, the 100% development scenario would require accepting a significant likelihood that target protections are exceeded. For the divers, grebes and scoters, the likelihood of exceeding at least one of the three target protection levels was 62%, 37% and 12% respectively. Under the 50% scenario, these risks were smaller (45%, <1%, 4.2%). It is worth noting that the diver species unit was estimated to already have a significant risk (>5%) of exceeding the displacement target under the status quo scenario, i.e., existing wind turbines. Some of this can attributed to knowledge uncertainty about the spatial extent of displacement and target protection level for this species unit. The associated probability distributions are bimodal with heavy tails (**Figure 3.1**), indicating that if the most concerned experts are correct, then the cumulative level of displacement from existing wind farms may already exceed acceptable levels.

The main risk analysis assumed that the placement of wind farms is the primary means by which the target protections can be achieved. However, if the planning of wind farms is constrained to be outside SPAs, and area-based protections are effective in protecting designated species from displacement and collision, then we can consider this as an additional measure that contributes to the target protection levels (Figure 2.2). The most notable reductions in the resulting cumulative risk ratios were seen for the grebes, common and velvet scoters (Figure 3.13). The risk ratio for the diver was similarly reduced, but the chance of exceeding the threshold remained high due to the uncertainty associated with knowledge and expert opinion (discussed above).

Nevertheless, these results underscore the potential for management measures to counter potential risks to seabird populations from offshore wind development. These management measures could include area-based protections, as tested here to achieve the target protection levels from offshore wind development, and other management measures to achieve overall management targets that incorporate other anthropogenic pressures as well.

4.3 Next steps and future developments

We outlined improvements and extensions to the spatial risk-ranking framework in Isojunno et al., 2025, and have in this report accomplished those identified as the highest priority. These include refining input parameter estimates through expert elicitation, target protection levels which are specific to each hazard, incorporation of all input parameter uncertainty, further testing and sensitivity analysis of the spatial risk-ranking algorithm, seasonal sensitivity maps, and time-weighting to account for the pooling of multiple years of survey data. Of the remaining proposed extensions, we consider the following as constituting the high priority for future iterations of the risk analysis:

- An interactive online tool, allowing users to modify input parameters for different use-cases and to generate and compare different scenarios, e.g., between different seasons, or under different assumptions about species-level impacts.
- A re-evaluation of species units included in the analysis. This would consider species currently combined to species units as individual species, given differences in their ecology and conservation status
- Incorporation of movement corridors, migration intensity, and barrier effects in the risk analysis. This would use tracking-based data as input to the analysis.
- Validation of the relative risk analysis approach. This could involve population modelling to validate and refine target protection levels, or individual-based modelling to evaluate the validity of the cross-sectional approach to estimating relative species risks

We foresee substantial scope to adapt and apply the relative risk analysis approach to a broader range of receptor groups than seabirds, and to different geographical areas. Though the specific impact pathways vary, the benchmarking of risk is readily generalisable to a broad range of species and phases of wind farm life cycle, thus providing consistency in the assessment approach. For example, for marine mammals with seasonal variation in distribution, the algorithm could be used to generate seasonal maps to compare potential risks from pile driving between summer versus winter. Similar to the multiple hazard maps presented here for seabirds, multiple impact pathways could be considered for noise impacts on marine mammals, such as auditory injury and avoidance or other behaviour response. Indeed, the impact pathways could be user-specified as part of a comprehensive, interactive assessment tool.

5 Acknowledgments

This project was funded by Energistyrelsen. Aarhus University/DCE and University of St. Andrews were subcontracted to conduct this relative risk assessment for birds under a contract between Energistyrelsen and NIRAS. We are grateful to Energistyrelsen and NIRAS for the support provided.

A number of pilots and ornithological observers have contributed to the collection of data. We are very grateful to air companies, pilots and observers for their flexibility and support in this work.

6 References

Band, W., M. Madders, and D. Whitfield. 2007. "Developing field and analytical methods to assess avian collision risk at wind farms". Pages 259–275 *in Birds and Wind Farms: Risk Assessment and Mitigation*.

Best, B. D., and P. N. Halpin. 2019. "Minimizing wildlife impacts for offshore wind energy development: Winning tradeoffs for seabirds in space and cetaceans in time". *PLoS ONE* 14: 1–26.

BirdLife International. 2021. "European Red List of Birds". *2021*.

Bradbury, G., M. Trinder, B. Furness, A. N. Banks, R. W. G. Caldow, and D. Hume. 2014. "Mapping Seabird Sensitivity to offshore wind farms". *PLoS ONE* 9.

Buckland, S. T., D. R. Anderson, K. P. Burnham, J. L. Laake, D. L. Borchers, and L. Thomas. 2001. "Introduction to Distance Sampling: Estimating Abundance of Biological Populations". Oxford University Press, United Kingdom.

Caneco, B., G. R. W. Humphries, A. Cook, and E. A. Masden. 2022. "Estimating Bird Collisions at Offshore Wind Farms with stochLAB". https://github.com/MarineScotlandScience/stochLAB.

Certain, G., L. L. Jørgensen, I. Christel, B. Planque, and V. Bretagnolle. 2015. "Mapping the vulnerability of animal community to pressure in marine systems: disentangling pressure types and integrating their impact from the individual to the community level". *ICES Journal of Marine Science* 72: 1470–1482.

CIEEM. 2024. "Guidelines for ecological impact assessment in the UK and Ireland". Chartered Institute of Ecology and Environmental Management (CIEEM), Winchester. https://cieem.net/wp-content/uploads/2018/08/EcIA-Guidelines-v1.3-Sept-2024.pdf.

Cook, A. S. C. P., E. M. Humphreys, F. Bennet, E. A. Masden, and N. H. K. Burton. 2018. "Quantifying avian avoidance of offshore wind turbines: Current evidence and key knowledge gaps". *Marine Environmental Research* 140: 278–288.

Cook, A. S. C. P., E. Salkanovic, E. Masden, H. E. Lee, and A. H. Kiilerich. 2025. "A critical appraisal of 40 years of avian collision risk modelling: How have we got here and where do we go next?". *Environmental Impact Assessment Review* 110: 107717.

Cox, L. A. 2008. "What's wrong with risk matrices?". *Risk Analysis* 28: 497–512.

Dierschke, V., R. W. Furness, and S. Garthe. 2016. "Seabirds and offshore wind farms in European waters: Avoidance and attraction". *Biological Conservation* 202: 59–68.

Duijm, N. J. 2015. "Recommendations on the use and design of risk matrices". *Safety Science* 76: 21–31.

Dunn, R. E., J. Duckworth, S. O. Brien, R. W. Furness, L. Buckingham, M. Bogdanova, and J. A. Green. 2024. "Temporal and spatial variability in availability bias has consequences for marine bird abundance estimates during the non-breeding season". *bioRxiv*: 1–25.

Fauchald, P., V. M. S. Ollus, M. Ballesteros, A. Breistøl, S. Christensen-Dalsgaard, S. Molværsmyr, A. Tarroux, G. H. Systad, and B. Moe. 2024. "Mapping seabird vulnerability to offshore wind farms in Norwegian waters". *Frontiers in Marine Science* 11: 1–15.

Furness, R. W., H. M. Wade, and E. A. Masden. 2013. "Assessing vulnerability of marine bird populations to offshore wind farms". *Journal of Environmental Management* 119: 56–66.

Garthe, S., and O. Hüppop. 2004. "Scaling possible adverse effects of marine wind farms on seabirds: Developing and applying a vulnerability index". *Journal of Applied Ecology* 41: 724–734.

Gibbs, M. T., and H. I. Browman. 2015. "Introduction: Risk assessment and risk management: A primer for marine scientists". *ICES Journal of Marine Science* 72: 992–996.

Gormley, A., S. Pollard, and S. Rocks. 2011. "Guidelines for Environmental Risk Assessment and Management". UK Department for Environment, Food & Rural Affairs (DEFRA). https://www.gov.uk/government/publications/guidelines-for-environmental-risk-assessment-and-management-green-leaves-iii .

Green, R. M. W., N. H. K. Burton, A. S. C. P. Cook, S. E. Franks, and J. A. Green. 2025. "Framework for assessing species vulnerability whilst on migration to a spatially explicit anthropogenic pressure". *Biological Conservation* 307: 111118.

Hemming, V., M. A. Burgman, A. M. Hanea, M. F. McBride, and B. C. Wintle. 2018. "A practical guide to structured expert elicitation using the IDEA protocol". *Methods in Ecology and Evolution* 9: 169–180.

Horswill, C., J. A. O. Miller, and M. J. Wood. 2022. "Impact assessments of wind farms on seabird populations that overlook existing drivers of demographic change should be treated with caution". *Conservation Science and Practice* 4: 1–10.

Horswill, C., and R. A. Robinson. 2015. "Review of seabird demographic rates and density dependence". Peterborough.

International Organization for Standardization [ISO]. 2018. "ISO 31000:2018 Risk Management".

Isojunno, S., L. Scott-Hayward, C. L. Pedersen, H. M. Thomsen, J. Chetcuti, M. Frederiksen, T. Bregnballe, J. Sterup, M. MacKenzie, and I. . Petersen. 2025. "Mapping relative risk to seabirds from offshore wind energy developments in Danish waters".

Johnston, A., A. S. C. P. Cook, L. J. Wright, E. M. Humphreys, and N. H. K. Burton. 2014. "Modelling flight heights of marine birds to more accurately assess collision risk with offshore wind turbines". *Journal of Applied Ecology* 51: 31–41.

Kelsey, E. C., J. J. Felis, M. Czapanskiy, D. M. Pereksta, and J. Adams. 2018. "Collision and displacement vulnerability to offshore wind energy infrastructure among marine birds of the Pacific Outer Continental Shelf". *Journal of Environmental Management* 227: 229–247.

Lamb, J., J. Gulka, E. Adams, A. Cook, and K. A. Williams. 2024. "A synthetic analysis of post-construction displacement and attraction of marine birds at offshore wind energy installations". *Environmental Impact Assessment Review* 108: 107611.

Linkov, I., D. Loney, S. Cormier, F. K. Satterstrom, and T. Bridges. 2009. "Weight-of-evidence evaluation in environmental assessment: Review of qualitative and quantitative approaches". *Science of the Total Environment* 407: 5199–5205.

MacMillan, D. C., and K. Marshall. 2005. "The Delphi process – an expert-based approach to ecological modelling in data-poor environments Knowledge engineering and the". *Animal Conservation* 9: 11–19.

Martin, T. G., M. A. Burgman, F. Fidler, P. M. Kuhnert, S. Low-choy, M. Mcbride, and K. Mengersen. 2011. "Eliciting Expert Knowledge in Conservation Science". *Conservation Biology* 26: 29–38.

Masden, E. A., and A. S. C. P. Cook. 2016. "Avian collision risk models for wind energy impact assessments". *Environmental Impact Assessment Review* 56: 43–49.

Merrall, E., J. A. Green, L. A. Robinson, A. Butler, M. J. Wood, M. A. Newell, J. Black, F. Daunt, and C. Horswill. 2024. "Incorporating density-dependent regulation into impact assessments for seabirds". *Journal of Applied Ecology* 61: 2510–2524.

Miller, J. A. O., R. W. Furness, M. Trinder, and J. Matthiopoulos. 2019. "The sensitivity of seabird populations to density-dependence, environmental stochasticity and anthropogenic mortality". *Journal of Applied Ecology* 56: 2118–2130.

Niel, C., and J. D. Lebreton. 2005. "Using demographic invariants to detect overharvested bird populations from incomplete data". *Conservation Biology* 19: 826–835.

O'Brien, S. H., A. S. C. P. Cook, and R. A. Robinson. 2017. "Implicit assumptions underlying simple harvest models of marine bird populations can mislead environmental management decisions". *Journal of Environmental Management* 201: 163–171.

R Core Team. 2024. "R: A Language and Environment for Statistical Computing". R Foundation for Statistical Computing.

Raimondo, S., M. Etterson, N. Pollesch, K. Garber, A. Kanarek, W. Lehmann, and J. Awkerman. 2018. "A framework for linking population model development with ecological risk assessment objectives". *Integrated Environmental Assessment and Management* 14: 369–380.

Scott-Hayward, L. A. S., M. L. Mackenzie, and C. G. Walker. 2023a. "MRSea R Package (V1.5.0): Spatially Adaptive Uni and Bi-Variate Regression Splines Using SALSA". University of St Andrews.

Scott-Hayward, L. A. S., M. L. Mackenzie, C. G. Walker, G. Shatumbu, W. Kilian, and P. du Preez. 2023b. "Automated surface feature selection using SALSA2D: Assessing distribution of Elephant carcasses in Etosha National Park".

Searle, K., D. Mobbs, F. Daunt, and A. Butler. 2019. "A Population Viability Analysis modelling tool for seabird species". *Centre for Ecology & Hydrology report for Natural England. Natural England Commissioned Report NECR274*.

Southall, B. L., D. Tollit, J. Amaral, C. W. Clark, and W. T. Ellison. 2023. "Managing human activity and marine mammals: A biologically based, relativistic risk assessment framework". *Frontiers in Marine Science* 10: 1–15.

Stelzenmüller, V., M. Coll, R. Cormier, A. D. Mazaris, M. Pascual, C. Loiseau, J. Claudet, S. Katsanevakis, E. Gissi, A. Evagelopoulos, B. Rumes, S. Degraer, H. Ojaveer, T. Moller, J. Giménez, C. Piroddi, V. Markantonatou, and C. Dimitriadis. 2020. "Operationalizing risk-based cumulative effect assessments in the marine environment". *Science of the Total Environment* 724.

Thieurmel, B. 2017. "R package for calculating sun/moon positions and phases". https://github.com/datastorm-open/suncalc.

Tyack, P. L., L. Thomas, D. P. Costa, A. J. Hall, C. M. Harris, J. Harwood, S. D. Kraus, P. J. O. Miller, M. Moore, T. Photopoulou, E. Pirotta, R. M. Rolland, L. H. Schwacke, S. E. Simmons, and B. L. Southall. 2022. "Managing the effects of multiple stressors on wildlife populations in their ecosystems: developing a cumulative risk approach". *Proceedings of the Royal Society B: Biological Sciences* 289: 20222058.

USEPA. 2016. "Generic Ecological Assessment Endpoints (GEAEs) For Ecological Risk Assessment: Second Edition With Generic Ecosystem Services Endpoints Added". *Usepa*. U.S. Environmental Protection Agency (USEPA), Washington, DC. https://www.epa.gov/sites/default/files/2016-08/documents/geae_2nd_edition.pdf.

Verling, E., R. Miralles Ricós, M. Bou-Cabo, G. Lara, M. Garagouni, J. M. Brignon, and T. O'Higgins. 2021. "Application of a risk-based approach to continuous underwater noise at local and subregional scales for the Marine Strategy Framework Directive". *Marine Policy* 134.

Wade, P. R. 1998. "Calculating limits to the allowable human-caused mortality of cetaceans and pinnipeds". *Marine Mammal Science* 14: 1–37.

Willmott, J. R., G. Forcey, and A. Kent. 2013. "The relative vulnerability of migratory bird species to offshore wind energy projects on the Atlantic outer continental shelf". *OCS Study BOEM 2013-207*: 275 pp.

7 Appendix 1: Glossary

Table 7.1. Glossary of terms

Term	Definition
Assessment metric	An explicit expression of the environmental value to be assessed. Analogous to assessment end-point: "An explicit expression of the environmental value to be protected, operationally defined as an ecological entity and its attributes" (USEPA, 2016). Here, we use three assessment metrics: the degree of overlap with core habitat, the expected number of seabirds at risk of displacement, and the expected number of birds at risk of collision.
Assessment outcome	The outcome value of assessment metrics following environmental (risk) assessment.
Assessment target or target protection level	The desired, or acceptable, value for each assessment metric, which can be used to benchmark the performance of assessment outcomes in achieving targets. Such benchmarking also enables the comparison of assessment outcomes of receptors with different targets. In this work, we defined target protection levels as a proportion of the population or habitat to be protected: • Habitat protection level (HPL, h_i^*): the proportion of each species' range that should be protected from any additional habitat alteration, reflecting the dependence of each species on spatially limited resources. Habitat overlap was used as an assessment metric for potential habitat alteration. HPL was used to benchmark the degree of overlap with core habitat metric. • Target protection level for displacement (TPLd, p_i^*): the desired level of protection for each species unit in Danish national waters, given current population status, trends, and resilience to existing threats. Specifically, the TPLd was defined as the proportion of the current population size in the national waters that should be protected from displacement, additional to existing pressures, to maintain or achieve favourable conservation status. The TPLd was derived from two expert-elicited parameters, population status and importance of Danish marine waters to the population status. TPLd was used to benchmark the assessment metric for displacement. In addition, TPLd was used to adjust HPL values to account for population status, and as the population "recovery factor" to calculate PBR, which informed TPLm (**Section 2.1.6**). • Target protection level for mortality (TPLd, m_i^*): the target protection level for added mortality for each species unit in Danish national waters. TPLm was used to benchmark the assessment metric for collision.
Cumulative risk	The combined risk to species or habitats from multiple developments or hazards over time, rather than from a single source or event. "Cumulative effects can result from individually insignificant but collectively significant actions taking place over a period of time or concentrated in a location" (CIEEM, 2024). In this report, cumulative risk refers to the relative increase in risk as more offshore wind turbines are installed under future build scenarios (**Section 2.1.4**).
Expert elicitation	A structured process for obtaining expert judgments to inform parameter values and uncertainty. "Expert knowledge is substantive information on a particular topic that is not widely known by others"…"When experts use their knowledge to predict what may happen in a particular context, we refer to these predictions as expert judgments" (Martin et al., 2011). We used a two-stage Delphi process, supported by an evidence dossier to ensure consistency in the type of empirical information experts used to inform their judgements (**Section 2.1.5,** Electronic supplementary material).
Hazard	The source of risk. "Element which alone or in combination has the intrinsic potential to give rise to risk" (International Organization for Standardization [ISO], 2018). Here, we considered three hazards: habitat overlap, displacement, and collision due to wind farm presence.
Potential Biological Removal (PBR)	A management metric estimating the maximum allowable human-caused mortality for a population while maintaining sustainability, originally proposed for marine mammals by Wade, 1998. Here, a PBR calculation adapted to seabirds (O'Brien et al., 2017) was used to inform TPLm.
Proxy collision rate	An estimated collision risk metric based on species flight behaviour and turbine characteristics, used as a computationally efficient alternative to full collision risk models. For a detailed calculation, see report section 2.1.6.

Risk	In the broadest sense, defined as “The effect of uncertainty on objectives” (ISO 2018 31000). Typically used to describe both the likelihood and consequence of unwanted or adverse effects, such as in ecological risk assessment (ERA) (Gormley et al., 2011; Gibbs & Browman, 2015). When the objective of the ERA is to protect individuals or populations of animals, risk can be defined as “The probability of harmful effects to the health of individuals or to populations integrated over a defined time period” (Tyack et al., 2022).
Risk-ranking	The ordinal ranking of risk from low to high values. Risk-rankings only contain information about the order of values, or the position of an element in an ordered series, not absolute value or magnitude differences in risk level.
Risk-tolerance and regret	Concepts used in decision-making under uncertainty. Risk tolerance refers to the acceptable level of uncertainty in planning; regret refers to the likelihood that a chosen option turns out to be higher risk than expected.
Relative species risk	Risk expressed relative to a population benchmark level of risk, such as a minimum viable population size. While relative risk does not express the absolute risk to a population, relative risk can be ranked, as well as inform about the magnitude differences in risk compared to the benchmark. In this work, we define relative species risk with respect to assessment targets. Relative species risks were calculated for each hazard as relative risk ratios, with the assessment metric as the numerator and assessment target in the denominator (**Figure 2.3**).
Risk ratio	A quantitative measure of relative risk, calculated as the ratio between expected outcomes (e.g., birds at risk) and allowable outcomes based on assessment targets. Values >1 indicate that expected risk exceeds allowable levels.
Sensitivity map	A spatial representation of relative risk across a study area, ranking locations from lowest to highest risk based on species distribution and susceptibility to hazards.
SPA	Special Protection Areas are sites designated under the EU Birds Directive to safeguard habitats for bird species listed in Annex I and for regularly occurring migratory species. In this report, SPA designations were considered in alternative risk scenarios.
Spatially relative risk	Risk expressed relative in space. Spatially relative risks may be benchmarked relative to a specific area or represent a ranking within the whole area. With the assessment objective being a spatially explicit risk-ranking (i.e., a sensitivity map), we chose the ranking approach, and thus the mapped risks are relative to the lowest and highest values in Danish marine waters.
Species unit	Individual species or ecologically similar species groups (**Section 2.2.1**) that were analysed together as a unit in the analysis. Individual species within species groups were assumed to have broadly similar distribution and habitat preference, target protection level, displacement rate and collision risk. Species units may combine ecologically similar species when identification from aerial surveys is challenging.
Time-weighting	A method applied to survey data to give greater weight to more recent observations when estimating species distributions, reflecting their relevance as baseline data for future planning (**Section 2.2.3**).

References

Band, W., M. Madders, and D. Whitfield. 2007. "Developing field and analytical methods to assess avian collision risk at wind farms". Pages 259–275 *in Birds and Wind Farms: Risk Assessment and Mitigation*.

Best, B. D., and P. N. Halpin. 2019. "Minimizing wildlife impacts for offshore wind energy development: Winning tradeoffs for seabirds in space and cetaceans in time". *PLoS ONE* 14: 1–26.

BirdLife International. 2021. "European Red List of Birds". *2021*.

Bradbury, G., M. Trinder, B. Furness, A. N. Banks, R. W. G. Caldow, and D. Hume. 2014. "Mapping Seabird Sensitivity to offshore wind farms". *PLoS ONE* 9.

Buckland, S. T., D. R. Anderson, K. P. Burnham, J. L. Laake, D. L. Borchers, and L. Thomas. 2001. "Introduction to Distance Sampling: Estimating Abundance of Biological Populations". Oxford University Press, United Kingdom.

Caneco, B., G. R. W. Humphries, A. Cook, and E. A. Masden. 2022. "Estimating Bird Collisions at Offshore Wind Farms with stochLAB". https://github.com/MarineScotlandScience/stochLAB.

Certain, G., L. L. Jørgensen, I. Christel, B. Planque, and V. Bretagnolle. 2015. "Mapping the vulnerability of animal community to pressure in marine systems: disentangling pressure types and integrating their impact from the individual to the community level". *ICES Journal of Marine Science* 72: 1470–1482.

CIEEM. 2024. "Guidelines for ecological impact assessment in the UK and Ireland". Chartered Institute of Ecology and Environmental Management (CIEEM), Winchester. https://cieem.net/wp-content/uploads/2018/08/EcIA-Guidelines-v1.3-Sept-2024.pdf.

Cook, A. S. C. P., E. M. Humphreys, F. Bennet, E. A. Masden, and N. H. K. Burton. 2018. "Quantifying avian avoidance of offshore wind turbines: Current evidence and key knowledge gaps". *Marine Environmental Research* 140: 278–288.

Cook, A. S. C. P., E. Salkanovic, E. Masden, H. E. Lee, and A. H. Kiilerich. 2025. "A critical appraisal of 40 years of avian collision risk modelling: How have we got here and where do we go next?". *Environmental Impact Assessment Review* 110: 107717.

Cox, L. A. 2008. "What's wrong with risk matrices?". *Risk Analysis* 28: 497–512.

Dierschke, V., R. W. Furness, and S. Garthe. 2016. "Seabirds and offshore wind farms in European waters: Avoidance and attraction". *Biological Conservation* 202: 59–68.

Duijm, N. J. 2015. "Recommendations on the use and design of risk matrices". *Safety Science* 76: 21–31.

Dunn, R. E., J. Duckworth, S. O. Brien, R. W. Furness, L. Buckingham, M. Bogdanova, and J. A. Green. 2024. "Temporal and spatial variability in availability bias has consequences for marine bird abundance estimates during the non-breeding season". *bioRxiv*: 1–25.

Fauchald, P., V. M. S. Ollus, M. Ballesteros, A. Breistøl, S. Christensen-Dalsgaard, S. Molværsmyr, A. Tarroux, G. H. Systad, and B. Moe. 2024. "Mapping seabird vulnerability to offshore wind farms in Norwegian waters". *Frontiers in Marine Science* 11: 1–15.

Furness, R. W., H. M. Wade, and E. A. Masden. 2013. "Assessing vulnerability of marine bird populations to offshore wind farms". *Journal of Environmental Management* 119: 56–66.

Garthe, S., and O. Hüppop. 2004. "Scaling possible adverse effects of marine wind farms on seabirds: Developing and applying a vulnerability index". *Journal of Applied Ecology* 41: 724–734.

Gibbs, M. T., and H. I. Browman. 2015. "Introduction: Risk assessment and risk management: A primer for marine scientists". *ICES Journal of Marine Science* 72: 992–996.

Gormley, A., S. Pollard, and S. Rocks. 2011. "Guidelines for Environmental Risk Assessment and Management". UK Department for Environment, Food & Rural Affairs (DEFRA). https://www.gov.uk/government/publications/guidelines-for-environmental-risk-assessment-and-management-green-leaves-iii.

Green, R. M. W., N. H. K. Burton, A. S. C. P. Cook, S. E. Franks, and J. A. Green. 2025. "Framework for assessing species vulnerability whilst on migration to a spatially explicit anthropogenic pressure". *Biological Conservation* 307: 111118.

Hemming, V., M. A. Burgman, A. M. Hanea, M. F. McBride, and B. C. Wintle. 2018. "A practical guide to structured expert elicitation using the IDEA protocol". *Methods in Ecology and Evolution* 9: 169–180.

Horswill, C., J. A. O. Miller, and M. J. Wood. 2022. "Impact assessments of wind farms on seabird populations that overlook existing drivers of demographic change should be treated with caution". *Conservation Science and Practice* 4: 1–10.

Horswill, C., and R. A. Robinson. 2015. "Review of seabird demographic rates and density dependence". Peterborough.

International Organization for Standardization [ISO]. 2018. "ISO 31000:2018 Risk Management".

Isojunno, S., L. Scott-Hayward, C. L. Pedersen, H. M. Thomsen, J. Chetcuti, M. Frederiksen, T. Bregnballe, J. Sterup, M. MacKenzie, and I. . Petersen. 2025. "Mapping relative risk to seabirds from offshore wind energy developments in Danish waters".

Johnston, A., A. S. C. P. Cook, L. J. Wright, E. M. Humphreys, and N. H. K. Burton. 2014. "Modelling flight heights of marine birds to more accurately assess collision risk with offshore wind turbines". *Journal of Applied Ecology* 51: 31–41.

Kelsey, E. C., J. J. Felis, M. Czapanskiy, D. M. Pereksta, and J. Adams. 2018. "Collision and displacement vulnerability to offshore wind energy infrastructure among marine birds of the Pacific Outer Continental Shelf". *Journal of Environmental Management* 227: 229–247.

Lamb, J., J. Gulka, E. Adams, A. Cook, and K. A. Williams. 2024. "A synthetic analysis of post-construction displacement and attraction of marine birds at offshore wind energy installations". *Environmental Impact Assessment Review* 108: 107611.

Linkov, I., D. Loney, S. Cormier, F. K. Satterstrom, and T. Bridges. 2009. "Weight-of-evidence evaluation in environmental assessment: Review of qualitative and quantitative approaches". *Science of the Total Environment* 407: 5199–5205.

MacMillan, D. C., and K. Marshall. 2005. "The Delphi process – an expert-based approach to ecological modelling in data-poor environments Knowledge engineering and the". *Animal Conservation* 9: 11–19.

Martin, T. G., M. A. Burgman, F. Fidler, P. M. Kuhnert, S. Low-choy, M. Mcbride, and K. Mengersen. 2011. "Eliciting Expert Knowledge in Conservation Science". *Conservation Biology* 26: 29–38.

Masden, E. A., and A. S. C. P. Cook. 2016. "Avian collision risk models for wind energy impact assessments". *Environmental Impact Assessment Review* 56: 43–49.

Merrall, E., J. A. Green, L. A. Robinson, A. Butler, M. J. Wood, M. A. Newell, J. Black, F. Daunt, and C. Horswill. 2024. "Incorporating density-dependent regulation into impact assessments for seabirds". *Journal of Applied Ecology* 61: 2510–2524.

Miller, J. A. O., R. W. Furness, M. Trinder, and J. Matthiopoulos. 2019. "The sensitivity of seabird populations to density-dependence, environmental stochasticity and anthropogenic mortality". *Journal of Applied Ecology* 56: 2118–2130.

Niel, C., and J. D. Lebreton. 2005. "Using demographic invariants to detect overharvested bird populations from incomplete data". *Conservation Biology* 19: 826–835.

O'Brien, S. H., A. S. C. P. Cook, and R. A. Robinson. 2017. "Implicit assumptions underlying simple harvest models of marine bird populations can mislead environmental management decisions". *Journal of Environmental Management* 201: 163–171.

R Core Team. 2024. "R: A Language and Environment for Statistical Computing". R Foundation for Statistical Computing.

Raimondo, S., M. Etterson, N. Pollesch, K. Garber, A. Kanarek, W. Lehmann, and J. Awkerman. 2018. "A framework for linking population model development with ecological risk assessment objectives". *Integrated Environmental Assessment and Management* 14: 369–380.

Scott-Hayward, L. A. S., M. L. Mackenzie, and C. G. Walker. 2023a. "MRSea R Package (V1.5.0): Spatially Adaptive Uni and Bi-Variate Regression Splines Using SALSA". University of St Andrews.

Scott-Hayward, L. A. S., M. L. Mackenzie, C. G. Walker, G. Shatumbu, W. Kilian, and P. du Preez. 2023b. "Automated surface feature selection using SALSA2D: Assessing distribution of Elephant carcasses in Etosha National Park".

Searle, K., D. Mobbs, F. Daunt, and A. Butler. 2019. "A Population Viability Analysis modelling tool for seabird species". *Centre for Ecology & Hydrology report for Natural England. Natural England Commissioned Report NECR274*.

Southall, B. L., D. Tollit, J. Amaral, C. W. Clark, and W. T. Ellison. 2023. "Managing human activity and marine mammals: A biologically based, relativistic risk assessment framework". *Frontiers in Marine Science* 10: 1–15.

Stelzenmüller, V., M. Coll, R. Cormier, A. D. Mazaris, M. Pascual, C. Loiseau, J. Claudet, S. Katsanevakis, E. Gissi, A. Evagelopoulos, B. Rumes, S. Degraer, H. Ojaveer, T. Moller, J. Giménez, C. Piroddi, V. Markantonatou, and C. Dimitriadis. 2020. "Operationalizing risk-based cumulative effect assessments in the marine environment". *Science of the Total Environment* 724.

Thieurmel, B. 2017. "R package for calculating sun/moon positions and phases". https://github.com/datastorm-open/suncalc.

Tyack, P. L., L. Thomas, D. P. Costa, A. J. Hall, C. M. Harris, J. Harwood, S. D. Kraus, P. J. O. Miller, M. Moore, T. Photopoulou, E. Pirotta, R. M. Rolland, L. H. Schwacke, S. E. Simmons, and B. L. Southall. 2022. "Managing the effects of multiple stressors on wildlife populations in their ecosystems: developing a cumulative risk approach". *Proceedings of the Royal Society B: Biological Sciences* 289: 20222058.

USEPA. 2016. "Generic Ecological Assessment Endpoints (GEAEs) For Ecological Risk Assessment: Second Edition With Generic Ecosystem Services Endpoints Added". *Usepa*. U.S. Environmental Protection Agency (USEPA), Washington, DC. https://www.epa.gov/sites/default/files/2016-08/documents/geae_2nd_edition.pdf.

Verling, E., R. Miralles Ricós, M. Bou-Cabo, G. Lara, M. Garagouni, J. M. Brignon, and T. O'Higgins. 2021. "Application of a risk-based approach to continuous underwater noise at local and subregional scales for the Marine Strategy Framework Directive". *Marine Policy* 134.

Wade, P. R. 1998. "Calculating limits to the allowable human-caused mortality of cetaceans and pinnipeds". *Marine Mammal Science* 14: 1–37.

Willmott, J. R., G. Forcey, and A. Kent. 2013. "The relative vulnerability of migratory bird species to offshore wind energy projects on the Atlantic outer continental shelf". *OCS Study BOEM 2013-207*: 275 pp.

8 Appendix 2: Spatial outputs, diagnostics and risk-mapping by species unit

The following outputs are shown for each species unit:

1. Modelled density distributions from the spatial distribution models and distance-corrected observation data for each season and where, in both cases, density represents birds/km^2. Distance-corrected data are shown as averaged (circles on top plots) and both time-weighted average (emphasizing newest data) and reverse time-weighted average (emphasizing historical data). Any differences between the forward- and reverse-weighted maps indicate changes in density distribution between the beginning and end of the study period (1999-2025). This is used as a diagnostic tool to evaluate any genuine shifts in distribution over time.
2. Spatial Modelling diagnostics – best selected model for each season and diagnostics to assess residual correlation and the assumed mean-variance relationships.
3. Species-specific risk-mapping outputs. The maps show the rescaling of estimated density distributions to habitat risk for each species unit, overlaid with existing and proposed turbine installations. Species unit abundance and top-use areas are shown as cumulative percentiles. If any SPAs are designated for one or more species in the species unit, they are shown. Otherwise, they are omitted.

8.1 Results by species unit

8.1.1 Razorbill/ common guillemot. Species unit “Alcid”

Spatial modelling data and results

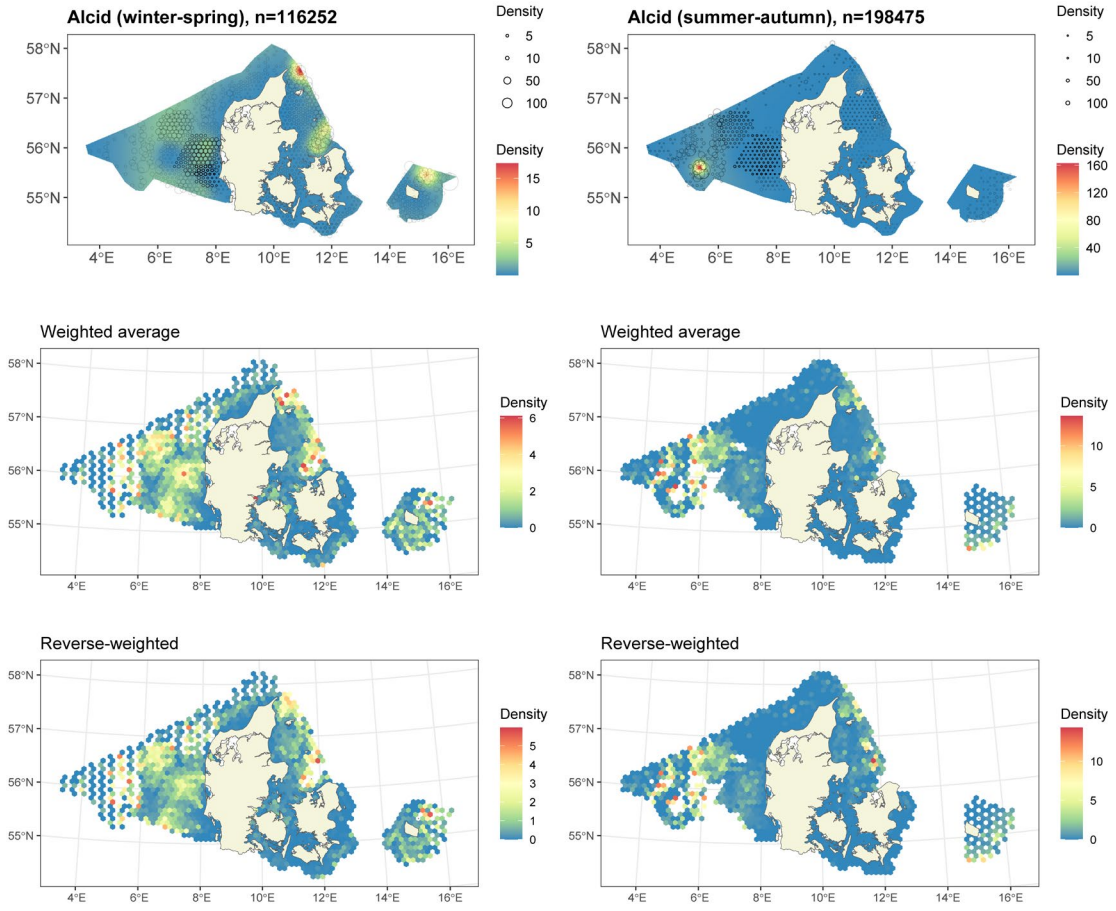

Aerial survey data and modelled density distributions. Top panel raster surface(s) show the modelled density distributions, overlaid with density corrected for detectability and averaged over segments in 10km hexagons (symbol size). Symbol transparency indicates time-weighted sample size in each hexagon. The average densities are provided both without any weighting (top), with time weighting (raster map in the middle), and with reverse time-weighting (raster map in the bottom). Time-weighting emphasizes the newest data, while reverse-weighting emphasizes the oldest data. Differences between the two can be used to indicate changes in density distribution between the beginning and end of the study period (1999-2025).

8.1.2 Diagnostics for the best spatial models

Species unit	Seasons	Best model	1D terms	2D term	Distribution	Tweedie parameter	Dispersion parameter
Alcid	winter, spring	Best 1D2D	s(distcoast, df=2)	s(x,y, df=14)	Tweedie	1.37	34
Alcid	summer, autumn	Best 1D2D	s(distcoast, df=2)	s(x,y, df=7)	Tweedie	1.38	63

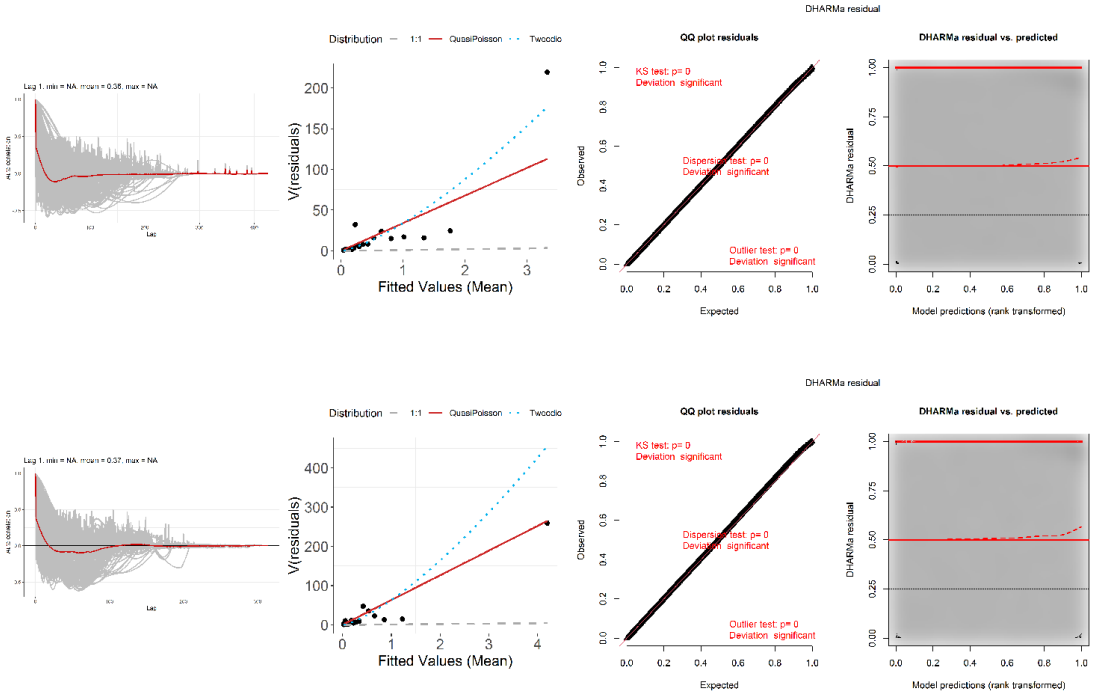

Diagnostics for the best spatial model(s) listed in the table above. For species present in Danish marine waters year-round, models were fitted separately for winter-spring (top) and summer-autumn (bottom). For strongly seasonal species, a single model was fitted to the months the species is present. Left: within-block autocorrelation function, with the grey lines representing the residual correlation observed in each transect and the red line the average of these values across transects. Second left: the estimated mean-variance relationship (Quasi-Poisson: red line, Tweedie: blue dashed line) against observed values (black symbols), with grey dashed line showing 1:1 relationship for reference. Right two panels: QQplot and residuals against predicted values. The red stars are outliers and the red line is a smooth spline around the mean of the residuals. Note: Whilst the tests on the QQ plot indicate that there might be an issue this is owing to the large volume of data and practically we find no significant deviations.

8.1.3 Risk-mapping

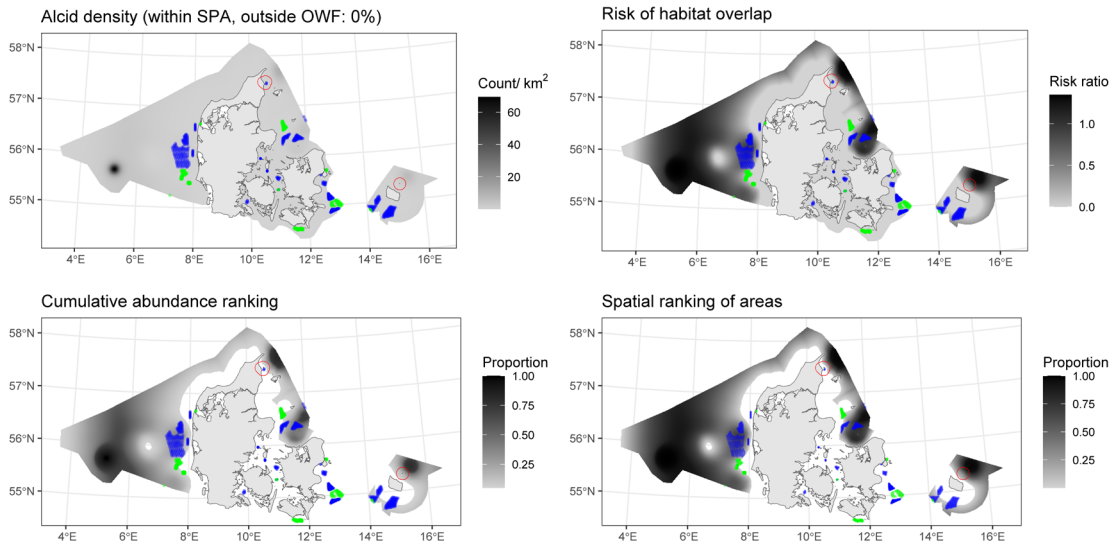

The rescaling of estimated density distribution (top left) to habitat risk for the species unit (top right). Bottom left and right: species unit abundance and top-use areas as cumulative percentiles (up to 0.95 abundance, defining species unit range). Red polygons: any SPAs designated for one or more species in the species unit. Existing wind turbines are shown in green and proposed future turbine locations in blue. Percentage population with area-based protections, defined as total density within SPA boundaries and >2 km away from existing or future turbine locations, is provided in the top-left panel title (rounded to nearest decimal place).

8.2 Red-throated diver/ black-throated diver. Species unit "Diver"

8.2.1 Spatial modelling data and results

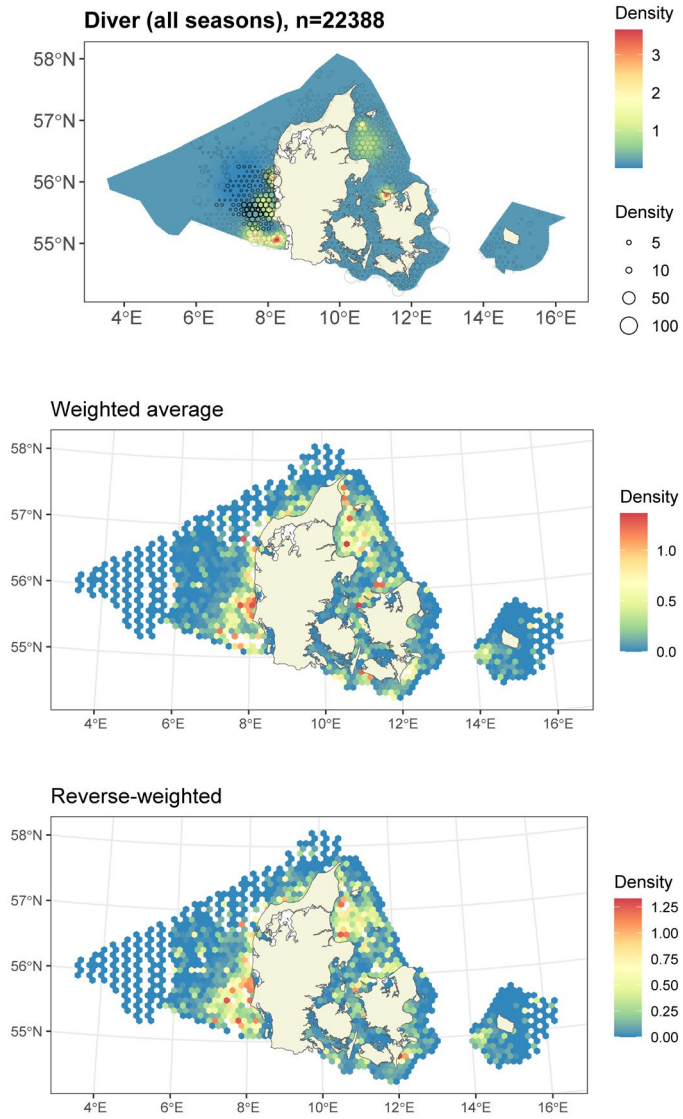

Aerial survey data and modelled density distributions. Top panel raster surface(s) show the modelled density distributions, overlaid with density corrected for detectability and averaged over segments in 10km hexagons (symbol size). Symbol transparency indicates time-weighted sample size in each hexagon. The average densities are provided both without any weighting (top), with time weighting (raster map in the middle), and with reverse time-weighting (raster map in the bottom). Time-weighting emphasizes the newest data, while reverse-weighting emphasizes the oldest data. Differences between the two can be used to indicate changes in density distribution between the beginning and end of the study period (1999-2025).

8.2.2 Diagnostics for the best spatial models

Species unit	Seasons	Best model	1D terms	2D term	Distribution	Tweedie parameter	Dispersion parameter
Diver	winter, spring, autumn	Best 1D2D	NA	s(x,y, df=13)	Tweedie	1.28	27

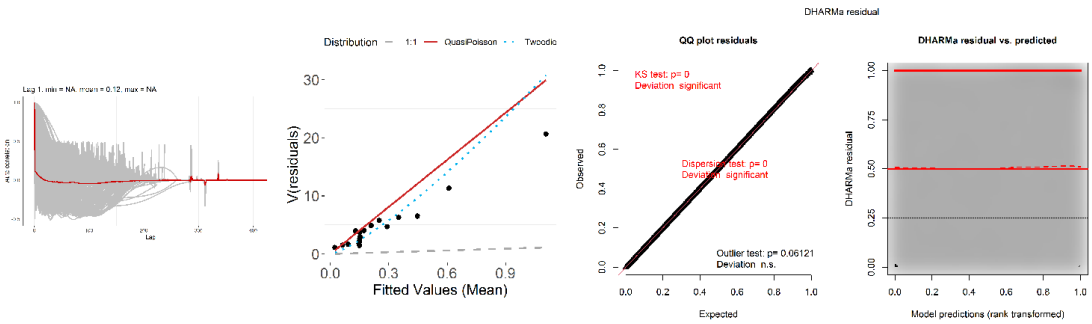

Diagnostics for the best spatial model(s) listed in the table above. For species present in Danish marine waters year-round, models were fitted separately for winter-spring (top) and summer-autumn (bottom). For strongly seasonal species, a single model was fitted to the months the species is present. Left: within-block autocorrelation function, with the grey lines representing the residual correlation observed in each transect and the red line the average of these values across transects. Second left: the estimated mean-variance relationship (Quasi-Poisson: red line, Tweedie: blue dashed line) against observed values (black symbols), with grey dashed line showing 1:1 relationship for reference. Right two panels: QQplot and residuals against predicted values. The red stars are outliers and the red line is a smooth spline around the mean of the residuals. Note: Whilst the tests on the QQ plot indicate that there might be an issue this is owing to the large volume of data and practically we find no significant deviations.

8.2.3 Risk-mapping

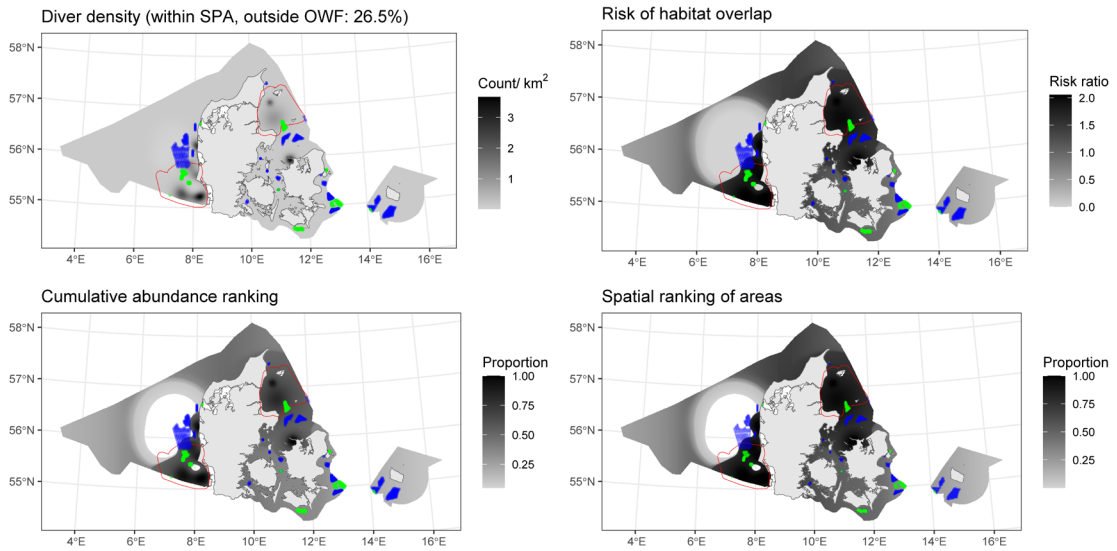

The rescaling of estimated density distribution (top left) to habitat risk for the species unit (top right). Bottom left and right: species unit abundance and top-use areas as cumulative percentiles (up to 0.95 abundance, defining species unit range). Red polygons: any SPAs designated for one or more species in the species unit. Existing wind turbines are shown in green and proposed future turbine locations in blue. Percentage population with area-based protections, defined as total density within SPA boundaries and >2 km away from existing or future turbine locations, is provided in the top-left panel title (rounded to nearest decimal place).

8.3 Common eider. Species unit “Eider”

8.3.1 Spatial modelling data and results

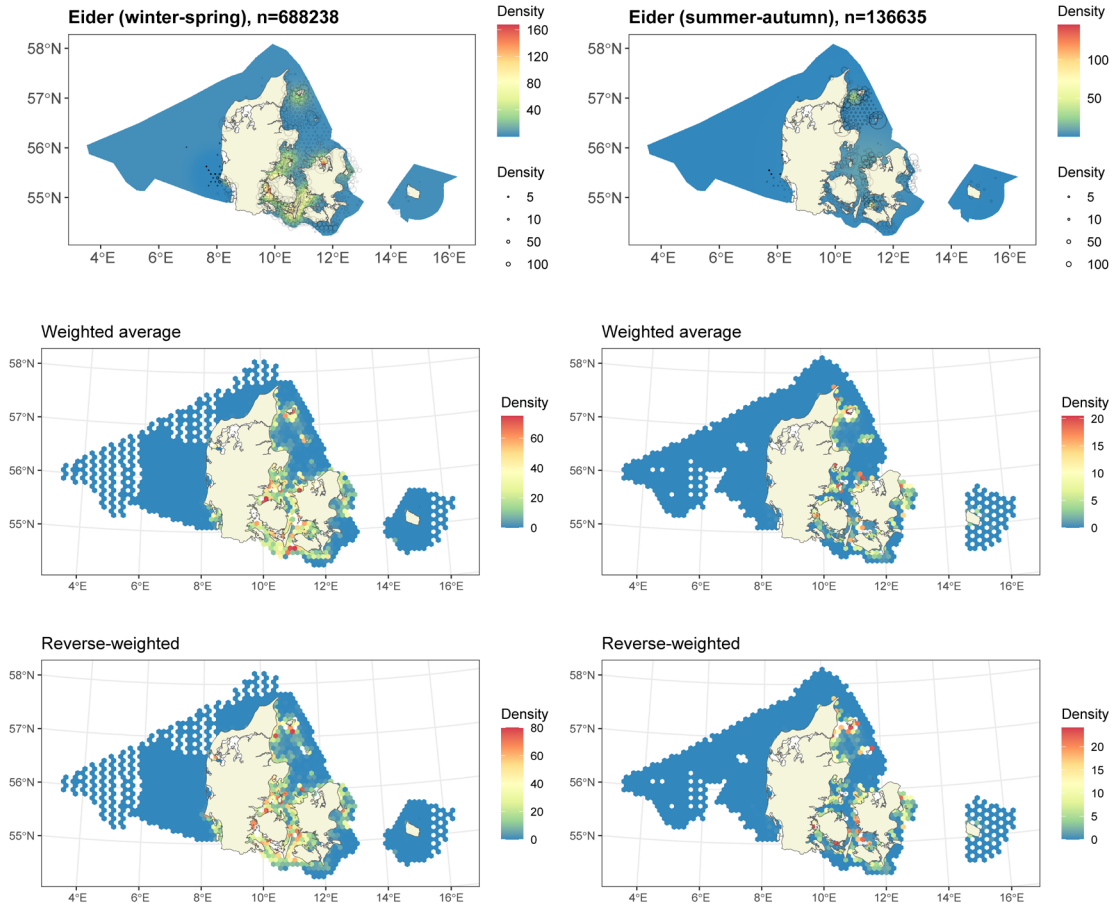

Aerial survey data and modelled density distributions. Top panel raster surface(s) show the modelled density distributions, overlaid with density corrected for detectability and averaged over segments in 10km hexagons (symbol size). Symbol transparency indicates time-weighted sample size in each hexagon. The average densities are provided both without any weighting (top), with time weighting (raster map in the middle), and with reverse time-weighting (raster map in the bottom). Time-weighting emphasizes the newest data, while reverse-weighting emphasizes the oldest data. Differences between the two can be used to indicate changes in density distribution between the beginning and end of the study period (1999-2025).

8.3.2 Diagnostics for the best spatial models

Species unit	Seasons	Best model	1D terms	2D term	Distribution	Tweedie parameter	Dispersion parameter
Eider	winter, spring	Best 1D2D	NA	s(x,y, df=11)	quasipoisson	NA	337.5
Eider	summer, autumn	Best 1D2D	NA	s(x,y, df=3)	quasipoisson	NA	362.7

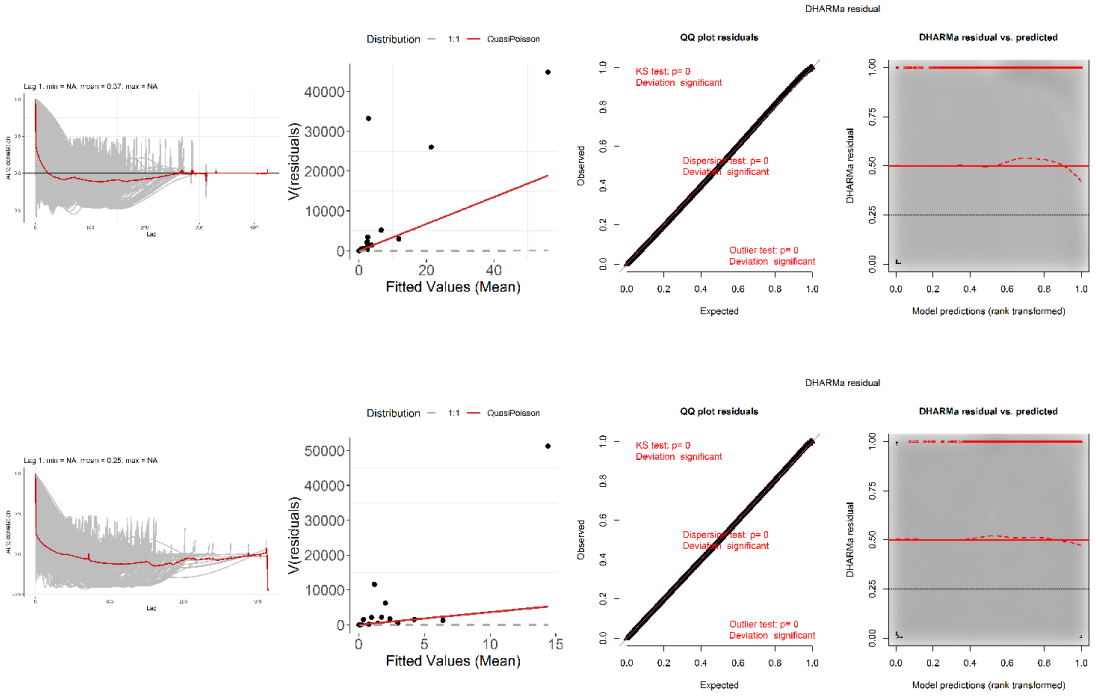

Diagnostics for the best spatial model(s) listed in the table above. For species present in Danish marine waters year-round, models were fitted separately for winter-spring (top) and summer-autumn (bottom). For strongly seasonal species, a single model was fitted to the months the species is present. Left: within-block autocorrelation function, with the grey lines representing the residual correlation observed in each transect and the red line the average of these values across transects. Second left: the estimated mean-variance relationship (Quasi-Poisson: red line, Tweedie: blue dashed line) against observed values (black symbols), with grey dashed line showing 1:1 relationship for reference. Right two panels: QQplot and residuals against predicted values. The red stars are outliers and the red line is a smooth spline around the mean of the residuals. Note: Whilst the tests on the QQ plot indicate that there might be an issue this is owing to the large volume of data and practically we find no significant deviations.

8.3.3 Risk-mapping

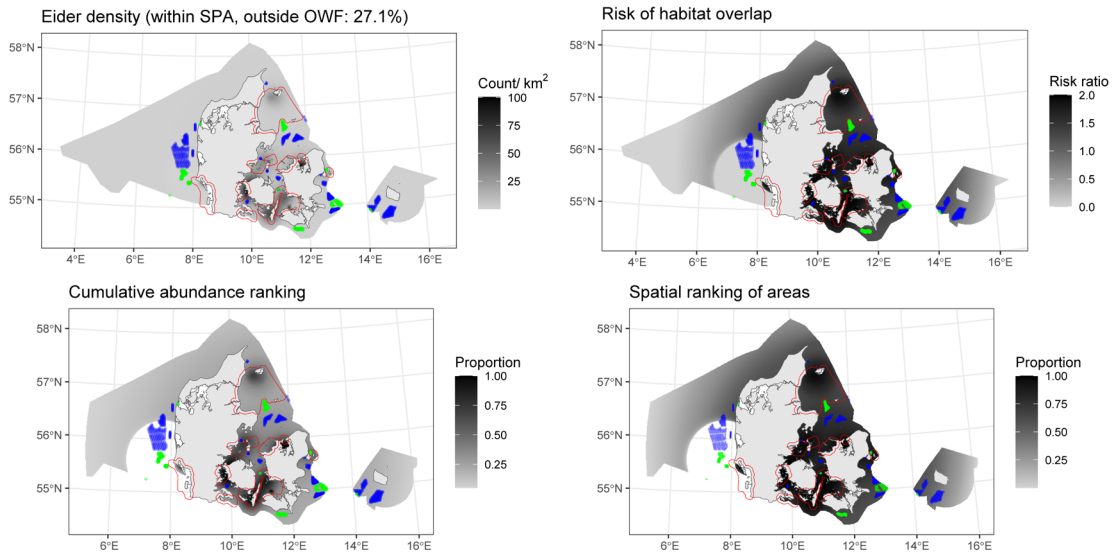

The rescaling of estimated density distribution (top left) to habitat risk for the species unit (top right). Bottom left and right: species unit abundance and top-use areas as cumulative percentiles (up to 0.95 abundance, defining species unit range). Red polygons: any SPAs designated for one or more species in the species unit. Existing wind turbines are shown in green and proposed future turbine locations in blue. Percentage population with area-based protections, defined as total density within SPA boundaries and >2 km away from existing or future turbine locations, is provided in the top-left panel title (rounded to nearest decimal place).

8.4 Northern fulmar. Species unit “Fulmar”

8.4.1 Spatial modelling data and results

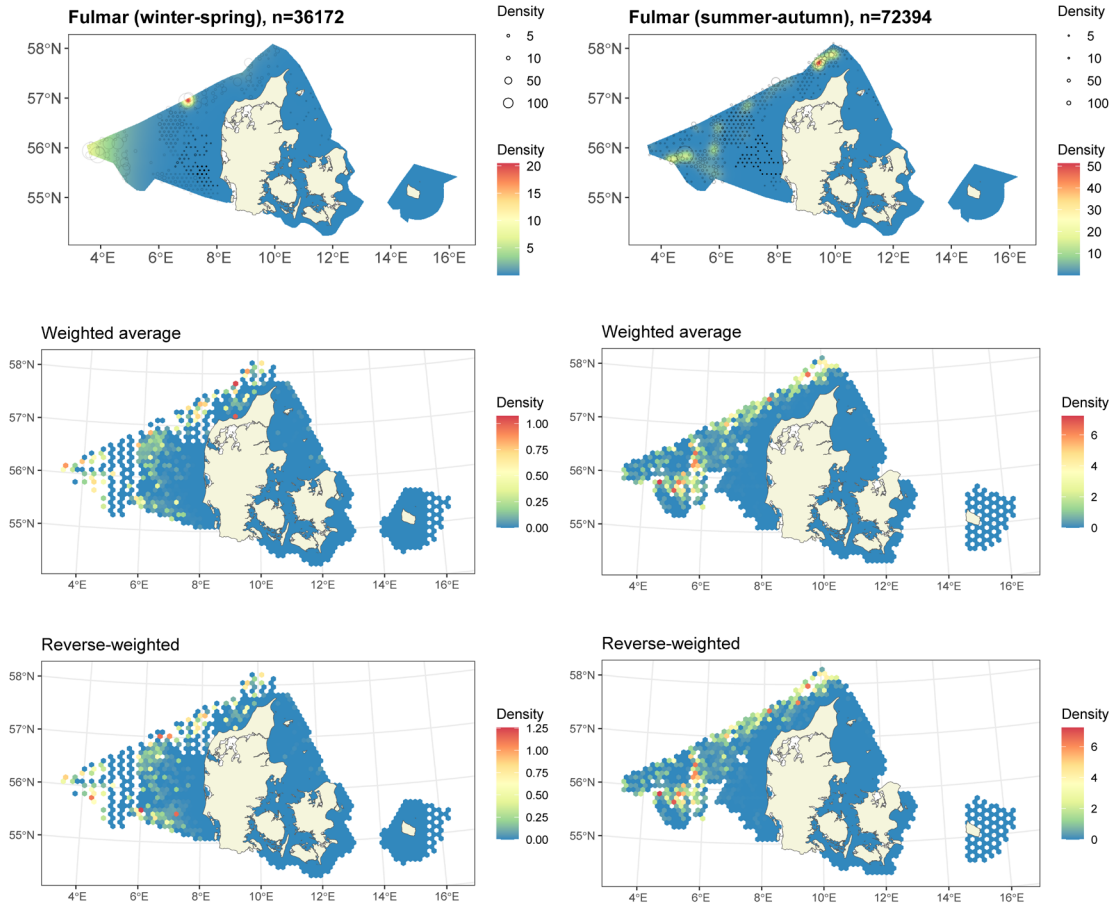

Aerial survey data and modelled density distributions. Top panel raster surface(s) show the modelled density distributions, overlaid with density corrected for detectability and averaged over segments in 10km hexagons (symbol size). Symbol transparency indicates time-weighted sample size in each hexagon. The average densities are provided both without any weighting (top), with time weighting (raster map in the middle), and with reverse time-weighting (raster map in the bottom). Time-weighting emphasizes the newest data, while reverse-weighting emphasizes the oldest data. Differences between the two can be used to indicate changes in density distribution between the beginning and end of the study period (1999-2025).

8.4.2 Diagnostics for the best spatial models

Species unit	Seasons	Best model	1D terms	2D term	Distribution	Tweedie parameter	Dispersion parameter
Fulmar	winter, spring	Best 1D2D	s(distcoast, df=2)	s(x,y, df=2)	Tweedie	1.39	148.8
Fulmar	summer, autumn	2D Only	NA	s(x,y, df=17)	Tweedie	1.39	29.5

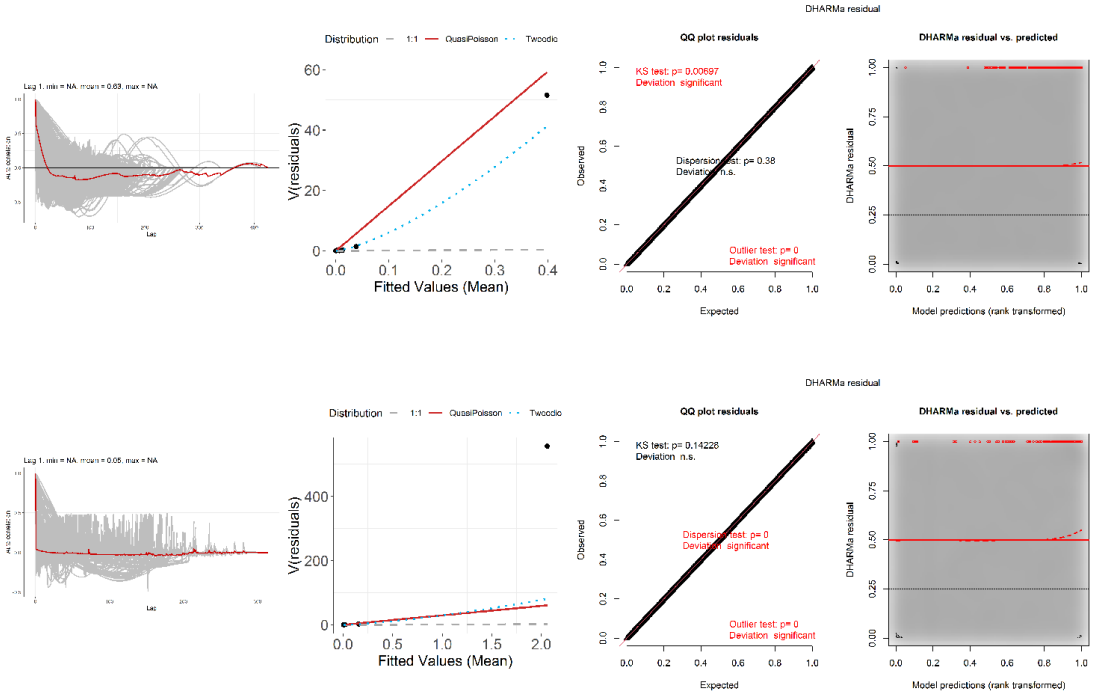

Diagnostics for the best spatial model(s) listed in the table above. For species present in Danish marine waters year-round, models were fitted separately for winter-spring (top) and summer-autumn (bottom). For strongly seasonal species, a single model was fitted to the months the species is present. Left: within-block autocorrelation function, with the grey lines representing the residual correlation observed in each transect and the red line the average of these values across transects. Second left: the estimated mean-variance relationship (Quasi-Poisson: red line, Tweedie: blue dashed line) against observed values (black symbols), with grey dashed line showing 1:1 relationship for reference. Right two panels: QQplot and residuals against predicted values. The red stars are outliers and the red line is a smooth spline around the mean of the residuals. Note: Whilst the tests on the QQ plot indicate that there might be an issue this is owing to the large volume of data and practically we find no significant deviations.

8.4.3 Risk-mapping

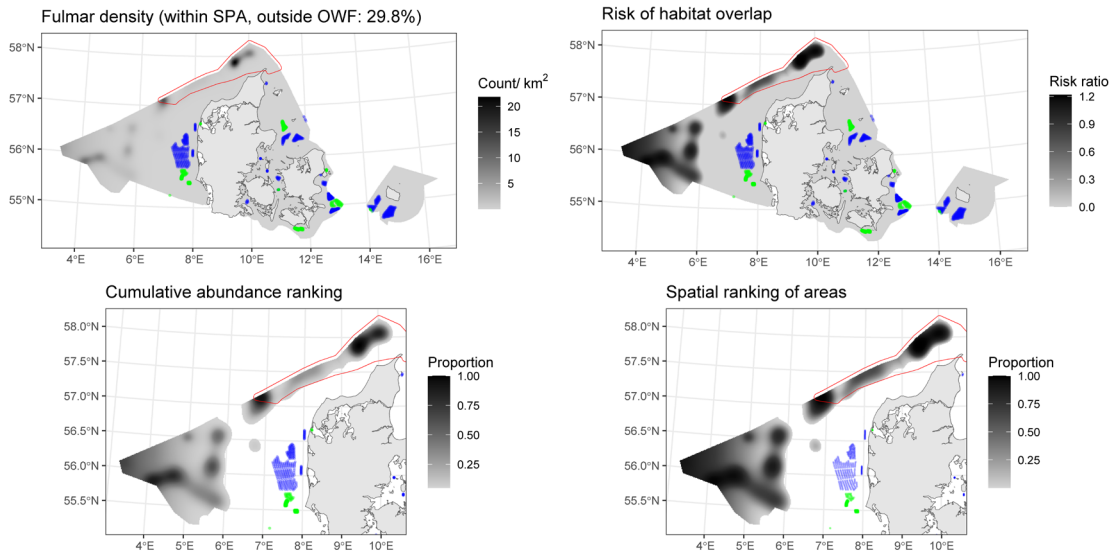

The rescaling of estimated density distribution (top left) to habitat risk for the species unit (top right). Bottom left and right: species unit abundance and top-use areas as cumulative percentiles (up to 0.95 abundance, defining species unit range). Red polygons: any SPAs designated for one or more species in the species unit. Existing wind turbines are shown in green and proposed future turbine locations in blue. Percentage population with area-based protections, defined as total density within SPA boundaries and >2 km away from existing or future turbine locations, is provided in the top-left panel title (rounded to nearest decimal place).

8.5 Northern gannet. Species unit “Gannet”

8.5.1 Spatial modelling data and results

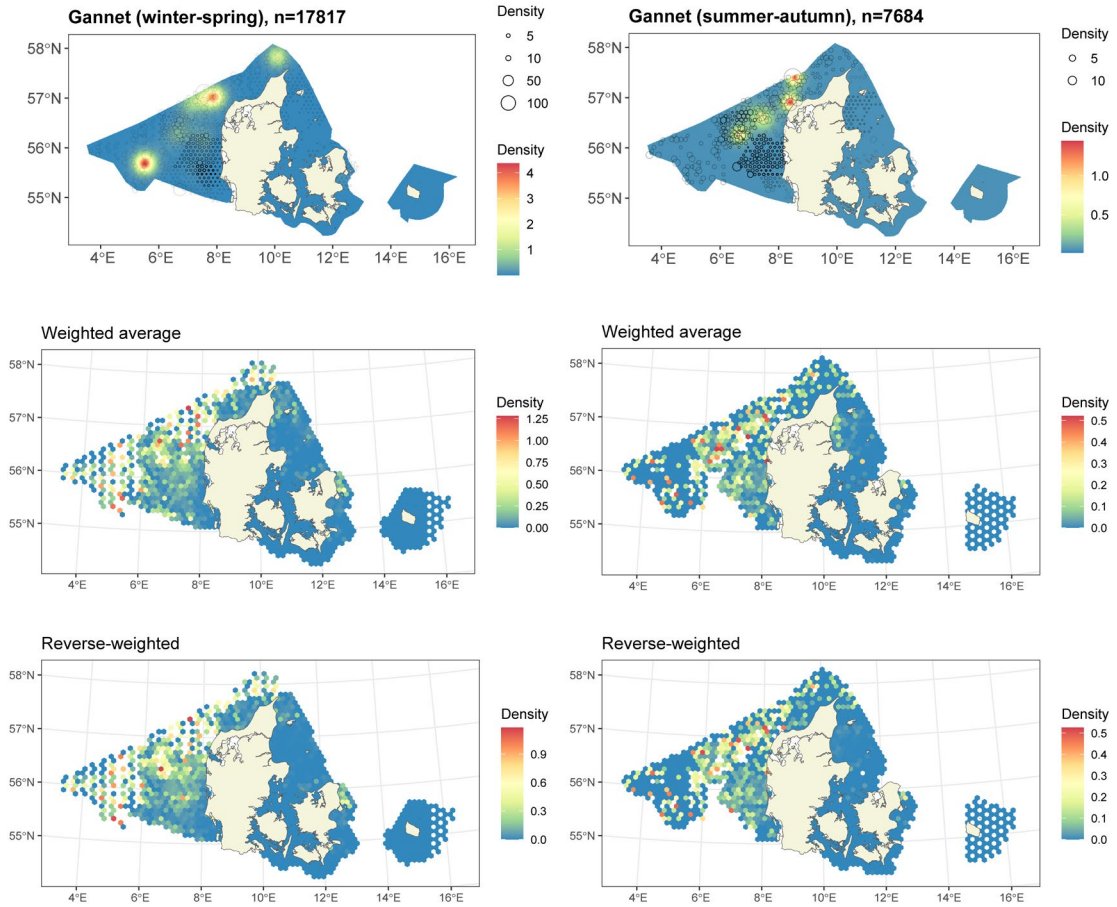

Aerial survey data and modelled density distributions. Top panel raster surface(s) show the modelled density distributions, overlaid with density corrected for detectability and averaged over segments in 10km hexagons (symbol size). Symbol transparency indicates time-weighted sample size in each hexagon. The average densities are provided both without any weighting (top), with time weighting (raster map in the middle), and with reverse time-weighting (raster map in the bottom). Time-weighting emphasizes the newest data, while reverse-weighting emphasizes the oldest data. Differences between the two can be used to indicate changes in density distribution between the beginning and end of the study period (1999-2025).

8.5.2 Diagnostics for the best spatial models

Species unit	Seasons	Best model	1D terms	2D term	Distribution	Tweedie parameter	Dispersion parameter
Gannet	winter, spring	Best 1D2D	NA	s(x,y, df=11)	Tweedie	1.28	22.9
Gannet	summer, autumn	2D Only	NA	s(x,y, df=5)	Tweedie	1.22	13.9

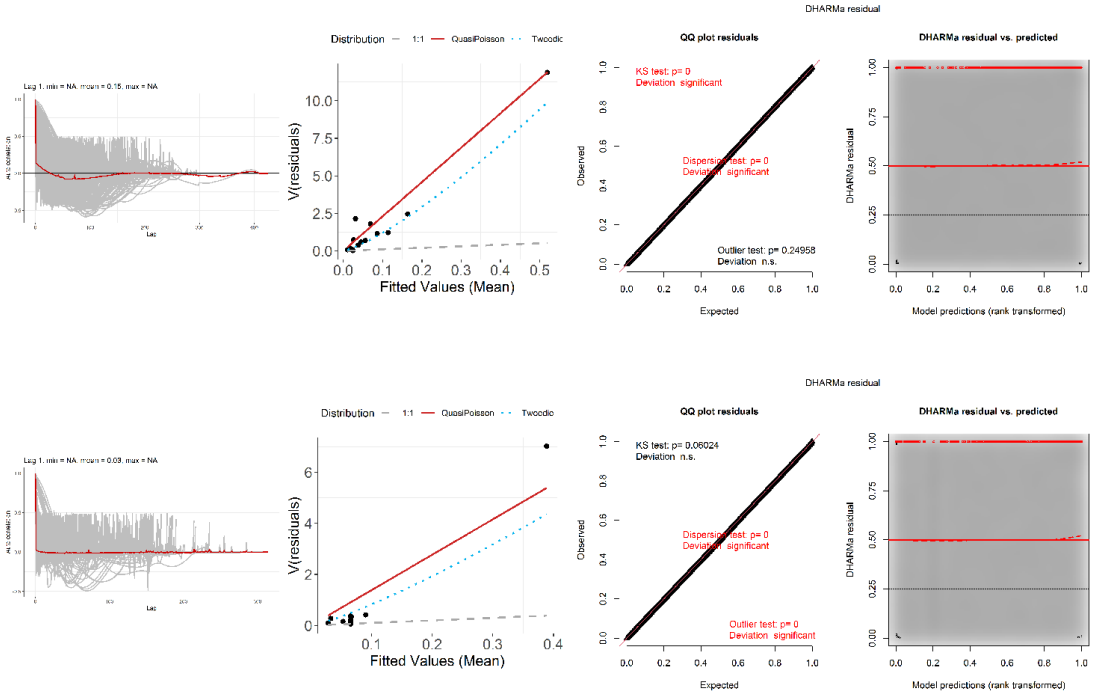

Diagnostics for the best spatial model(s) listed in the table above. For species present in Danish marine waters year-round, models were fitted separately for winter-spring (top) and summer-autumn (bottom). For strongly seasonal species, a single model was fitted to the months the species is present. Left: within-block autocorrelation function, with the grey lines representing the residual correlation observed in each transect and the red line the average of these values across transects. Second left: the estimated mean-variance relationship (Quasi-Poisson: red line, Tweedie: blue dashed line) against observed values (black symbols), with grey dashed line showing 1:1 relationship for reference. Right two panels: QQplot and residuals against predicted values. The red stars are outliers and the red line is a smooth spline around the mean of the residuals. Note: Whilst the tests on the QQ plot indicate that there might be an issue this is owing to the large volume of data and practically we find no significant deviations.

8.5.3 Risk-mapping

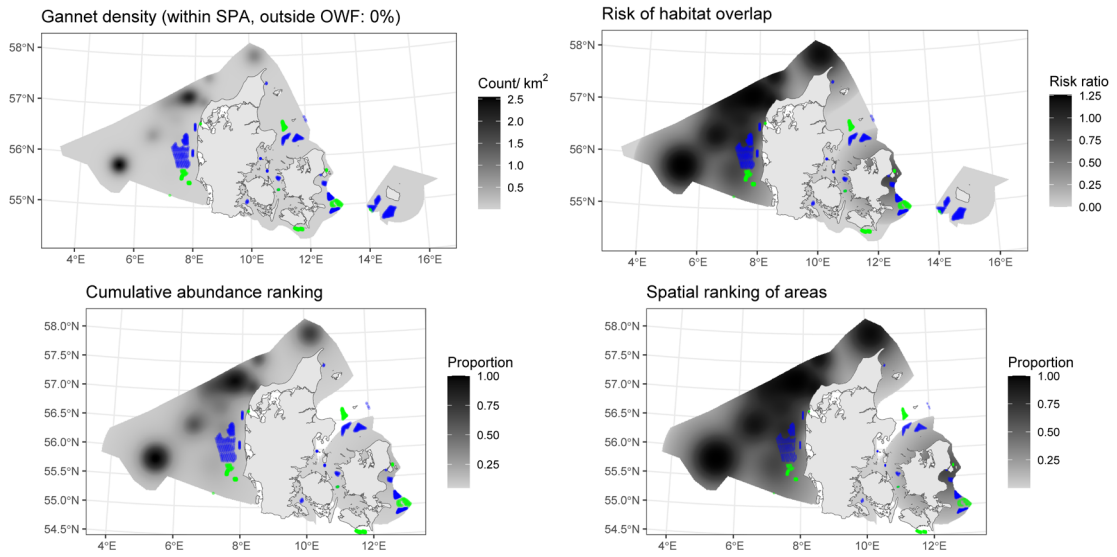

The rescaling of estimated density distribution (top left) to habitat risk for the species unit (top right). Bottom left and right: species unit abundance and top-use areas as cumulative percentiles (up to 0.95 abundance, defining species unit range). Red polygons: any SPAs designated for one or more species in the species unit. Existing wind turbines are shown in green and proposed future turbine locations in blue. Percentage population with area-based protections, defined as total density within SPA boundaries and >2 km away from existing or future turbine locations, is provided in the top-left panel title (rounded to nearest decimal place).

8.6 Great black-backed gull. Species unit “GBBG”

8.6.1 Spatial modelling data and results

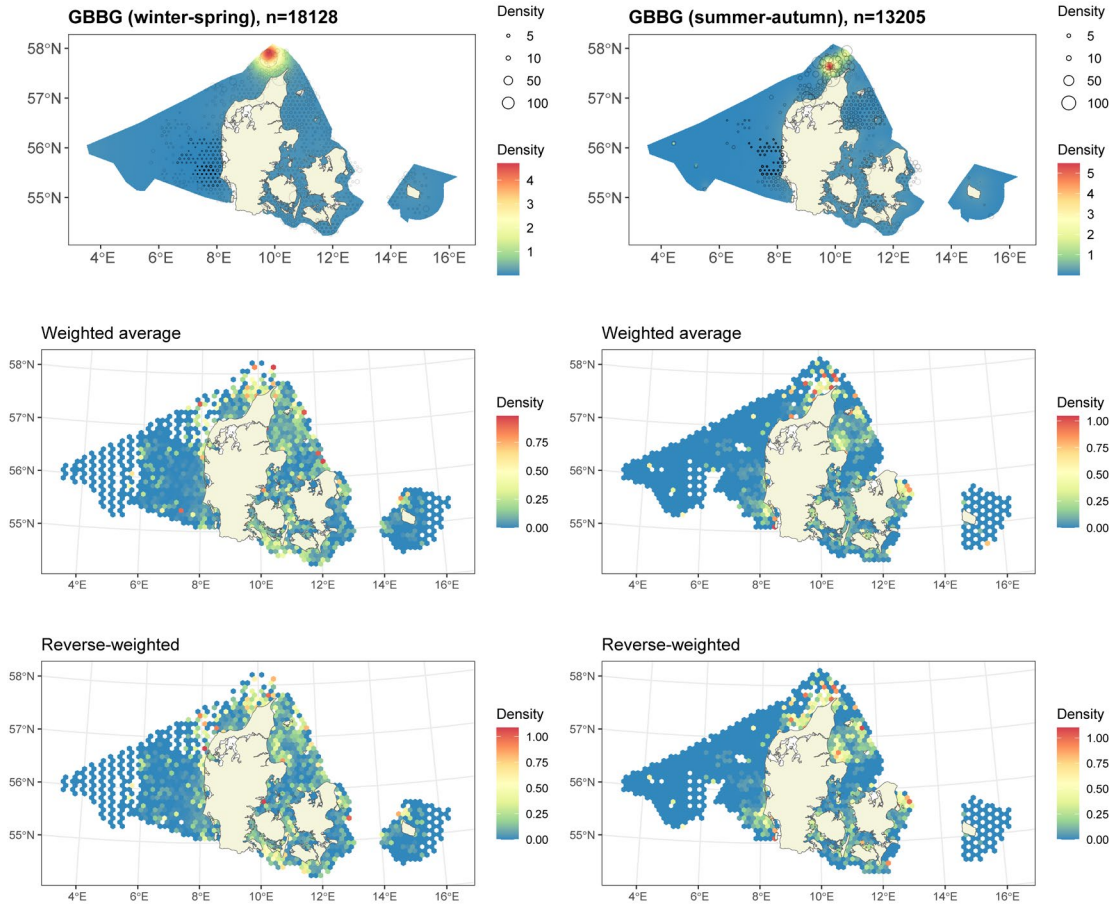

Aerial survey data and modelled density distributions. Top panel raster surface(s) show the modelled density distributions, overlaid with density corrected for detectability and averaged over segments in 10km hexagons (symbol size). Symbol transparency indicates time-weighted sample size in each hexagon. The average densities are provided both without any weighting (top), with time weighting (raster map in the middle), and with reverse time-weighting (raster map in the bottom). Time-weighting emphasizes the newest data, while reverse-weighting emphasizes the oldest data. Differences between the two can be used to indicate changes in density distribution between the beginning and end of the study period (1999-2025).

8.6.2 Diagnostics for the best spatial models

Species unit	Seasons	Best model	1D terms	2D term	Distribution	Tweedie parameter	Dispersion parameter
GBBG	winter, spring	Best 1D2D	s(distcoast, df=2)	s(x,y, df=2)	Tweedie	1.35	62.0
GBBG	summer, autumn	Best 1D2D	distcoast, df=1	s(x,y, df=6)	Tweedie	1.22	27.1

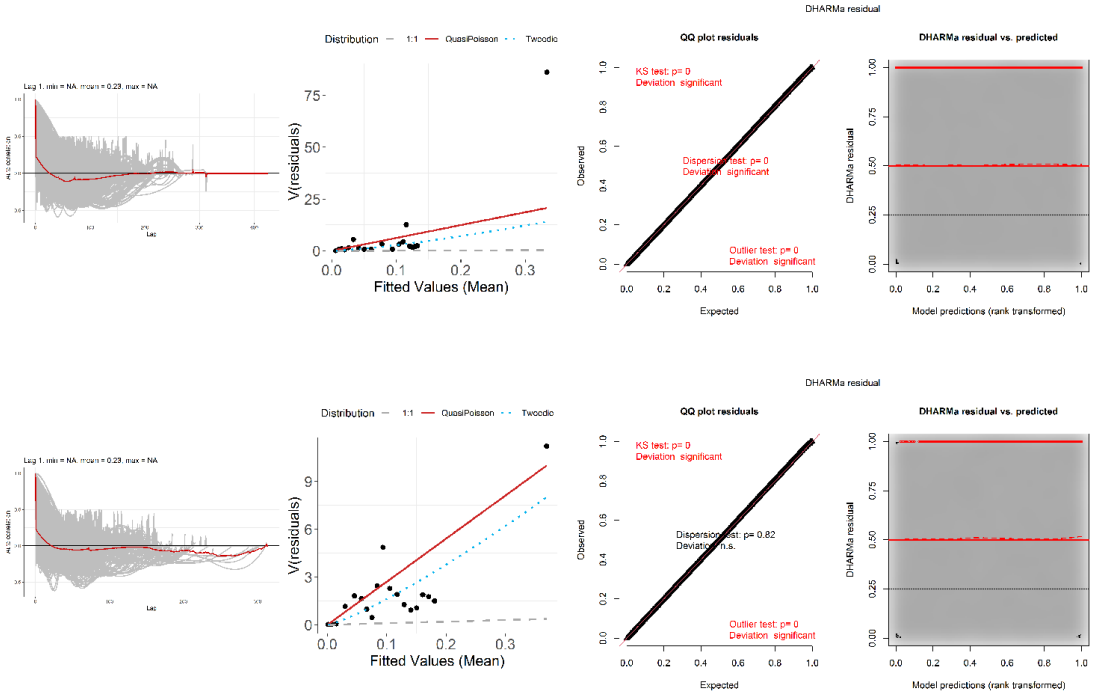

Diagnostics for the best spatial model(s) listed in the table above. For species present in Danish marine waters year-round, models were fitted separately for winter-spring (top) and summer-autumn (bottom). For strongly seasonal species, a single model was fitted to the months the species is present. Left: within-block autocorrelation function, with the grey lines representing the residual correlation observed in each transect and the red line the average of these values across transects. Second left: the estimated mean-variance relationship (Quasi-Poisson: red line, Tweedie: blue dashed line) against observed values (black symbols), with grey dashed line showing 1:1 relationship for reference. Right two panels: QQplot and residuals against predicted values. The red stars are outliers and the red line is a smooth spline around the mean of the residuals. Note: Whilst the tests on the QQ plot indicate that there might be an issue this is owing to the large volume of data and practically we find no significant deviations.

8.6.3 Risk-mapping

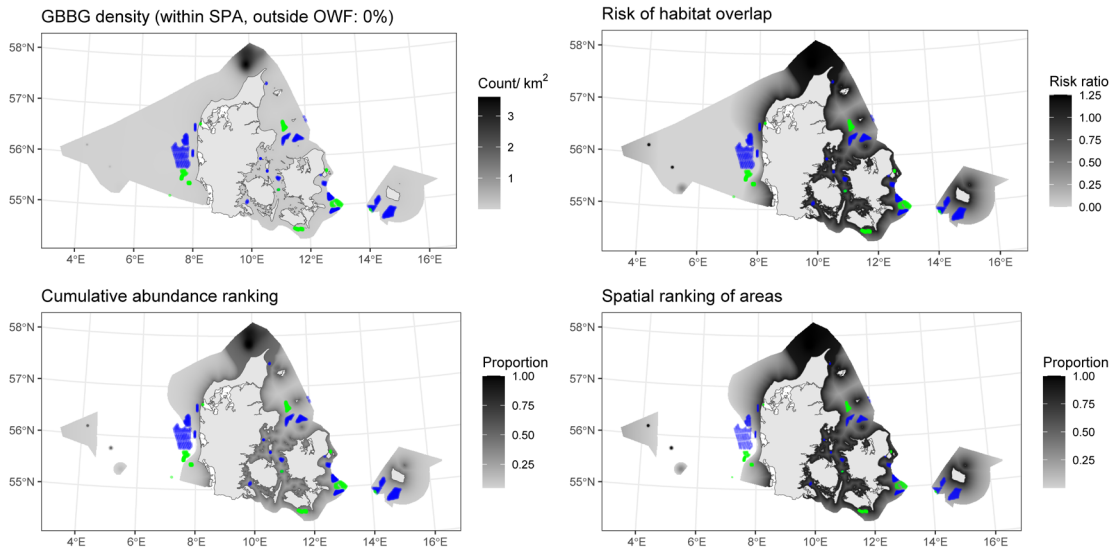

The rescaling of estimated density distribution (top left) to habitat risk for the species unit (top right). Bottom left and right: species unit abundance and top-use areas as cumulative percentiles (up to 0.95 abundance, defining species unit range). Red polygons: any SPAs designated for one or more species in the species unit. Existing wind turbines are shown in green and proposed future turbine locations in blue. Percentage population with area-based protections, defined as total density within SPA boundaries and >2 km away from existing or future turbine locations, is provided in the top-left panel title (rounded to nearest decimal place).

8.7 Common Goldeneye. Species unit “Goldeneye”

8.7.1 Spatial modelling data and results

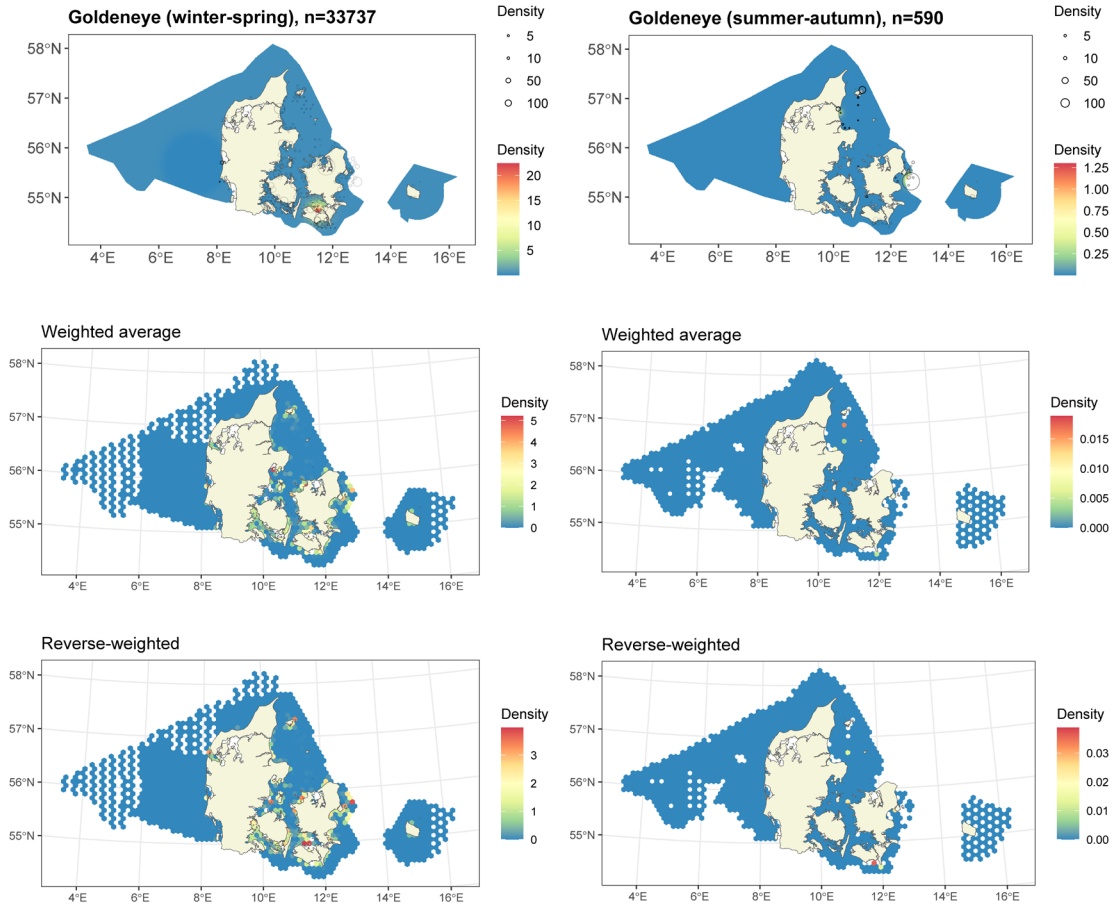

Aerial survey data and modelled density distributions. Top panel raster surface(s) show the modelled density distributions, overlaid with density corrected for detectability and averaged over segments in 10km hexagons (symbol size). Symbol transparency indicates time-weighted sample size in each hexagon. The average densities are provided both without any weighting (top), with time weighting (raster map in the middle), and with reverse time-weighting (raster map in the bottom). Time-weighting emphasizes the newest data, while reverse-weighting emphasizes the oldest data. Differences between the two can be used to indicate changes in density distribution between the beginning and end of the study period (1999-2025).

8.7.2 Diagnostics for the best spatial models

Species unit	Seasons	Best model	1D terms	2D term	Distribution	Tweedie parameter	Dispersion parameter
Goldeneye	winter, spring	Best 1D2D	NA	s(x,y, df=2)	Tweedie	1.37	368.4
Goldeneye	summer, autumn	Best 1D2D	NA	s(x,y, df=2)	Tweedie	1.41	2204.9

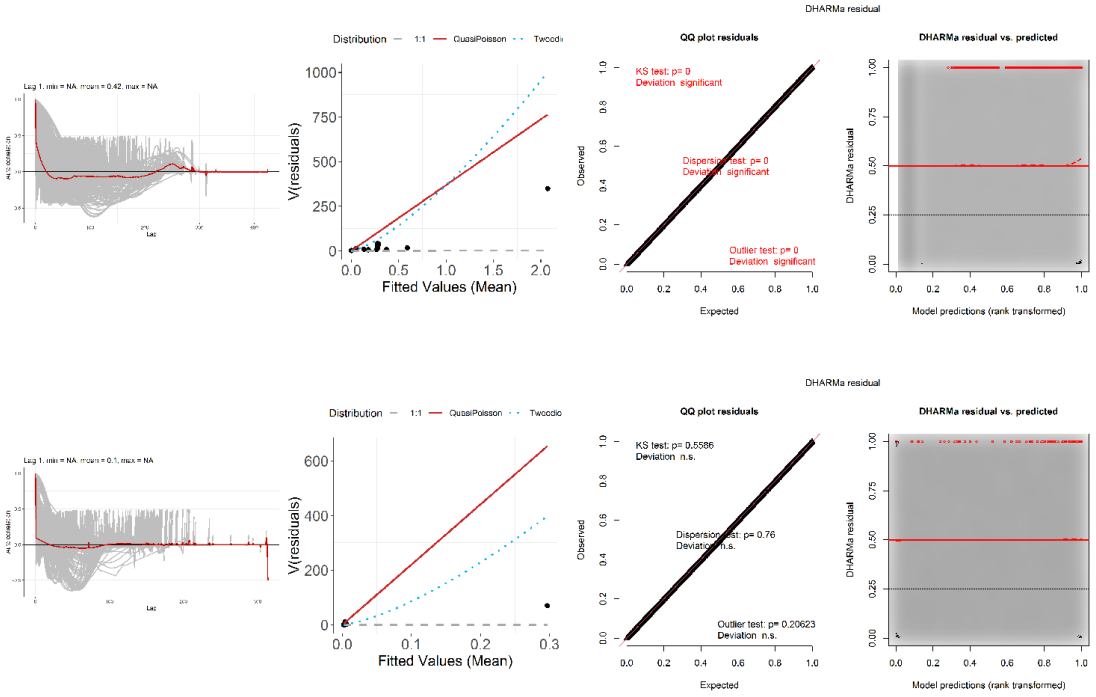

Diagnostics for the best spatial model(s) listed in the table above. For species present in Danish marine waters year-round, models were fitted separately for winter-spring (top) and summer-autumn (bottom). For strongly seasonal species, a single model was fitted to the months the species is present. Left: within-block autocorrelation function, with the grey lines representing the residual correlation observed in each transect and the red line the average of these values across transects. Second left: the estimated mean-variance relationship (Quasi-Poisson: red line, Tweedie: blue dashed line) against observed values (black symbols), with grey dashed line showing 1:1 relationship for reference. Right two panels: QQplot and residuals against predicted values. The red stars are outliers and the red line is a smooth spline around the mean of the residuals. Note: Whilst the tests on the QQ plot indicate that there might be an issue this is owing to the large volume of data and practically we find no significant deviations.

8.7.3 Risk-mapping

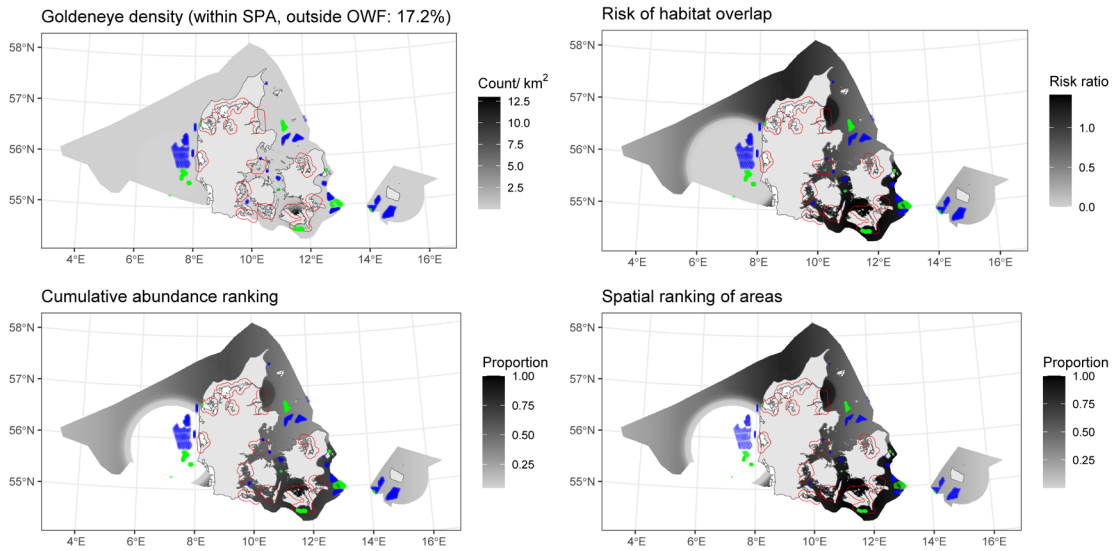

The rescaling of estimated density distribution (top left) to habitat risk for the species unit (top right). Bottom left and right: species unit abundance and top-use areas as cumulative percentiles (up to 0.95 abundance, defining species unit range). Red polygons: any SPAs designated for one or more species in the species unit. Existing wind turbines are shown in green and proposed future turbine locations in blue. Percentage population with area-based protections, defined as total density within SPA boundaries and >2 km away from existing or future turbine locations, is provided in the top-left panel title (rounded to nearest decimal place).

8.8 Crested grebe/ red-necked grebe. Species unit “Grebe”

8.8.1 Spatial modelling data and results

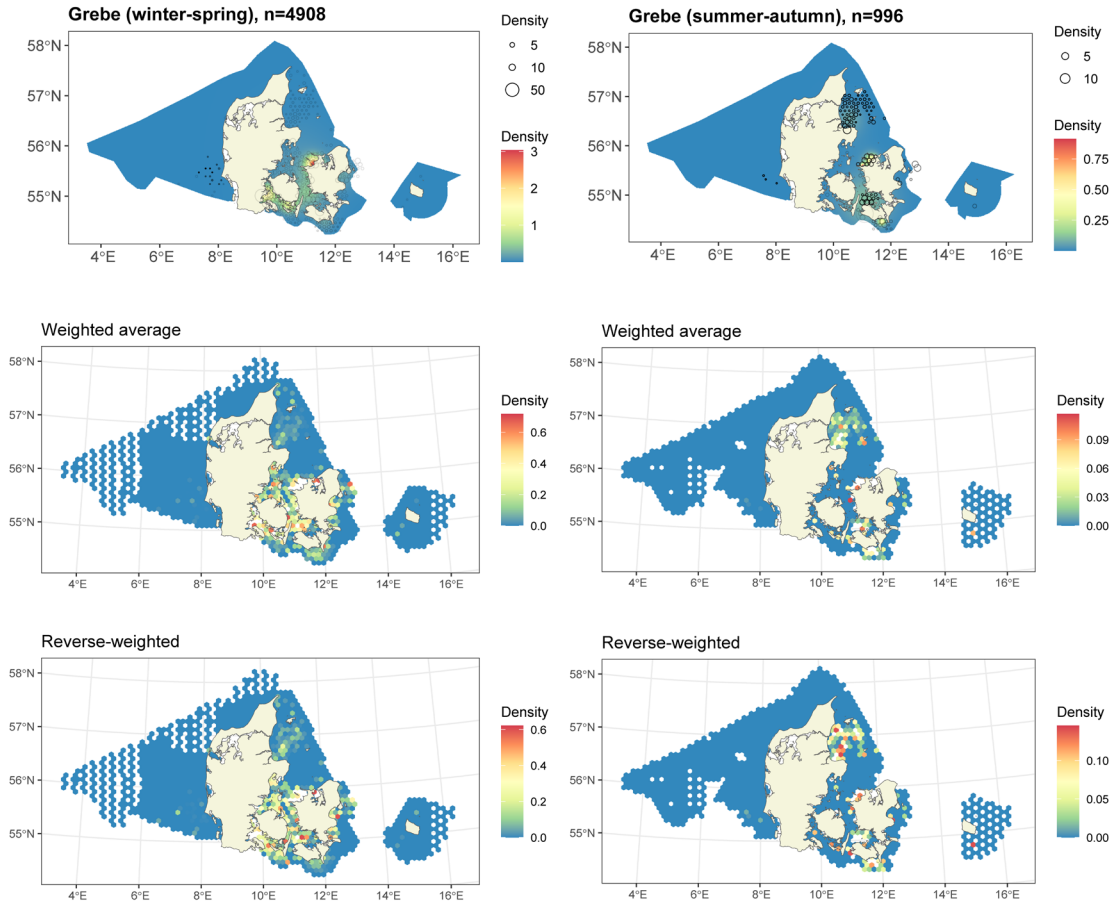

Aerial survey data and modelled density distributions. Top panel raster surface(s) show the modelled density distributions, overlaid with density corrected for detectability and averaged over segments in 10km hexagons (symbol size). Symbol transparency indicates time-weighted sample size in each hexagon. The average densities are provided both without any weighting (top), with time weighting (raster map in the middle), and with reverse time-weighting (raster map in the bottom). Time-weighting emphasizes the newest data, while reverse-weighting emphasizes the oldest data. Differences between the two can be used to indicate changes in density distribution between the beginning and end of the study period (1999-2025).

8.8.2 Diagnostics for the best spatial models

Species unit	Seasons	Best model	1D terms	2D term	Distribution	Tweedie parameter	Dispersion parameter
Grebe	winter, spring	Best 1D2D	NA	s(x,y, df=8)	Tweedie	1.32	101.3
Grebe	summer, autumn	Best 1D2D	NA	s(x,y, df=5)	quasipoisson	NA	7.7

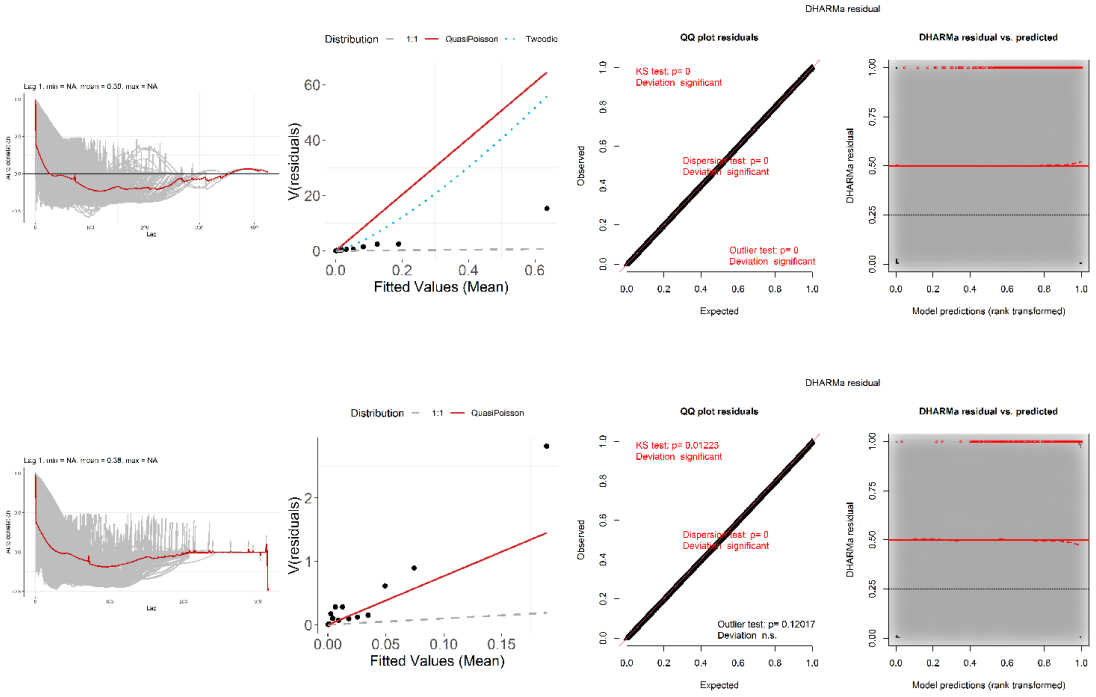

Diagnostics for the best spatial model(s) listed in the table above. For species present in Danish marine waters year-round, models were fitted separately for winter-spring (top) and summer-autumn (bottom). For strongly seasonal species, a single model was fitted to the months the species is present. Left: within-block autocorrelation function, with the grey lines representing the residual correlation observed in each transect and the red line the average of these values across transects. Second left: the estimated mean-variance relationship (Quasi-Poisson: red line, Tweedie: blue dashed line) against observed values (black symbols), with grey dashed line showing 1:1 relationship for reference. Right two panels: QQplot and residuals against predicted values. The red stars are outliers and the red line is a smooth spline around the mean of the residuals. Note: Whilst the tests on the QQ plot indicate that there might be an issue this is owing to the large volume of data and practically we find no significant deviations.

8.8.3 Risk-mapping

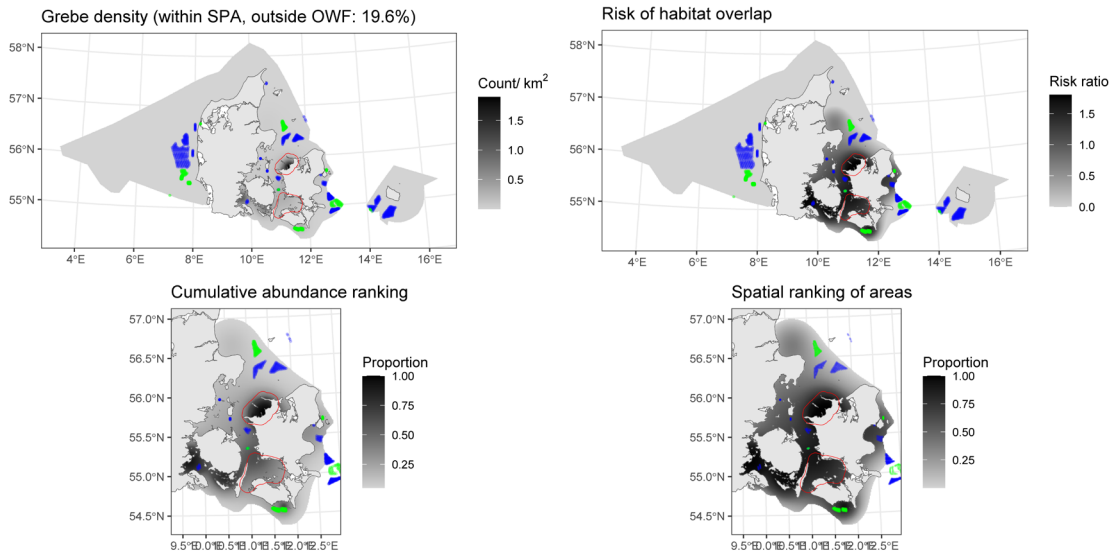

The rescaling of estimated density distribution (top left) to habitat risk for the species unit (top right). Bottom left and right: species unit abundance and top-use areas as cumulative percentiles (up to 0.95 abundance, defining species unit range). Red polygons: any SPAs designated for one or more species in the species unit. Existing wind turbines are shown in green and proposed future turbine locations in blue. Percentage population with area-based protections, defined as total density within SPA boundaries and >2 km away from existing or future turbine locations, is provided in the top-left panel title (rounded to nearest decimal place).

8.9 Herring gull/ common gull. Species unit “Gull”

8.9.1 Spatial modelling data and results

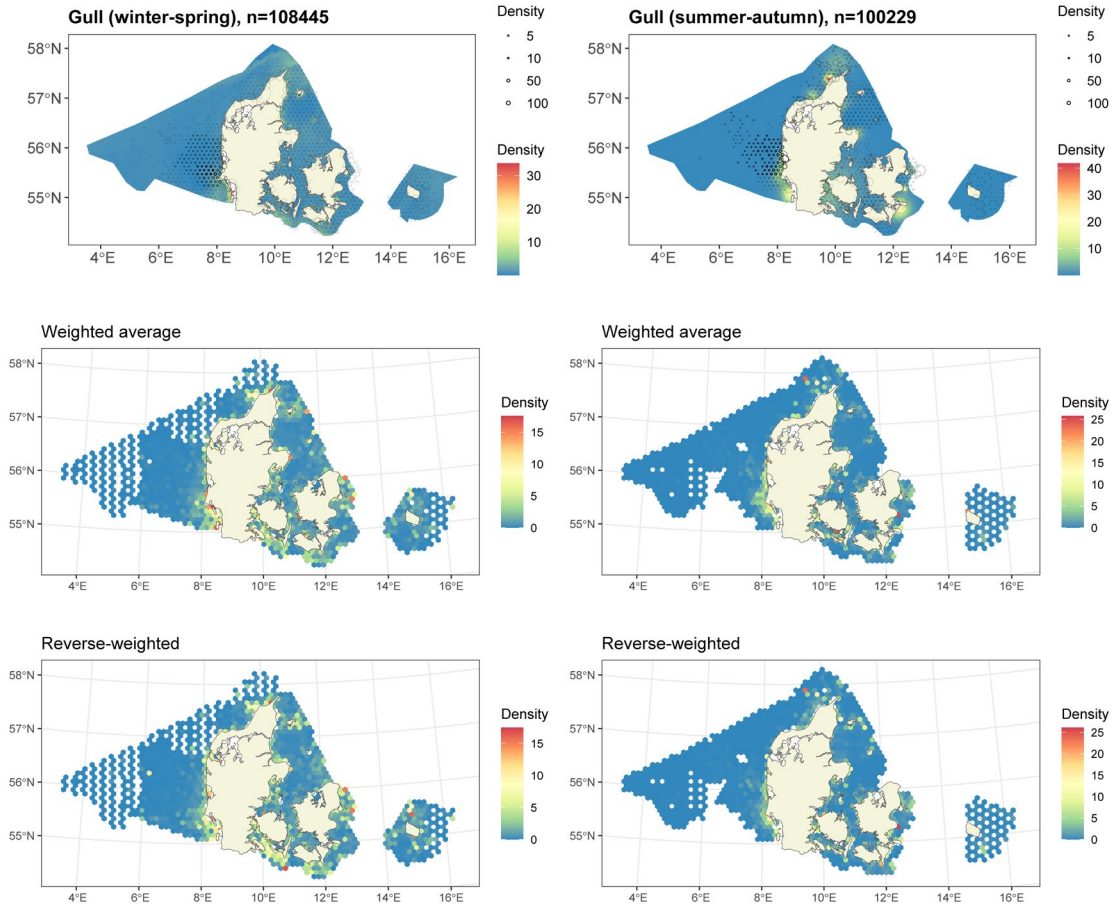

Aerial survey data and modelled density distributions. Top panel raster surface(s) show the modelled density distributions, overlaid with density corrected for detectability and averaged over segments in 10km hexagons (symbol size). Symbol transparency indicates time-weighted sample size in each hexagon. The average densities are provided both without any weighting (top), with time weighting (raster map in the middle), and with reverse time-weighting (raster map in the bottom). Time-weighting emphasizes the newest data, while reverse-weighting emphasizes the oldest data. Differences between the two can be used to indicate changes in density distribution between the beginning and end of the study period (1999-2025).

8.9.2 Diagnostics for the best spatial models

Species unit	Seasons	Best model	1D terms	2D term	Distribution	Tweedie parameter	Dispersion parameter
Gull	winter, spring	Best 1D2D	s(depth, df=5)	s(x,y, df=10)	quasipoisson	NA	117.3
Gull	summer, autumn	Best 1D2D	NA	s(x,y, df=14)	quasipoisson	NA	145.6

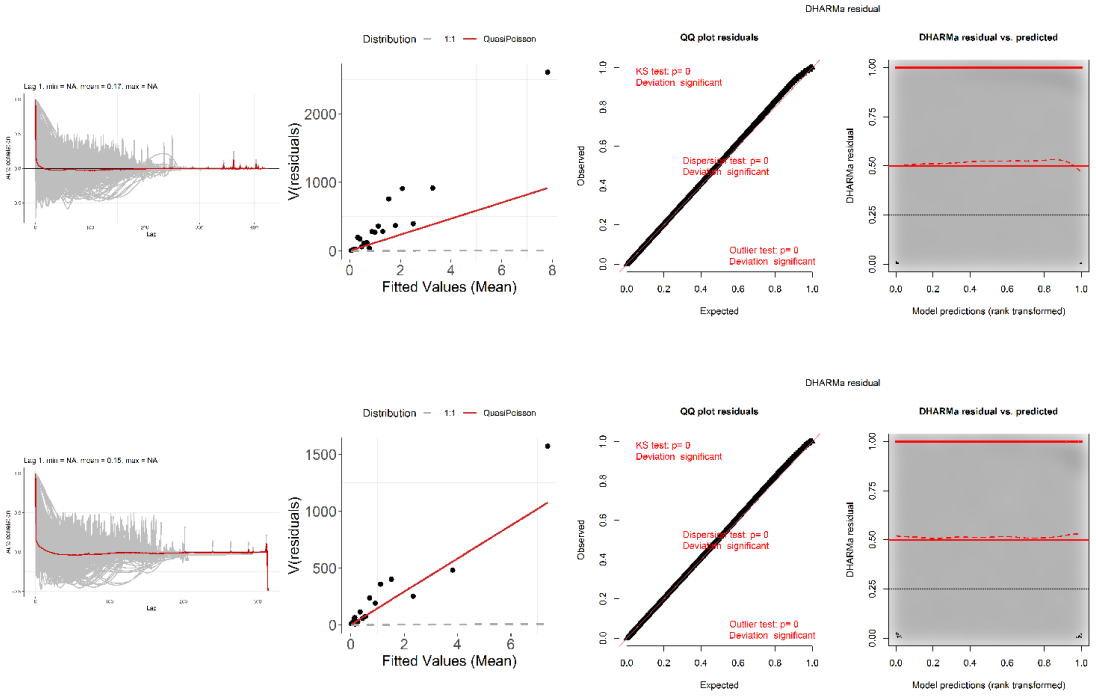

Diagnostics for the best spatial model(s) listed in the table above. For species present in Danish marine waters year-round, models were fitted separately for winter-spring (top) and summer-autumn (bottom). For strongly seasonal species, a single model was fitted to the months the species is present. Left: within-block autocorrelation function, with the grey lines representing the residual correlation observed in each transect and the red line the average of these values across transects. Second left: the estimated mean-variance relationship (Quasi-Poisson: red line, Tweedie: blue dashed line) against observed values (black symbols), with grey dashed line showing 1:1 relationship for reference. Right two panels: QQplot and residuals against predicted values. The red stars are outliers and the red line is a smooth spline around the mean of the residuals. Note: Whilst the tests on the QQ plot indicate that there might be an issue this is owing to the large volume of data and practically we find no significant deviations.

8.9.3 Risk-mapping

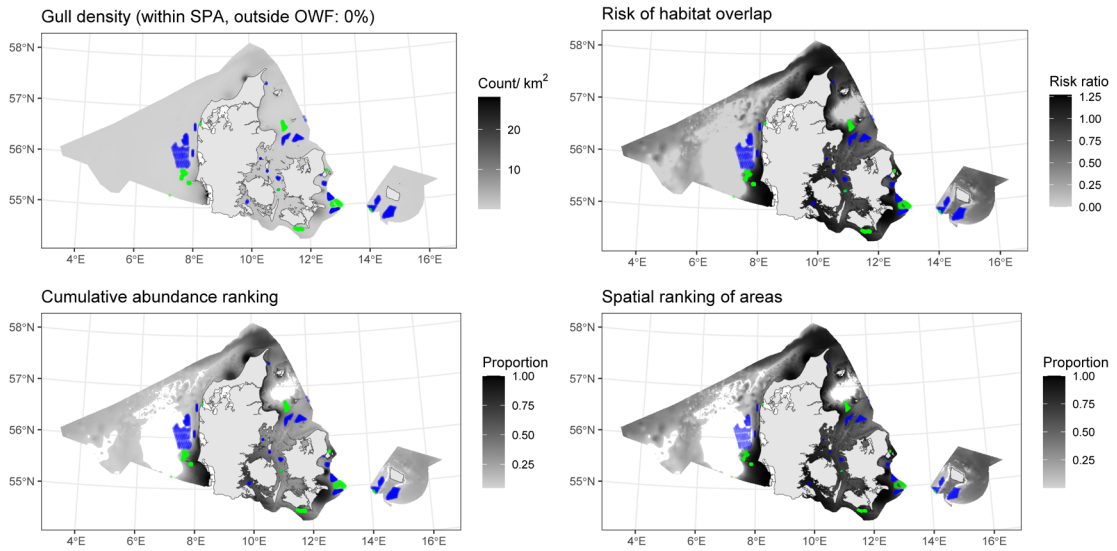

The rescaling of estimated density distribution (top left) to habitat risk for the species unit (top right). Bottom left and right: species unit abundance and top-use areas as cumulative percentiles (up to 0.95 abundance, defining species unit range). Red polygons: any SPAs designated for one or more species in the species unit. Existing wind turbines are shown in green and proposed future turbine locations in blue. Percentage population with area-based protections, defined as total density within SPA boundaries and >2 km away from existing or future turbine locations, is provided in the top-left panel title (rounded to nearest decimal place).

8.10 Black-legged kittiwake. Species unit “Kittiwake”

8.10.1 Spatial modelling data and results

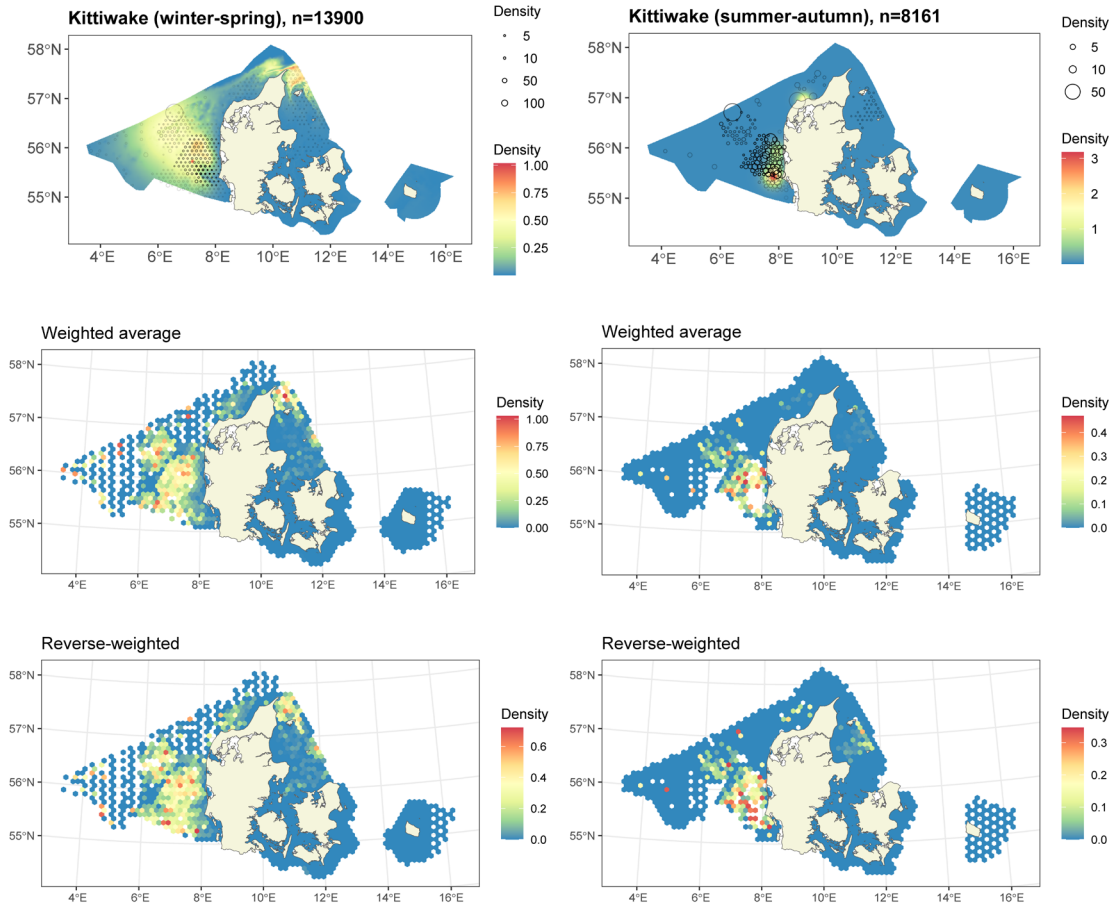

Aerial survey data and modelled density distributions. Top panel raster surface(s) show the modelled density distributions, overlaid with density corrected for detectability and averaged over segments in 10km hexagons (symbol size). Symbol transparency indicates time-weighted sample size in each hexagon. The average densities are provided both without any weighting (top), with time weighting (raster map in the middle), and with reverse time-weighting (raster map in the bottom). Time-weighting emphasizes the newest data, while reverse-weighting emphasizes the oldest data. Differences between the two can be used to indicate changes in density distribution between the beginning and end of the study period (1999-2025).

8.10.2 Diagnostics for the best spatial models

Species unit	Seasons	Best model	1D terms	2D term	Distribution	Tweedie parameter	Dispersion parameter
Kittiwake	winter, spring	Best 1D2D	s(depth, df=2)	s(x,y, df=6)	Tweedie	1.30	34.1
Kittiwake	summer, autumn	Best 1D2D	NA	s(x,y, df=3)	Tweedie	1.32	66.9

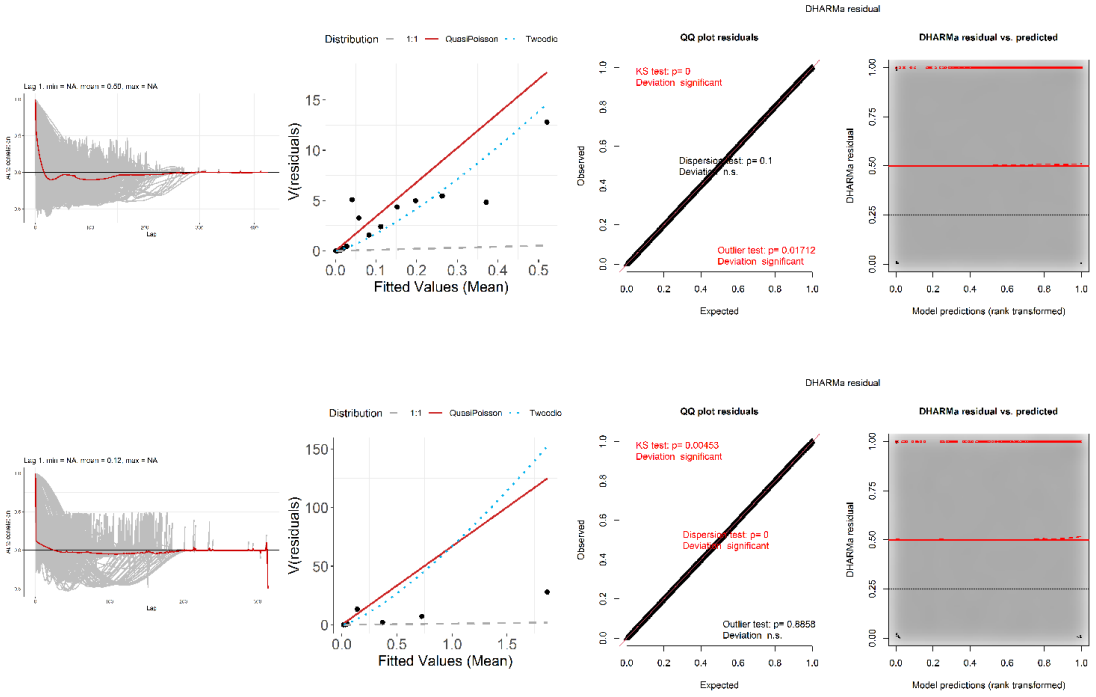

Diagnostics for the best spatial model(s) listed in the table above. For species present in Danish marine waters year-round, models were fitted separately for winter-spring (top) and summer-autumn (bottom). For strongly seasonal species, a single model was fitted to the months the species is present. Left: within-block autocorrelation function, with the grey lines representing the residual correlation observed in each transect and the red line the average of these values across transects. Second left: the estimated mean-variance relationship (Quasi-Poisson: red line, Tweedie: blue dashed line) against observed values (black symbols), with grey dashed line showing 1:1 relationship for reference. Right two panels: QQplot and residuals against predicted values. The red stars are outliers and the red line is a smooth spline around the mean of the residuals. Note: Whilst the tests on the QQ plot indicate that there might be an issue this is owing to the large volume of data and practically we find no significant deviations.

8.10.3 Risk-mapping

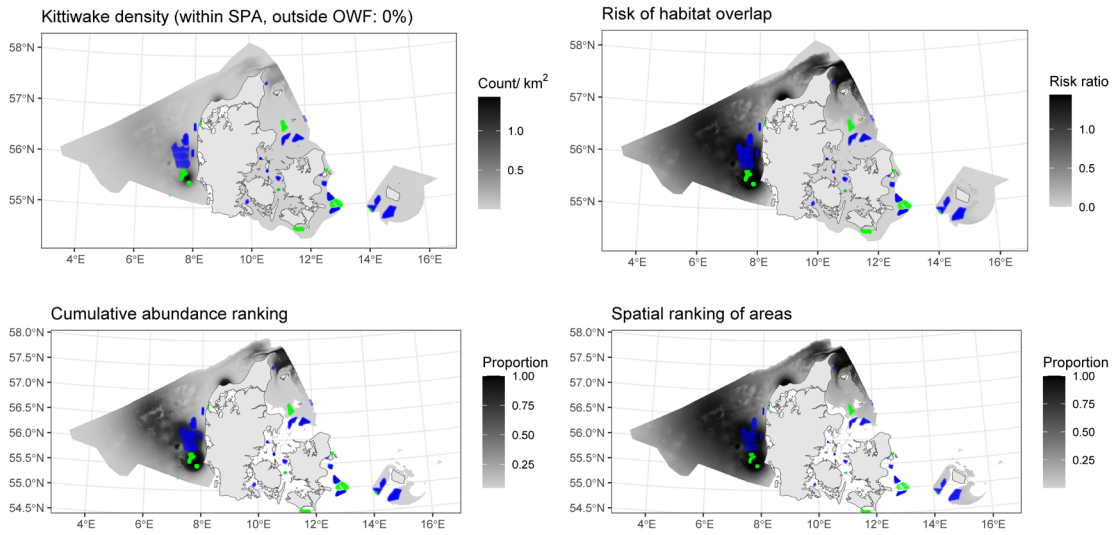

The rescaling of estimated density distribution (top left) to habitat risk for the species unit (top right). Bottom left and right: species unit abundance and top-use areas as cumulative percentiles (up to 0.95 abundance, defining species unit range). Red polygons: any SPAs designated for one or more species in the species unit. Existing wind turbines are shown in green and proposed future turbine locations in blue. Percentage population with area-based protections, defined as total density within SPA boundaries and >2 km away from existing or future turbine locations, is provided in the top-left panel title (rounded to nearest decimal place).

8.11 Lesser black-backed gull. Species unit “LBBG”

8.11.1 Spatial modelling data and results

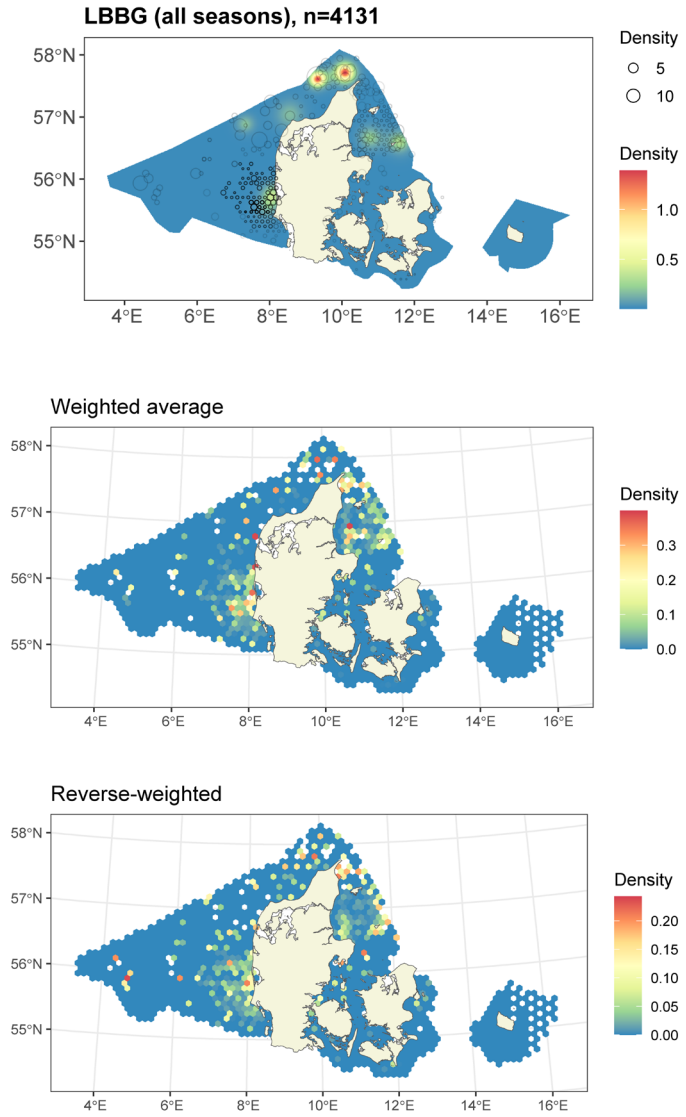

Aerial survey data and modelled density distributions. Top panel raster surface(s) show the modelled density distributions, overlaid with density corrected for detectability and averaged over segments in 10km hexagons (symbol size). Symbol transparency indicates time-weighted sample size in each hexagon. The average densities are provided both without any weighting (top), with time weighting (raster map in the middle), and with reverse time-weighting (raster map in the bottom). Time-weighting emphasizes the newest data, while reverse-weighting emphasizes the oldest data. Differences between the two can be used to indicate changes in density distribution between the beginning and end of the study period (1999-2025).

8.11.2 Diagnostics for the best spatial models

Species unit	Seasons	Best model	1D terms	2D term	Distribution	Tweedie parameter	Dispersion parameter
LBBG	spring, summer, autumn	Best 1D2D	NA	s(x,y, df=8)	Tweedie	1.32	33.1

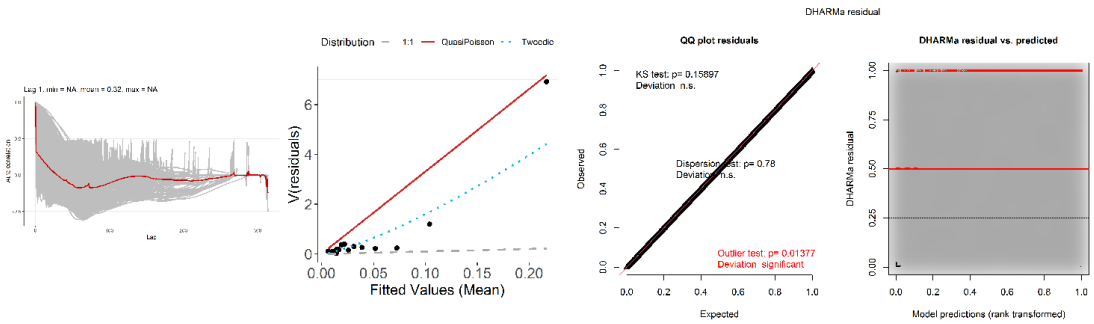

Diagnostics for the best spatial model(s) listed in the table above. For species present in Danish marine waters year-round, models were fitted separately for winter-spring (top) and summer-autumn (bottom). For strongly seasonal species, a single model was fitted to the months the species is present. Left: within-block autocorrelation function, with the grey lines representing the residual correlation observed in each transect and the red line the average of these values across transects. Second left: the estimated mean-variance relationship (Quasi-Poisson: red line, Tweedie: blue dashed line) against observed values (black symbols), with grey dashed line showing 1:1 relationship for reference. Right two panels: QQplot and residuals against predicted values. The red stars are outliers and the red line is a smooth spline around the mean of the residuals. Note: Whilst the tests on the QQ plot indicate that there might be an issue this is owing to the large volume of data and practically we find no significant deviations.

8.11.3 Risk-mapping

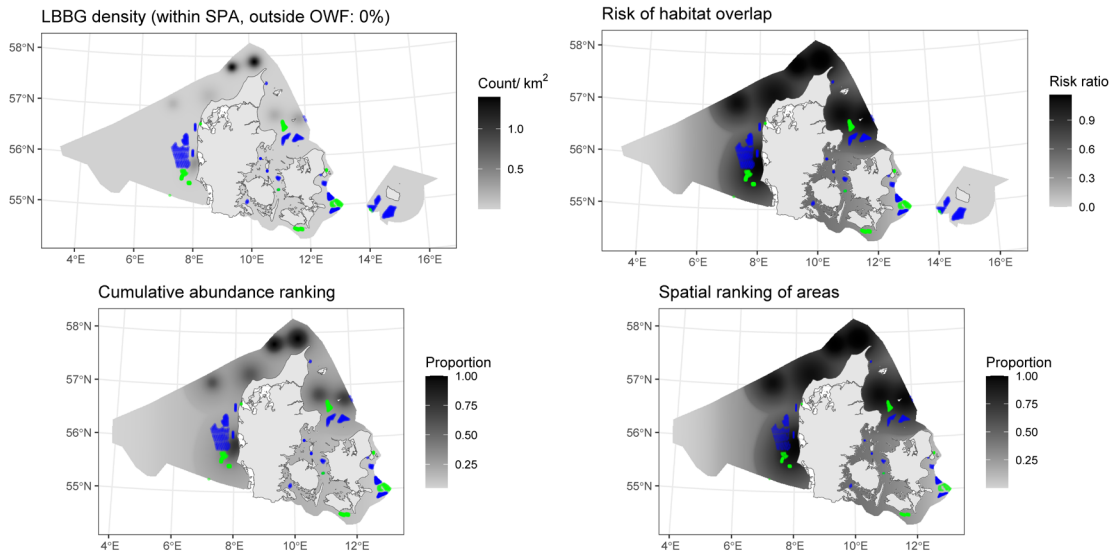

The rescaling of estimated density distribution (top left) to habitat risk for the species unit (top right). Bottom left and right: species unit abundance and top-use areas as cumulative percentiles (up to 0.95 abundance, defining species unit range). Red polygons: any SPAs designated for one or more species in the species unit. Existing wind turbines are shown in green and proposed future turbine locations in blue. Percentage population with area-based protections, defined as total density within SPA boundaries and >2 km away from existing or future turbine locations, is provided in the top-left panel title (rounded to nearest decimal place).

8.12 Little gull. Species unit “Littlegull”

8.12.1 Spatial modelling data and results

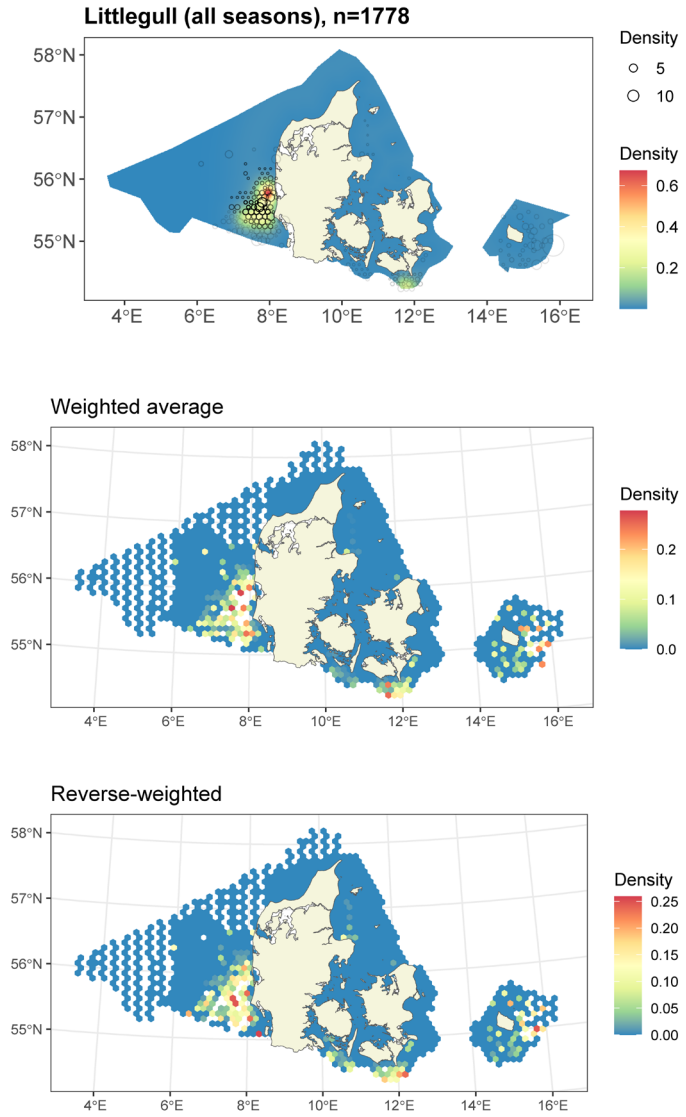

Aerial survey data and modelled density distributions. Top panel raster surface(s) show the modelled density distributions, overlaid with density corrected for detectability and averaged over segments in 10km hexagons (symbol size). Symbol transparency indicates time-weighted sample size in each hexagon. The average densities are provided both without any weighting (top), with time weighting (raster map in the middle), and with reverse time-weighting (raster map in the bottom). Time-weighting emphasizes the newest data, while reverse-weighting emphasizes the oldest data. Differences between the two can be used to indicate changes in density distribution between the beginning and end of the study period (1999-2025).

8.12.2 Diagnostics for the best spatial models

Species unit	Seasons	Best model	1D terms	2D term	Distribution	Tweedie parameter	Dispersion parameter
Littlegull	winter, spring, autumn	Best 1D2D	s(distcoast, df=2)	s(x,y, df=4)	Tweedie	1.37	148.8

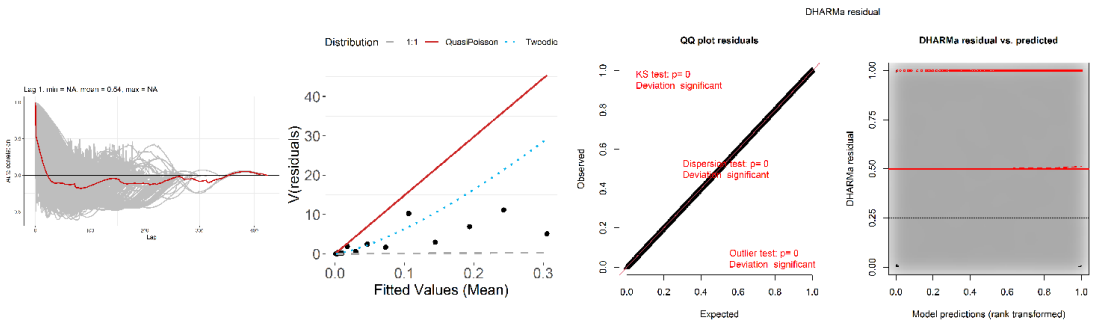

Diagnostics for the best spatial model(s) listed in the table above. For species present in Danish marine waters year-round, models were fitted separately for winter-spring (top) and summer-autumn (bottom). For strongly seasonal species, a single model was fitted to the months the species is present. Left: within-block autocorrelation function, with the grey lines representing the residual correlation observed in each transect and the red line the average of these values across transects. Second left: the estimated mean-variance relationship (Quasi-Poisson: red line, Tweedie: blue dashed line) against observed values (black symbols), with grey dashed line showing 1:1 relationship for reference. Right two panels: QQplot and residuals against predicted values. The red stars are outliers and the red line is a smooth spline around the mean of the residuals. Note: Whilst the tests on the QQ plot indicate that there might be an issue this is owing to the large volume of data and practically we find no significant deviations.

8.12.3 Risk-mapping

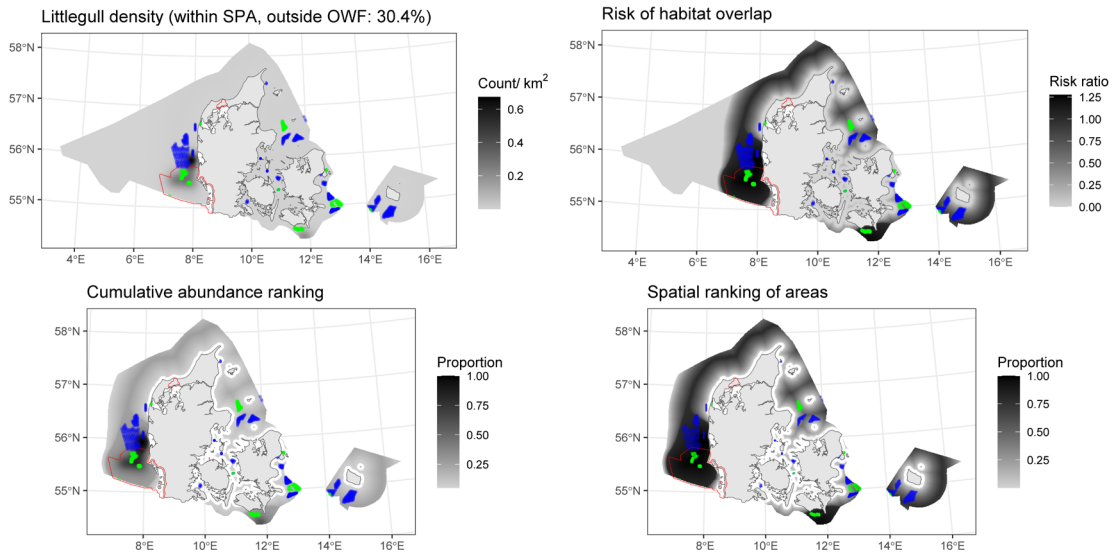

The rescaling of estimated density distribution (top left) to habitat risk for the species unit (top right). Bottom left and right: species unit abundance and top-use areas as cumulative percentiles (up to 0.95 abundance, defining species unit range). Red polygons: any SPAs designated for one or more species in the species unit. Existing wind turbines are shown in green and proposed future turbine locations in blue. Percentage population with area-based protections, defined as total density within SPA boundaries and >2 km away from existing or future turbine locations, is provided in the top-left panel title (rounded to nearest decimal place).

8.13 Long-tailed duck. Species unit “Longtailed”

8.13.1 Spatial modelling data and results

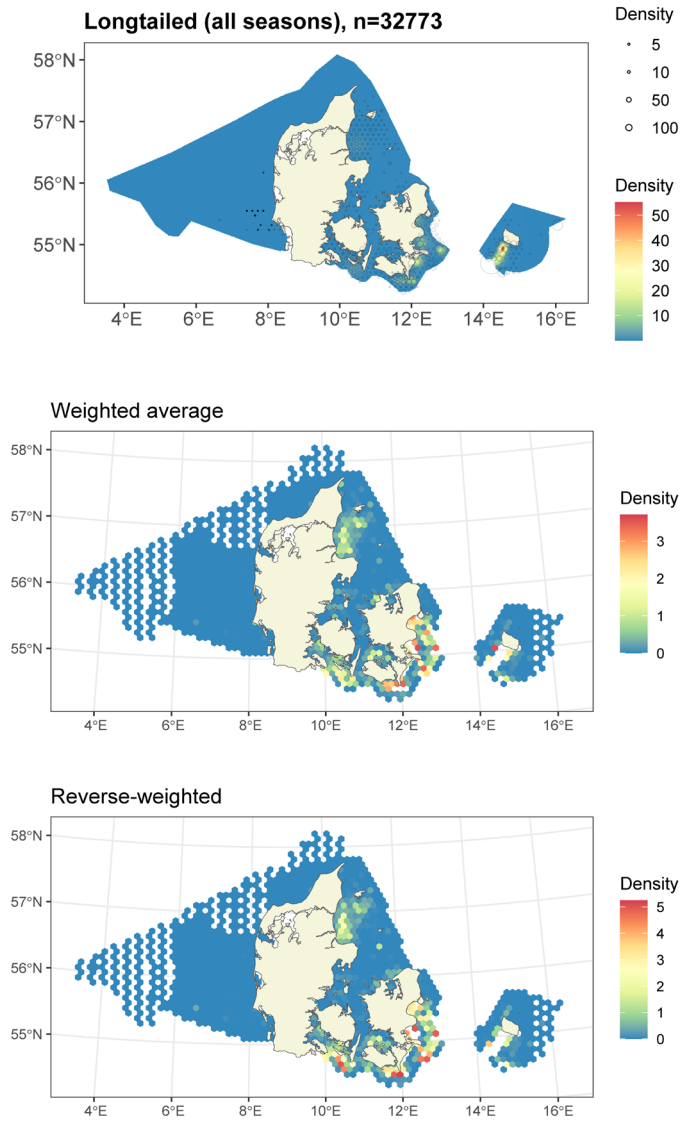

Aerial survey data and modelled density distributions. Top panel raster surface(s) show the modelled density distributions, overlaid with density corrected for detectability and averaged over segments in 10km hexagons (symbol size). Symbol transparency indicates time-weighted sample size in each hexagon. The average densities are provided both without any weighting (top), with time weighting (raster map in the middle), and with reverse time-weighting (raster map in the bottom). Time-weighting emphasizes the newest data, while reverse-weighting emphasizes the oldest data. Differences between the two can be used to indicate changes in density distribution between the beginning and end of the study period (1999-2025).

8.13.2 Diagnostics for the best spatial models

Species unit	Seasons	Best model	1D terms	2D term	Distribution	Tweedie parameter	Dispersion parameter
Longtailed	winter, spring	Best 1D2D	NA	s(x,y, df=14)	quasipoisson	NA	29.4

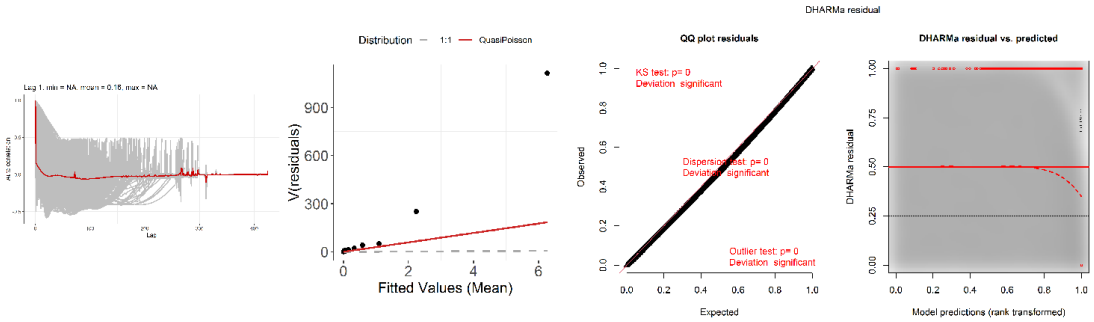

Diagnostics for the best spatial model(s) listed in the table above. For species present in Danish marine waters year-round, models were fitted separately for winter-spring (top) and summer-autumn (bottom). For strongly seasonal species, a single model was fitted to the months the species is present. Left: within-block autocorrelation function, with the grey lines representing the residual correlation observed in each transect and the red line the average of these values across transects. Second left: the estimated mean-variance relationship (Quasi-Poisson: red line, Tweedie: blue dashed line) against observed values (black symbols), with grey dashed line showing 1:1 relationship for reference. Right two panels: QQplot and residuals against predicted values. The red stars are outliers and the red line is a smooth spline around the mean of the residuals. Note: Whilst the tests on the QQ plot indicate that there might be an issue this is owing to the large volume of data and practically we find no significant deviations.

8.13.3 Risk-mapping

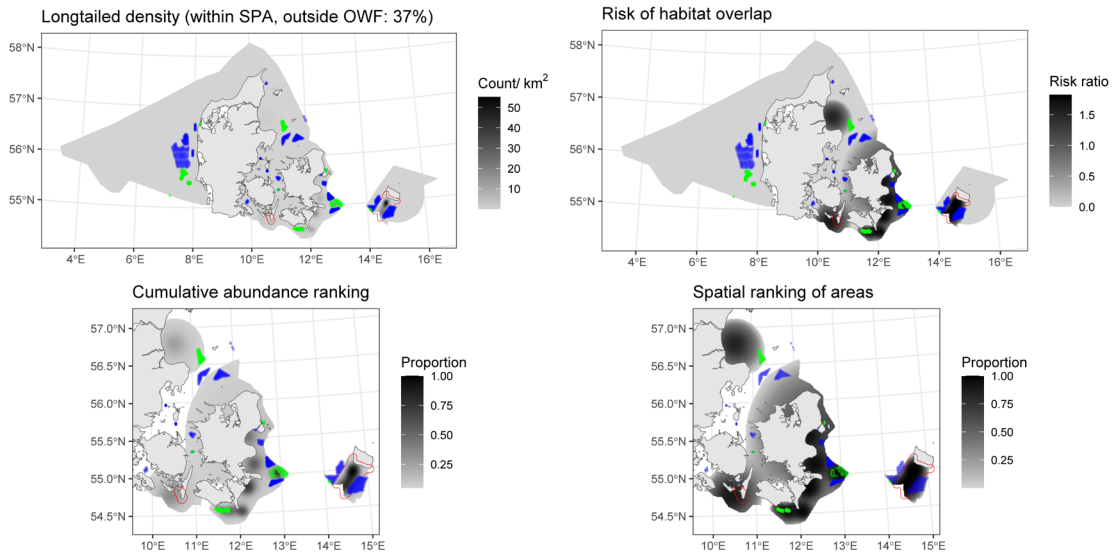

The rescaling of estimated density distribution (top left) to habitat risk for the species unit (top right). Bottom left and right: species unit abundance and top-use areas as cumulative percentiles (up to 0.95 abundance, defining species unit range). Red polygons: any SPAs designated for one or more species in the species unit. Existing wind turbines are shown in green and proposed future turbine locations in blue. Percentage population with area-based protections, defined as total density within SPA boundaries and >2 km away from existing or future turbine locations, is provided in the top-left panel title (rounded to nearest decimal place).

8.14 Red-breasted merganser. Species unit “Merganser”

8.14.1 Spatial modelling data and results

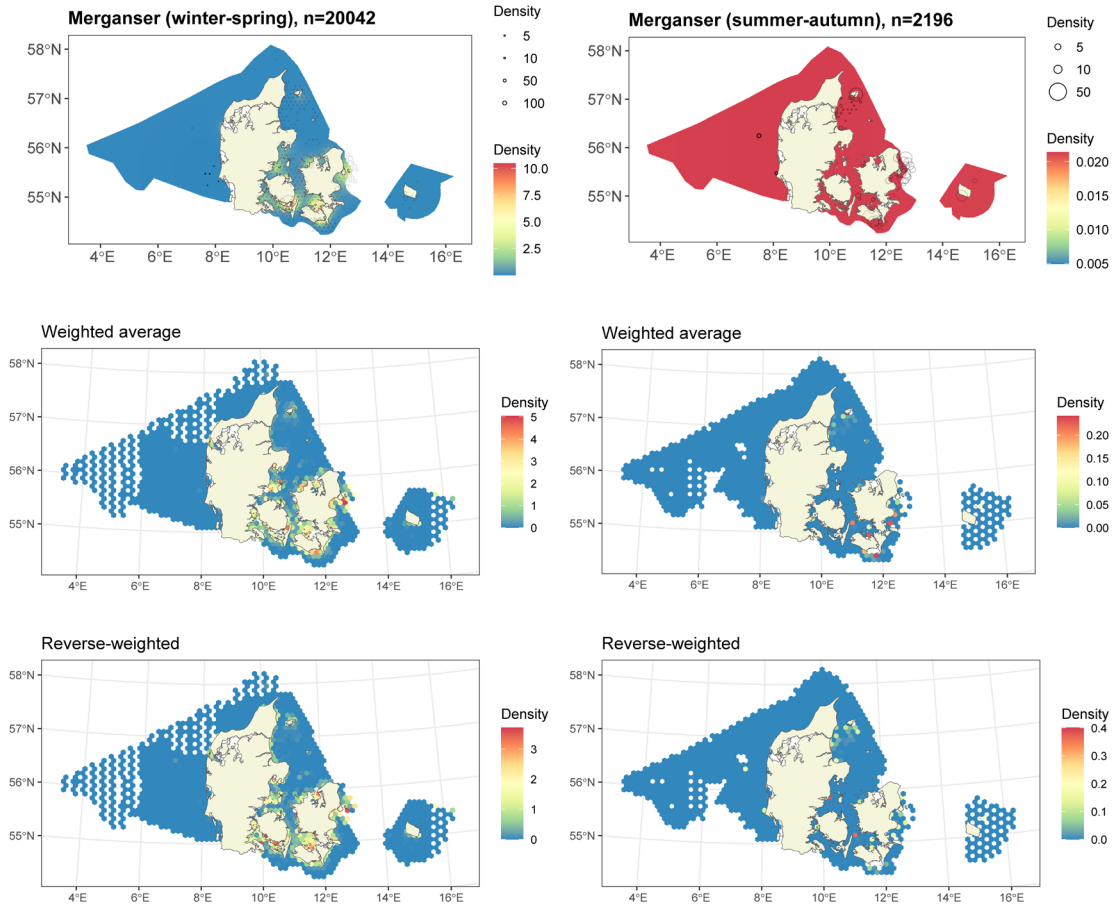

Aerial survey data and modelled density distributions. Top panel raster surface(s) show the modelled density distributions, overlaid with density corrected for detectability and averaged over segments in 10km hexagons (symbol size). Symbol transparency indicates time-weighted sample size in each hexagon. The average densities are provided both without any weighting (top), with time weighting (raster map in the middle), and with reverse time-weighting (raster map in the bottom). Time-weighting emphasizes the newest data, while reverse-weighting emphasizes the oldest data. Differences between the two can be used to indicate changes in density distribution between the beginning and end of the study period (1999-2025).

8.14.2 Diagnostics for the best spatial models

Species unit	Seasons	Best model	1D terms	2D term	Distribution	Tweedie parameter	Dispersion parameter
Merganser	winter, spring	Best 1D2D	NA	s(x,y, df=17)	quasipoisson	NA	39.8
Merganser	summer, autumn	Initial Model	NA	NA	Tweedie	1.39	511.1

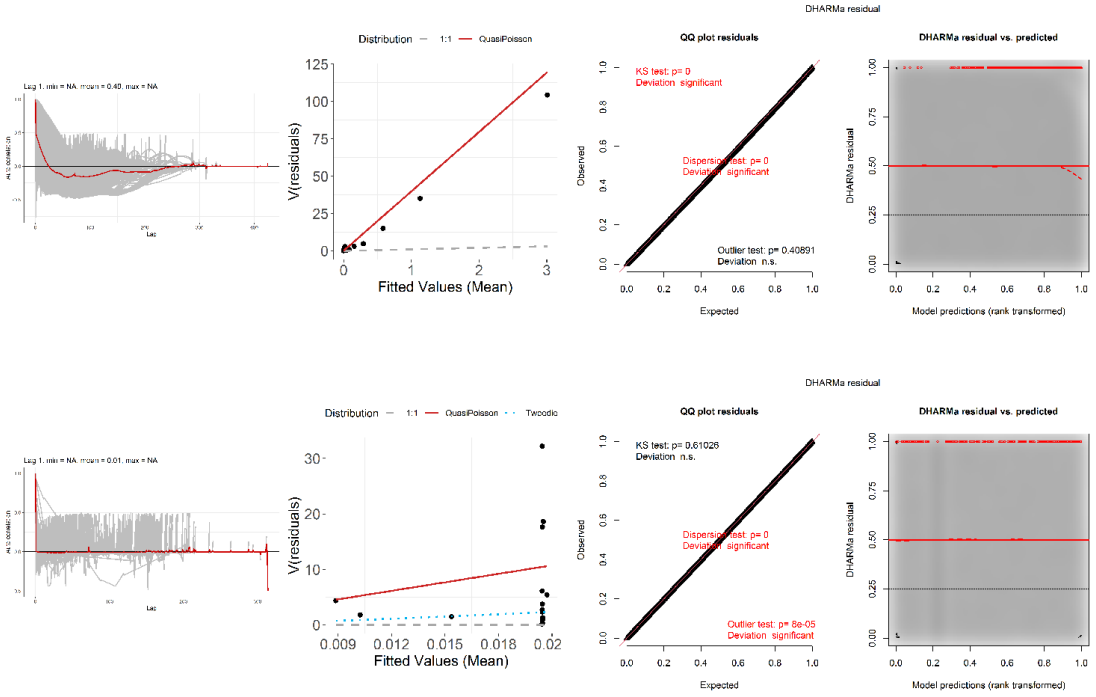

Diagnostics for the best spatial model(s) listed in the table above. For species present in Danish marine waters year-round, models were fitted separately for winter-spring (top) and summer-autumn (bottom). For strongly seasonal species, a single model was fitted to the months the species is present. Left: within-block autocorrelation function, with the grey lines representing the residual correlation observed in each transect and the red line the average of these values across transects. Second left: the estimated mean-variance relationship (Quasi-Poisson: red line, Tweedie: blue dashed line) against observed values (black symbols), with grey dashed line showing 1:1 relationship for reference. Right two panels: QQplot and residuals against predicted values. The red stars are outliers and the red line is a smooth spline around the mean of the residuals. Note: Whilst the tests on the QQ plot indicate that there might be an issue this is owing to the large volume of data and practically we find no significant deviations.

8.14.3 Risk-mapping

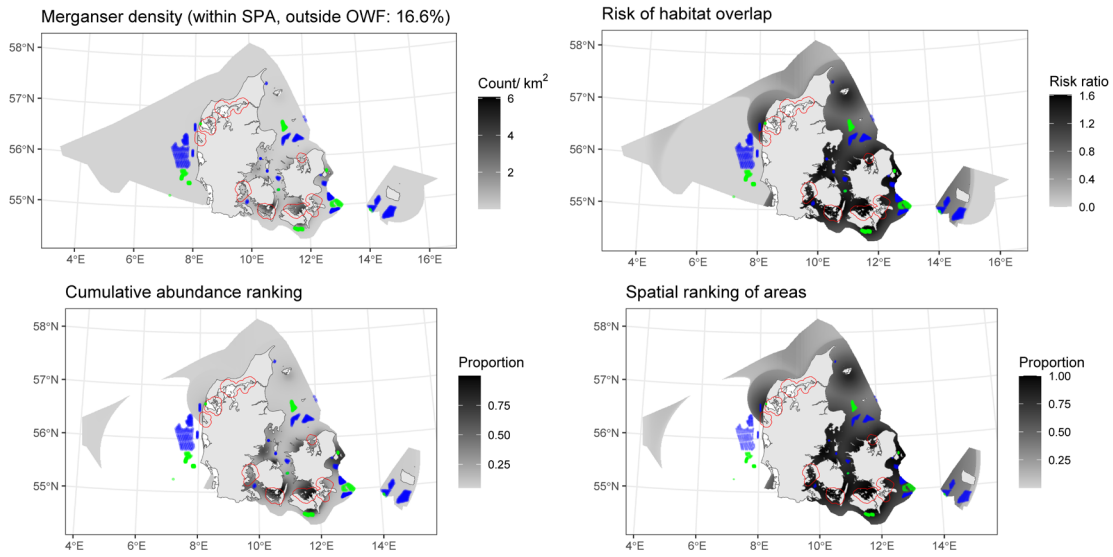

The rescaling of estimated density distribution (top left) to habitat risk for the species unit (top right). Bottom left and right: species unit abundance and top-use areas as cumulative percentiles (up to 0.95 abundance, defining species unit range). Red polygons: any SPAs designated for one or more species in the species unit. Existing wind turbines are shown in green and proposed future turbine locations in blue. Percentage population with area-based protections, defined as total density within SPA boundaries and >2 km away from existing or future turbine locations, is provided in the top-left panel title (rounded to nearest decimal place).

8.15 Common scoter. Species unit “Scoter”

8.15.1 Spatial modelling data and results

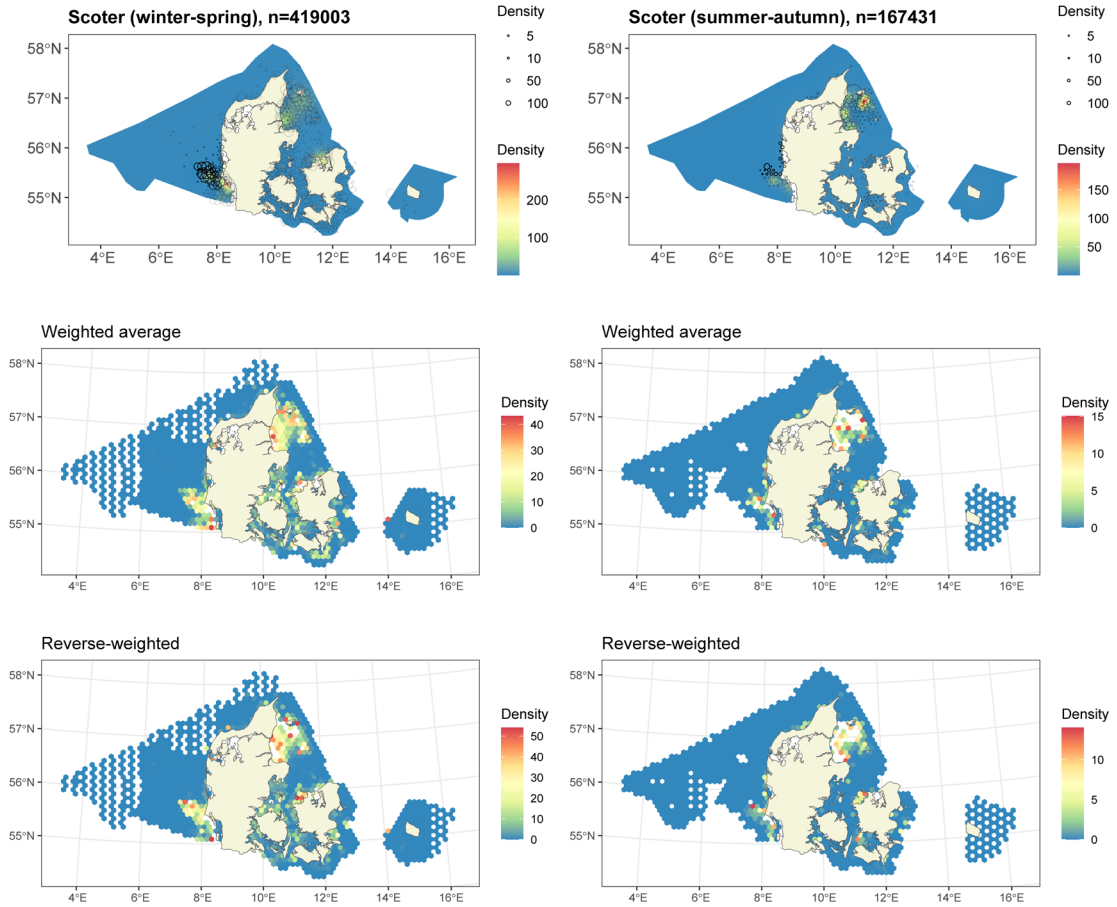

Aerial survey data and modelled density distributions. Top panel raster surface(s) show the modelled density distributions, overlaid with density corrected for detectability and averaged over segments in 10km hexagons (symbol size). Symbol transparency indicates time-weighted sample size in each hexagon. The average densities are provided both without any weighting (top), with time weighting (raster map in the middle), and with reverse time-weighting (raster map in the bottom). Time-weighting emphasizes the newest data, while reverse-weighting emphasizes the oldest data. Differences between the two can be used to indicate changes in density distribution between the beginning and end of the study period (1999-2025).

8.15.2 Diagnostics for the best spatial models

Species unit	Seasons	Best model	1D terms	2D term	Distribution	Tweedie parameter	Dispersion parameter
Scoter	winter, spring	Best 1D2D	NA	s(x,y, df=9)	quasipoisson	NA	523.3
Scoter	summer, autumn	Best 1D2D	s(distcoast, df=2)	s(x,y, df=8)	quasipoisson	NA	223.1

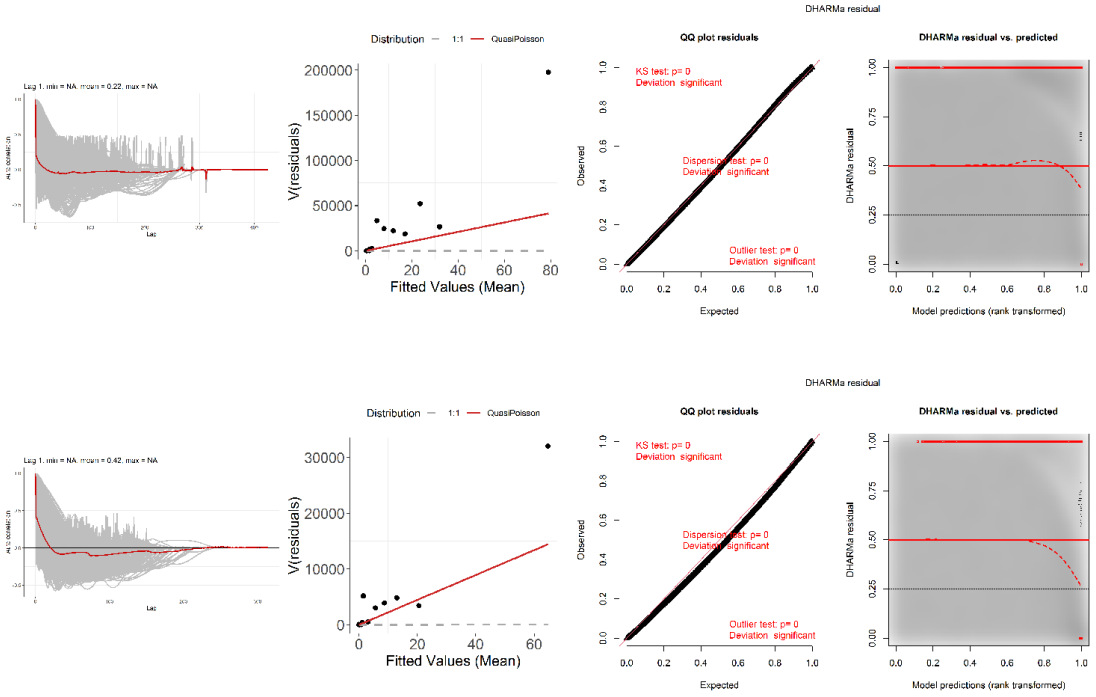

Diagnostics for the best spatial model(s) listed in the table above. For species present in Danish marine waters year-round, models were fitted separately for winter-spring (top) and summer-autumn (bottom). For strongly seasonal species, a single model was fitted to the months the species is present. Left: within-block autocorrelation function, with the grey lines representing the residual correlation observed in each transect and the red line the average of these values across transects. Second left: the estimated mean-variance relationship (Quasi-Poisson: red line, Tweedie: blue dashed line) against observed values (black symbols), with grey dashed line showing 1:1 relationship for reference. Right two panels: QQplot and residuals against predicted values. The red stars are outliers and the red line is a smooth spline around the mean of the residuals. Note: Whilst the tests on the QQ plot indicate that there might be an issue this is owing to the large volume of data and practically we find no significant deviations.

8.15.3 Risk-mapping

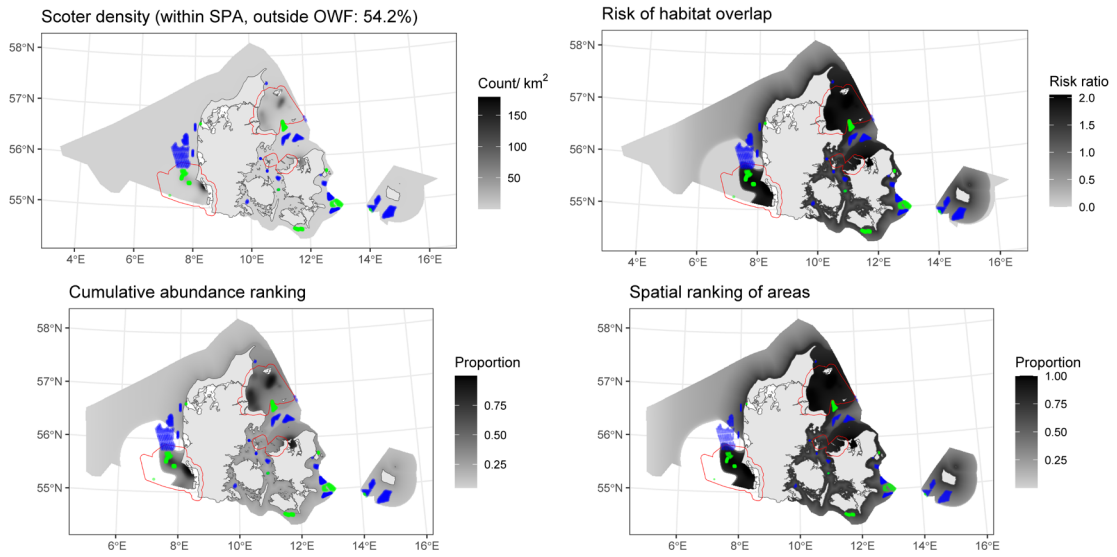

The rescaling of estimated density distribution (top left) to habitat risk for the species unit (top right). Bottom left and right: species unit abundance and top-use areas as cumulative percentiles (up to 0.95 abundance, defining species unit range). Red polygons: any SPAs designated for one or more species in the species unit. Existing wind turbines are shown in green and proposed future turbine locations in blue. Percentage population with area-based protections, defined as total density within SPA boundaries and >2 km away from existing or future turbine locations, is provided in the top-left panel title (rounded to nearest decimal place).

8.16 Common tern/ arctic tern/ Sandwich tern. Species unit "Tern"

8.16.1 Spatial modelling data and results

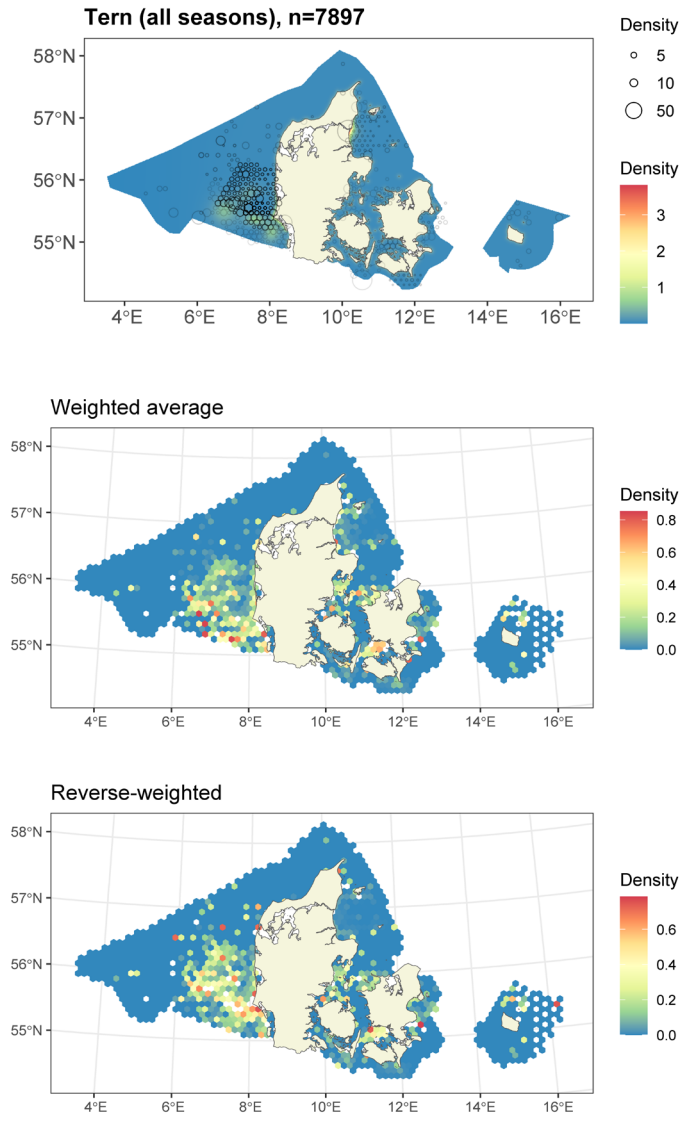

Aerial survey data and modelled density distributions. Top panel raster surface(s) show the modelled density distributions, overlaid with density corrected for detectability and averaged over segments in 10km hexagons (symbol size). Symbol transparency indicates time-weighted sample size in each hexagon. The average densities are provided both without any weighting (top), with time weighting (raster map in the middle), and with reverse time-weighting (raster map in the bottom). Time-weighting emphasizes the newest data, while reverse-weighting emphasizes the oldest data. Differences between the two can be used to indicate changes in density distribution between the beginning and end of the study period (1999-2025).

8.16.2 Diagnostics for the best spatial models

Species unit	Seasons	Best model	1D terms	2D term	Distribution	Tweedie parameter	Dispersion parameter
Tern	spring, summer	Best 1D2D	s(distcoast, df=3)	s(x,y, df=9)	quasipoisson	NA	38

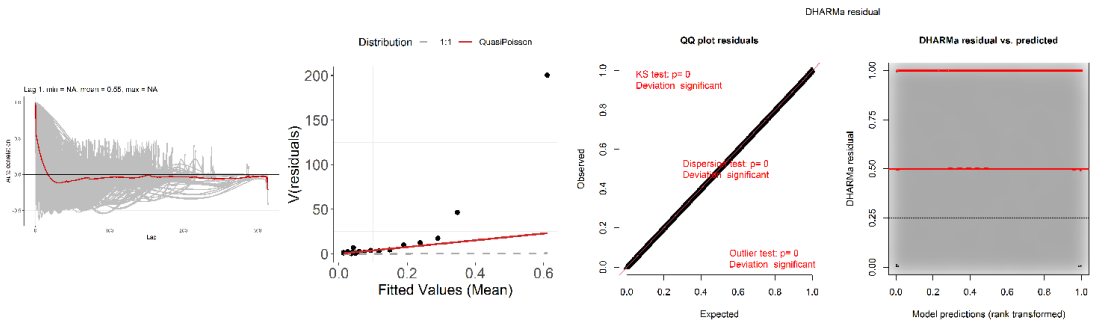

Diagnostics for the best spatial model(s) listed in the table above. For species present in Danish marine waters year-round, models were fitted separately for winter-spring (top) and summer-autumn (bottom). For strongly seasonal species, a single model was fitted to the months the species is present. Left: within-block autocorrelation function, with the grey lines representing the residual correlation observed in each transect and the red line the average of these values across transects. Second left: the estimated mean-variance relationship (Quasi-Poisson: red line, Tweedie: blue dashed line) against observed values (black symbols), with grey dashed line showing 1:1 relationship for reference. Right two panels: QQplot and residuals against predicted values. The red stars are outliers and the red line is a smooth spline around the mean of the residuals. Note: Whilst the tests on the QQ plot indicate that there might be an issue this is owing to the large volume of data and practically we find no significant deviations.

8.16.3 Risk-mapping

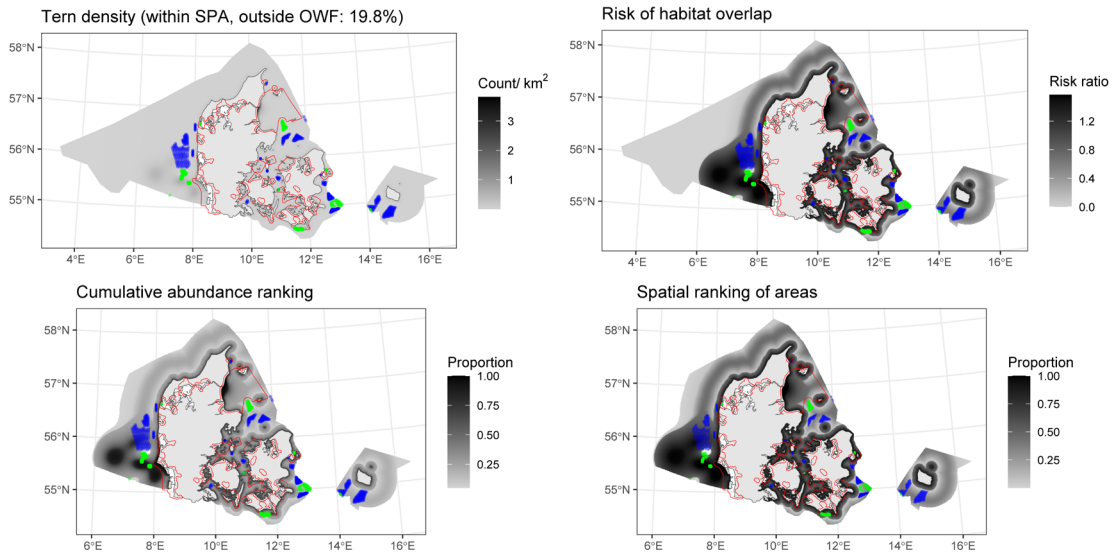

The rescaling of estimated density distribution (top left) to habitat risk for the species unit (top right). Bottom left and right: species unit abundance and top-use areas as cumulative percentiles (up to 0.95 abundance, defining species unit range). Red polygons: any SPAs designated for one or more species in the species unit. Existing wind turbines are shown in green and proposed future turbine locations in blue. Percentage population with area-based protections, defined as total density within SPA boundaries and >2 km away from existing or future turbine locations, is provided in the top-left panel title (rounded to nearest decimal place).

8.17 Velvet scoter. Species unit “Velvetscoter”

8.17.1 Spatial modelling data and results

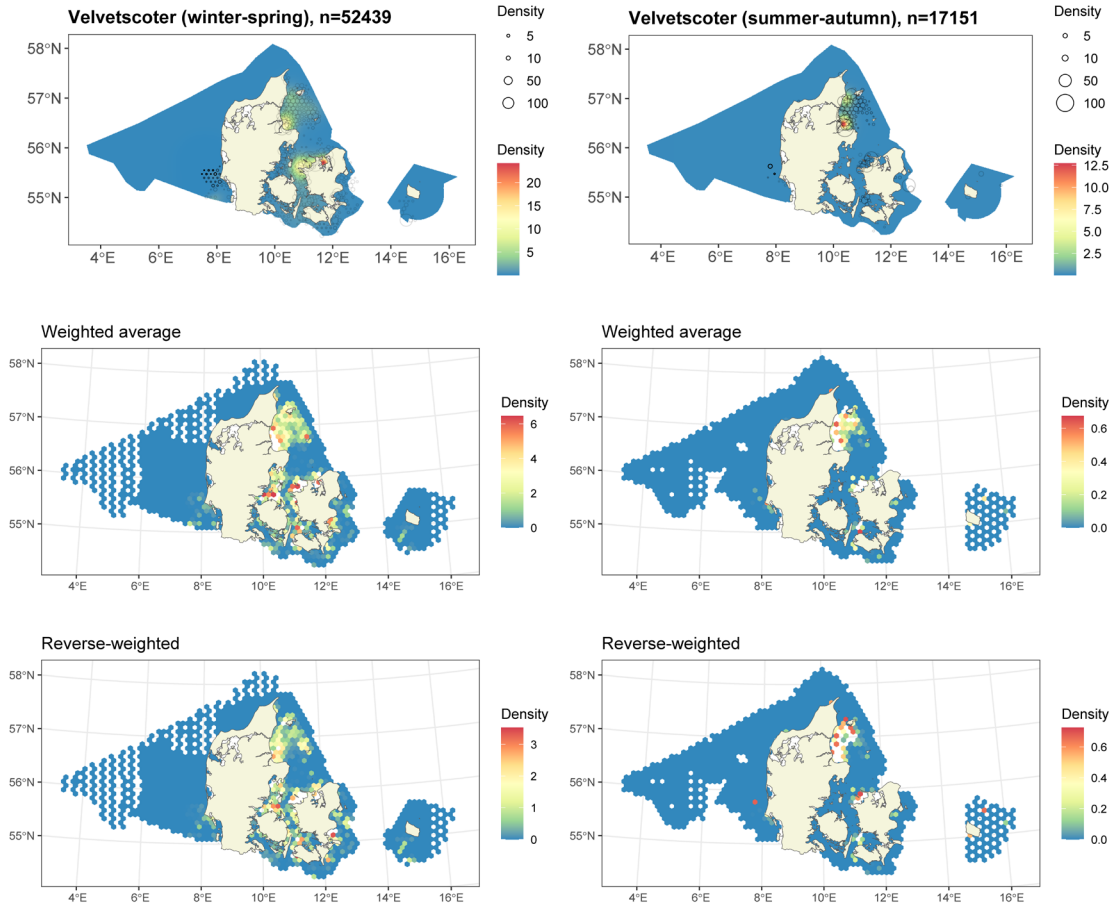

Aerial survey data and modelled density distributions. Top panel raster surface(s) show the modelled density distributions, overlaid with density corrected for detectability and averaged over segments in 10km hexagons (symbol size). Symbol transparency indicates time-weighted sample size in each hexagon. The average densities are provided both without any weighting (top), with time weighting (raster map in the middle), and with reverse time-weighting (raster map in the bottom). Time-weighting emphasizes the newest data, while reverse-weighting emphasizes the oldest data. Differences between the two can be used to indicate changes in density distribution between the beginning and end of the study period (1999-2025).

8.17.2 Diagnostics for the best spatial models

Species unit	Seasons	Best model	1D terms	2D term	Distribution	Tweedie parameter	Dispersion parameter
Velvetscoter	winter, spring	Best 1D2D	NA	s(x,y, df=11)	Tweedie	1.38	54.6
Velvetscoter	summer, autumn	2D Only	NA	s(x,y, df=2)	Tweedie	1.43	218.7

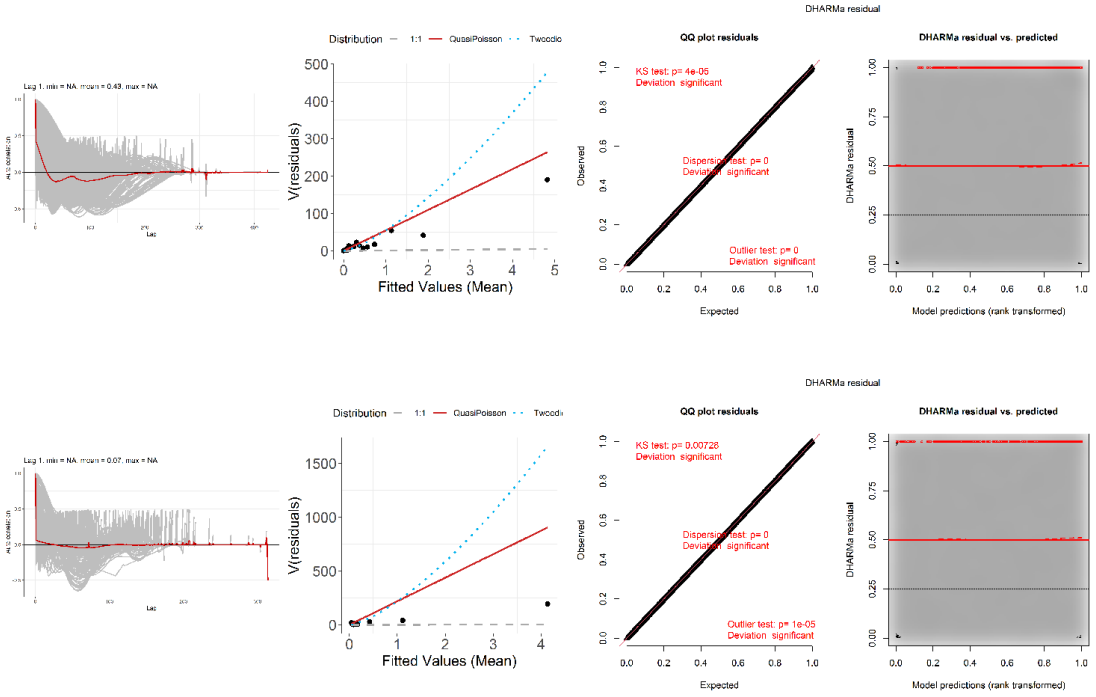

Diagnostics for the best spatial model(s) listed in the table above. For species present in Danish marine waters year-round, models were fitted separately for winter-spring (top) and summer-autumn (bottom). For strongly seasonal species, a single model was fitted to the months the species is present. Left: within-block autocorrelation function, with the grey lines representing the residual correlation observed in each transect and the red line the average of these values across transects. Second left: the estimated mean-variance relationship (Quasi-Poisson: red line, Tweedie: blue dashed line) against observed values (black symbols), with grey dashed line showing 1:1 relationship for reference. Right two panels: QQplot and residuals against predicted values. The red stars are outliers and the red line is a smooth spline around the mean of the residuals. Note: Whilst the tests on the QQ plot indicate that there might be an issue this is owing to the large volume of data and practically we find no significant deviations.

8.17.3 Risk-mapping

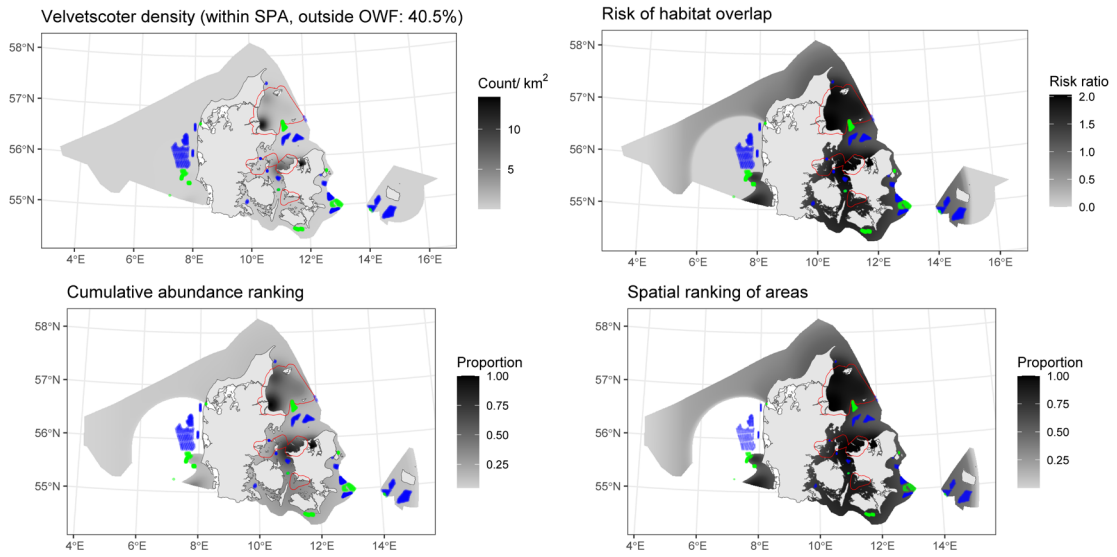

The rescaling of estimated density distribution (top left) to habitat risk for the species unit (top right). Bottom left and right: species unit abundance and top-use areas as cumulative percentiles (up to 0.95 abundance, defining species unit range). Red polygons: any SPAs designated for one or more species in the species unit. Existing wind turbines are shown in green and proposed future turbine locations in blue. Percentage population with area-based protections, defined as total density within SPA boundaries and >2 km away from existing or future turbine locations, is provided in the top-left panel title (rounded to nearest decimal place).

9 Appendix 3: Risk analysis additional figures

9.1 Collision risk

9.1.1 Proxy collision rate with/without flight speed

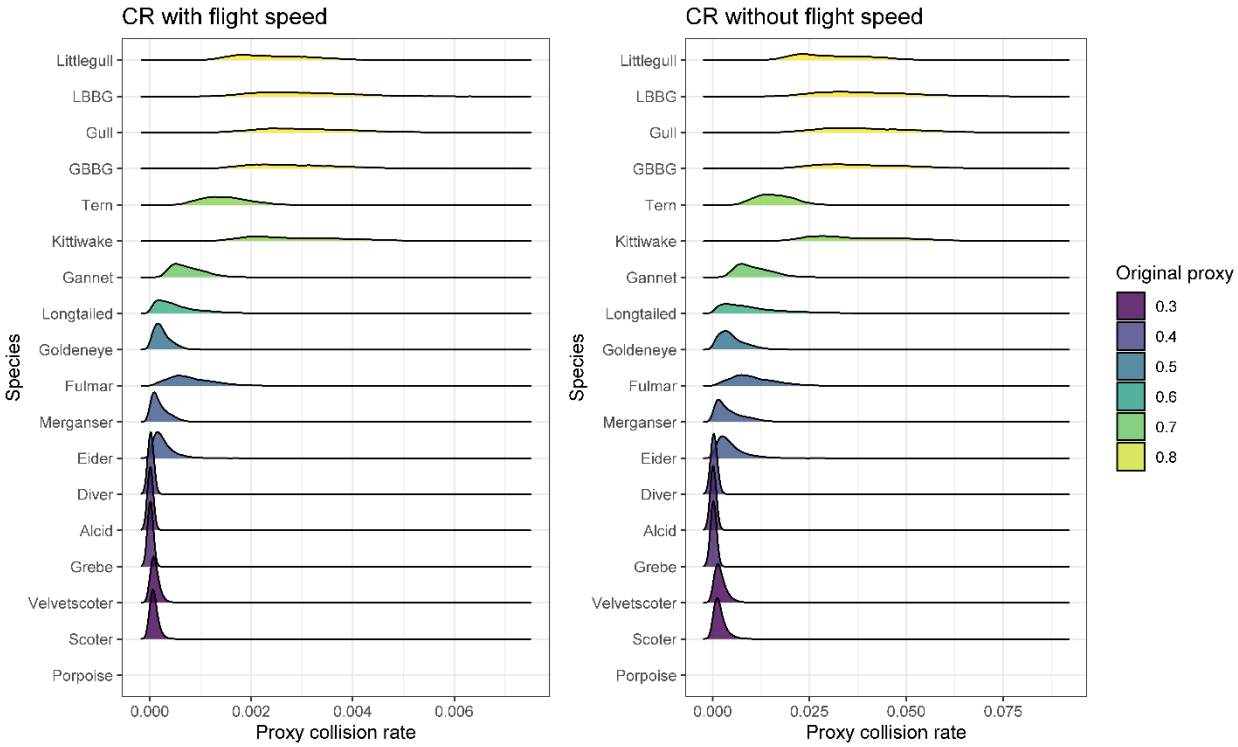

Figure A3.1 Proxy collision rate (CR) distributions when including (left panel) and excluding the flight speed parameter (right panel). The distributions were generated by bootstrapping from the expert-elicited values 10,000 times (**Section 2.1.5** and **Section 2.1.6**). Each species unit is colored by the original collision rate proxy from Isojunno et al., 2025, which was based on collision risk vulnerability scoring carried out by Fauchald et al., 2024.

9.1.2 Comparison with collision risk model output

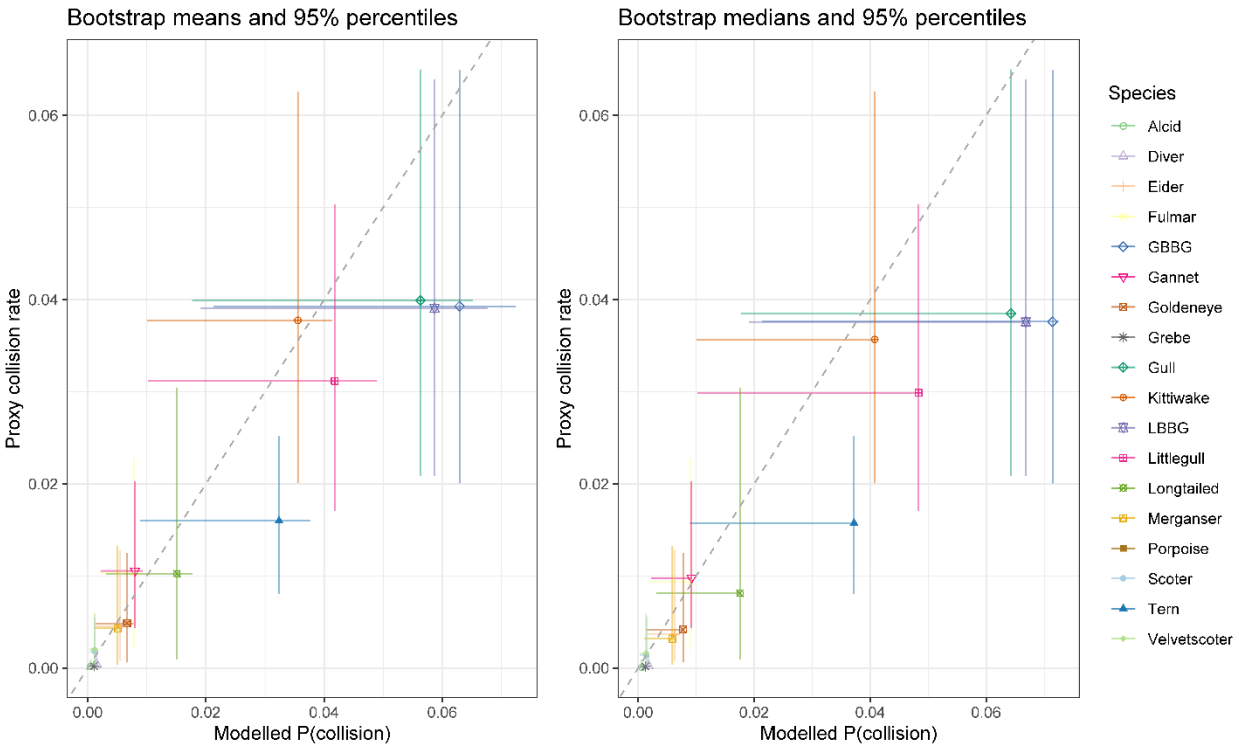

Figure A3.2 Comparison of the proxy collision rate (y-axis) and collision risk model (CRM) outputs (probability of collision per bird and per turbine, x-axis) for each species unit. Symbols show bootstrap means (left panel) and medians (right panel) for each species unit, while lines show 95% confidence intervals derived from the percentiles of the bootstrap distributions. Grey dashed line shows 1:1 line as a reference. The CRM was run in stochastic mode to generate uncertainty around wind farm activity, but without uncertainty on species-specific input parameters, and assuming flight height distribution was uniform within the rotor-swept zone (**Section 2.1.6**).

9.2 Seasonal maps

9.2.1 Number of species exceeding HPL by season

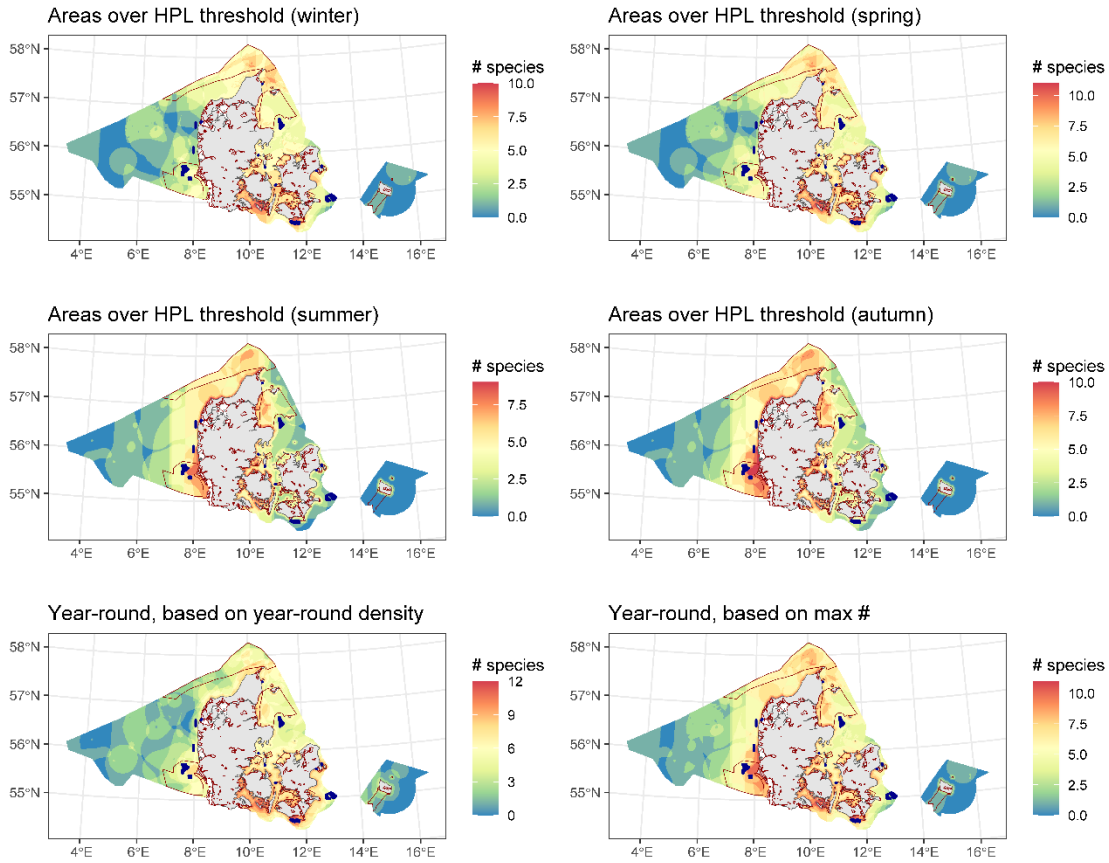

Figure A3.3 Number of species exceeding habitat protection level (HPL) in each season (top four panels) and year-round (bottom panels). Year-round risk is presented in two alternate ways. In the bottom left panel, the year-round risk is calculated based on average year-round density maps. This is the main method used to present risk analysis results in the report. In the bottom right panel, the year-round risk is shown as maximum values across the four season-specific maps.

9.3 Exploring alternatives to calculate year-round risk

9.3.1 Risk ratios

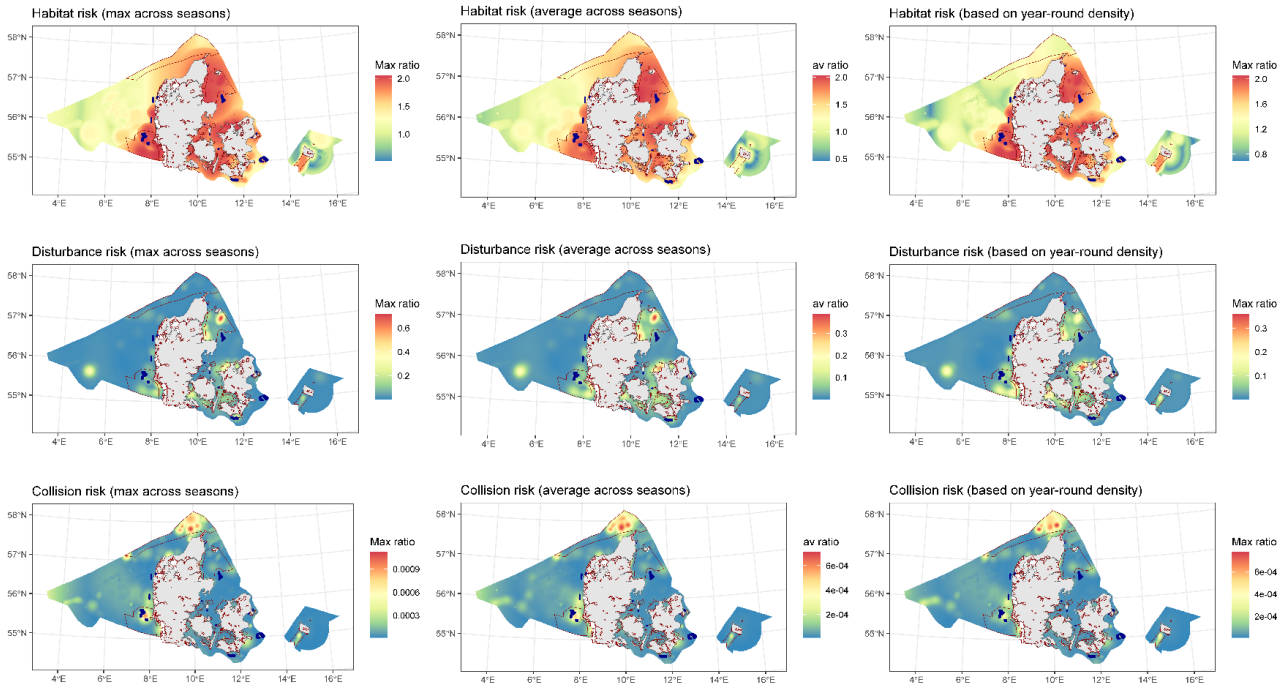

Figure A3.4 Three different methods to calculate year-round risk ratios for each hazard. The first two methods generated seasonal risk maps and then summarized the risk ratios across the seasonal maps, either as maximum (left panels) or average (middle panels). The third method calculated year-round risk based on year-round density distribution maps for each species (right panels). For species that were modelled density distribution separately for winter-spring and summer-autumn (**Section 2.2.1**), this involved averaging the density distributions, with season duration in days as weights.

9.3.2 Spatially relative risk

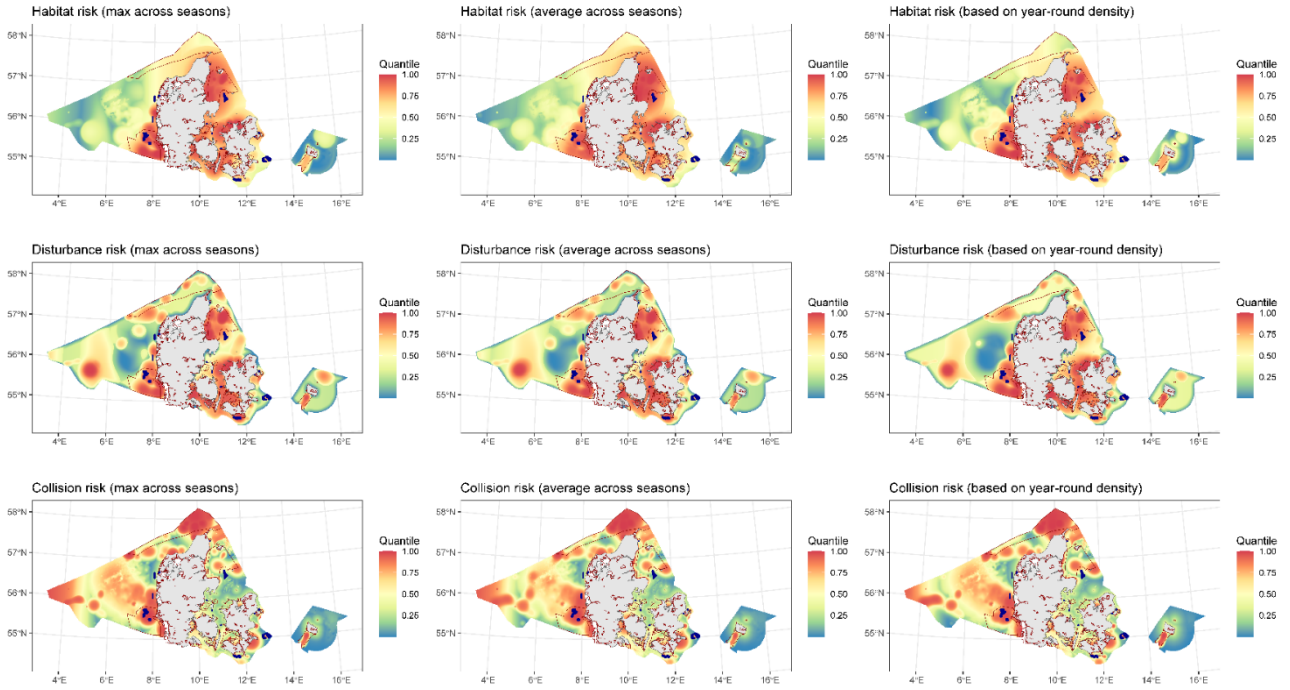

Figure A3.5 Three different methods to calculate year-round risk, shown as spatially relative risk (quantiles). The first two methods generated seasonal risk maps, and then summarized the risk ratios across the seasonal maps, either as maximum (left panels) or average (middle panels). The third method calculated year-round risk based on year-round density distribution maps for each species (right panels). For species that were modelled density distribution separately for winter-spring and summer-autumn (**Section 2.2.1**, "Modelled species and seasons"), this involved averaging the density distributions, with season duration in days as weights.

References

Band, W., M. Madders, and D. Whitfield. 2007. "Developing field and analytical methods to assess avian collision risk at wind farms". Pages 259–275 *in Birds and Wind Farms: Risk Assessment and Mitigation*.

Best, B. D., and P. N. Halpin. 2019. "Minimizing wildlife impacts for offshore wind energy development: Winning tradeoffs for seabirds in space and cetaceans in time". *PLoS ONE* 14: 1–26.

BirdLife International. 2021. "European Red List of Birds". *2021*.

Bradbury, G., M. Trinder, B. Furness, A. N. Banks, R. W. G. Caldow, and D. Hume. 2014. "Mapping Seabird Sensitivity to offshore wind farms". *PLoS ONE* 9.

Buckland, S. T., D. R. Anderson, K. P. Burnham, J. L. Laake, D. L. Borchers, and L. Thomas. 2001. "Introduction to Distance Sampling: Estimating Abundance of Biological Populations". Oxford University Press, United Kingdom.

Caneco, B., G. R. W. Humphries, A. Cook, and E. A. Masden. 2022. "Estimating Bird Collisions at Offshore Wind Farms with stochLAB". https://github.com/MarineScotlandScience/stochLAB.

Certain, G., L. L. Jørgensen, I. Christel, B. Planque, and V. Bretagnolle. 2015. "Mapping the vulnerability of animal community to pressure in marine

systems: disentangling pressure types and integrating their impact from the individual to the community level". *ICES Journal of Marine Science* 72: 1470–1482.

CIEEM. 2024. "Guidelines for ecological impact assessment in the UK and Ireland". Chartered Institute of Ecology and Environmental Management (CIEEM), Winchester. https://cieem.net/wp-content/uploads/2018/08/EcIA-Guidelines-v1.3-Sept-2024.pdf.

Cook, A. S. C. P., E. M. Humphreys, F. Bennet, E. A. Masden, and N. H. K. Burton. 2018. "Quantifying avian avoidance of offshore wind turbines: Current evidence and key knowledge gaps". *Marine Environmental Research* 140: 278–288.

Cook, A. S. C. P., E. Salkanovic, E. Masden, H. E. Lee, and A. H. Kiilerich. 2025. "A critical appraisal of 40 years of avian collision risk modelling: How have we got here and where do we go next?". *Environmental Impact Assessment Review* 110: 107717.

Cox, L. A. 2008. "What's wrong with risk matrices?". *Risk Analysis* 28: 497–512.

Dierschke, V., R. W. Furness, and S. Garthe. 2016. "Seabirds and offshore wind farms in European waters: Avoidance and attraction". *Biological Conservation* 202: 59–68.

Duijm, N. J. 2015. "Recommendations on the use and design of risk matrices". *Safety Science* 76: 21–31.

Dunn, R. E., J. Duckworth, S. O. Brien, R. W. Furness, L. Buckingham, M. Bogdanova, and J. A. Green. 2024. "Temporal and spatial variability in availability bias has consequences for marine bird abundance estimates during the non-breeding season". *bioRxiv*: 1–25.

Fauchald, P., V. M. S. Ollus, M. Ballesteros, A. Breistøl, S. Christensen-Dalsgaard, S. Molværsmyr, A. Tarroux, G. H. Systad, and B. Moe. 2024. "Mapping seabird vulnerability to offshore wind farms in Norwegian waters". *Frontiers in Marine Science* 11: 1–15.

Furness, R. W., H. M. Wade, and E. A. Masden. 2013. "Assessing vulnerability of marine bird populations to offshore wind farms". *Journal of Environmental Management* 119: 56–66.

Garthe, S., and O. Hüppop. 2004. "Scaling possible adverse effects of marine wind farms on seabirds: Developing and applying a vulnerability index". *Journal of Applied Ecology* 41: 724–734.

Gibbs, M. T., and H. I. Browman. 2015. "Introduction: Risk assessment and risk management: A primer for marine scientists". *ICES Journal of Marine Science* 72: 992–996.

Gormley, A., S. Pollard, and S. Rocks. 2011. "Guidelines for Environmental Risk Assessment and Management". UK Department for Environment, Food & Rural Affairs (DEFRA). https://www.gov.uk/government/publications/guidelines-for-environmental-risk-assessment-and-management-green-leaves-iii.

Green, R. M. W., N. H. K. Burton, A. S. C. P. Cook, S. E. Franks, and J. A. Green. 2025. "Framework for assessing species vulnerability whilst on migration to a spatially explicit anthropogenic pressure". *Biological Conservation* 307: 111118.

Hemming, V., M. A. Burgman, A. M. Hanea, M. F. McBride, and B. C. Wintle. 2018. "A practical guide to structured expert elicitation using the IDEA protocol". *Methods in Ecology and Evolution* 9: 169–180.

Horswill, C., J. A. O. Miller, and M. J. Wood. 2022. "Impact assessments of wind farms on seabird populations that overlook existing drivers of demographic change should be treated with caution". *Conservation Science and Practice* 4: 1–10.

Horswill, C., and R. A. Robinson. 2015. "Review of seabird demographic rates and density dependence". Peterborough.

International Organization for Standardization [ISO]. 2018. "ISO 31000:2018 Risk Management".

Isojunno, S., L. Scott-Hayward, C. L. Pedersen, H. M. Thomsen, J. Chetcuti, M. Frederiksen, T. Bregnballe, J. Sterup, M. MacKenzie, and I. . Petersen. 2025. "Mapping relative risk to seabirds from offshore wind energy developments in Danish waters".

Johnston, A., A. S. C. P. Cook, L. J. Wright, E. M. Humphreys, and N. H. K. Burton. 2014. "Modelling flight heights of marine birds to more accurately assess collision risk with offshore wind turbines". *Journal of Applied Ecology* 51: 31–41.

Kelsey, E. C., J. J. Felis, M. Czapanskiy, D. M. Pereksta, and J. Adams. 2018. "Collision and displacement vulnerability to offshore wind energy infrastructure among marine birds of the Pacific Outer Continental Shelf". *Journal of Environmental Management* 227: 229–247.

Lamb, J., J. Gulka, E. Adams, A. Cook, and K. A. Williams. 2024. "A synthetic analysis of post-construction displacement and attraction of marine birds at offshore wind energy installations". *Environmental Impact Assessment Review* 108: 107611.

Linkov, I., D. Loney, S. Cormier, F. K. Satterstrom, and T. Bridges. 2009. "Weight-of-evidence evaluation in environmental assessment: Review of qualitative and quantitative approaches". *Science of the Total Environment* 407: 5199–5205.

MacMillan, D. C., and K. Marshall. 2005. "The Delphi process – an expert-based approach to ecological modelling in data-poor environments Knowledge engineering and the". *Animal Conservation* 9: 11–19.

Martin, T. G., M. A. Burgman, F. Fidler, P. M. Kuhnert, S. Low-choy, M. Mcbride, and K. Mengersen. 2011. "Eliciting Expert Knowledge in Conservation Science". *Conservation Biology* 26: 29–38.

Masden, E. A., and A. S. C. P. Cook. 2016. "Avian collision risk models for wind energy impact assessments". *Environmental Impact Assessment Review* 56: 43–49.

Merrall, E., J. A. Green, L. A. Robinson, A. Butler, M. J. Wood, M. A. Newell, J. Black, F. Daunt, and C. Horswill. 2024. "Incorporating density-dependent regulation into impact assessments for seabirds". *Journal of Applied Ecology* 61: 2510–2524.

Miller, J. A. O., R. W. Furness, M. Trinder, and J. Matthiopoulos. 2019. "The sensitivity of seabird populations to density-dependence, environmental stochasticity and anthropogenic mortality". *Journal of Applied Ecology* 56: 2118–2130.

Niel, C., and J. D. Lebreton. 2005. "Using demographic invariants to detect overharvested bird populations from incomplete data". *Conservation Biology* 19: 826–835.

O'Brien, S. H., A. S. C. P. Cook, and R. A. Robinson. 2017. "Implicit assumptions underlying simple harvest models of marine bird populations can mislead environmental management decisions". *Journal of Environmental Management* 201: 163–171.

R Core Team. 2024. "R: A Language and Environment for Statistical Computing". R Foundation for Statistical Computing.

Raimondo, S., M. Etterson, N. Pollesch, K. Garber, A. Kanarek, W. Lehmann, and J. Awkerman. 2018. "A framework for linking population model development with ecological risk assessment objectives". *Integrated Environmental Assessment and Management* 14: 369–380.

Scott-Hayward, L. A. S., M. L. Mackenzie, and C. G. Walker. 2023a. "MRSea R Package (V1.5.0): Spatially Adaptive Uni and Bi-Variate Regression Splines Using SALSA". University of St Andrews.

Scott-Hayward, L. A. S., M. L. Mackenzie, C. G. Walker, G. Shatumbu, W. Kilian, and P. du Preez. 2023b. "Automated surface feature selection using SALSA2D: Assessing distribution of Elephant carcasses in Etosha National Park".

Searle, K., D. Mobbs, F. Daunt, and A. Butler. 2019. "A Population Viability Analysis modelling tool for seabird species". *Centre for Ecology & Hydrology report for Natural England. Natural England Commissioned Report NECR274*.

Southall, B. L., D. Tollit, J. Amaral, C. W. Clark, and W. T. Ellison. 2023. "Managing human activity and marine mammals: A biologically based, relativistic risk assessment framework". *Frontiers in Marine Science* 10: 1–15.

Stelzenmüller, V., M. Coll, R. Cormier, A. D. Mazaris, M. Pascual, C. Loiseau, J. Claudet, S. Katsanevakis, E. Gissi, A. Evagelopoulos, B. Rumes, S. Degraer, H. Ojaveer, T. Moller, J. Giménez, C. Piroddi, V. Markantonatou, and C. Dimitriadis. 2020. "Operationalizing risk-based cumulative effect assessments in the marine environment". *Science of the Total Environment* 724.

Thieurmel, B. 2017. "R package for calculating sun/moon positions and phases". https://github.com/datastorm-open/suncalc .

Tyack, P. L., L. Thomas, D. P. Costa, A. J. Hall, C. M. Harris, J. Harwood, S. D. Kraus, P. J. O. Miller, M. Moore, T. Photopoulou, E. Pirotta, R. M. Rolland, L. H. Schwacke, S. E. Simmons, and B. L. Southall. 2022. "Managing the effects of multiple stressors on wildlife populations in their ecosystems: developing a cumulative risk approach". *Proceedings of the Royal Society B: Biological Sciences* 289: 20222058.

USEPA. 2016. "Generic Ecological Assessment Endpoints (GEAEs) For Ecological Risk Assessment: Second Edition With Generic Ecosystem Services Endpoints Added". *Usepa*. U.S. Environmental Protection Agency (USEPA), Washington, DC. https://www.epa.gov/sites/default/files/2016-08/documents/geae_2nd_edition.pdf

Verling, E., R. Miralles Ricós, M. Bou-Cabo, G. Lara, M. Garagouni, J. M. Brignon, and T. O'Higgins. 2021. "Application of a risk-based approach to continuous underwater noise at local and subregional scales for the Marine Strategy Framework Directive". *Marine Policy* 134.

Wade, P. R. 1998. "Calculating limits to the allowable human-caused mortality of cetaceans and pinnipeds". *Marine Mammal Science* 14: 1–37.

Willmott, J. R., G. Forcey, and A. Kent. 2013. "The relative vulnerability of migratory bird species to offshore wind energy projects on the Atlantic outer continental shelf". *OCS Study BOEM 2013-207*: 275 pp.

RELATIVE RISK TO SEABIRDS FROM FUTURE OFFSHORE WIND ENERGY DEVELOPMENTS IN DANISH WATERS: SPATIAL DISTRIBUTION AND CUMULATIVE DEVELOPMENT SCENARIOS

Based on 352 days of aerial Distance Sampling line transect surveys of birds in Danish marine areas over the past 24 years, we developed a relative risk analysis for birds and offshore wind farm development. The assessment was based on abundance estimates for 17 marine bird species and their susceptibility towards offshore wind farm development. Using habitat, displacement and collision risk layers we classified the Danish marine areas in least and greatest risk of impacts to marine birds, as well as considered the potential relative risks under future cumulative development scenarios.

ISBN: 978-87-7648-021-9
ISSN: 2244-999X